Gitter-QCD-Test der Hypothese einer effektiven Restaurierung der chiralen Symmetrie bei Hadronenresonanzen

von

Johannes Gerer

aus

Traunstein

durchgeführt am Institut Physik I - Theoretische Physik der
Universität Regensburg unter Anleitung von
Prof. Dr. Andreas Schäfer

September 2009

Contents

1 Introduction

The aim of this work was to test the hypothesis of an effective restoration of chiral symmetry in the low lying baryon spectrum. The test was to check if a certain consequence of chiral symmetry restoration can be observed. The considered consequence is the smallness of the axial charge of baryons that exhibit parity doubling.

Thus, in this work the axial charge of the two lowest negative parity nucleon states, which is a highly non-perturbative quantity, is calculated using lattice quantum chromodynamics (QCD). For lattice QCD provides the means to compute properties of hadrons that are inaccessible via perturbative methods.

This thesis will start with a general introduction to the formulation of QCD and lattice QCD. Then it explains the methods of how to derive hadron properties using lattice QCD and gives an insight into numerical aspects of the calculation. The next part will deal with chiral symmetry. What it is, how it is broken and what consequences an effective restoration would have. The last section contains the results of the calculations and plots.

2 Notations

Throughout the work summation conventions are used for Minkowski, colour and Dirac indices and indices of the adjoint $SU(3)_{\text{colour}}$ representation.

Indices, labels and spacetime arguments will be omitted if possible.

The following notation will be used:

Natural units	$c = \hbar = 1$	(2.1)
Contravariant vector	$x^\mu = \left(x^0, x^1, x^2, x^3\right) = (t, x, y, z) = (t, \vec{x})$	(2.2)
Metric tensor	$g^{\mu\nu} = g_{\mu\nu} = \text{diag}\,(1, -1, -1, -1)$	(2.3)
Covariant vector	$x_\mu = g_{\mu\nu} x^\nu = (t, -\vec{x})$	(2.4)
Scalar product	$x \cdot y = x^\mu y_\mu = x^0 y^0 - \vec{x} \cdot \vec{y}$	(2.5)
Unit vectors	$\hat{\mu}^\nu = \delta_\mu{}^\nu$	(2.6)
Four-momentum	$p^\mu = (E, -\vec{p}) = i\partial^\mu = i\frac{\partial}{\partial x_\mu} = i\left(\frac{\partial}{\partial t}, -\vec{\nabla}\right)$	(2.7)
Four-spin	$(0, \vec{s}) \xrightarrow{\text{Lorentz boost}} s^\mu(\vec{p})$, with $p^\mu s_\mu(\vec{p}) = 0$	(2.8)

	and $s^2 = -m^2$	
Dirac matrices	$\gamma^\mu = (\gamma^0, \vec{\gamma})$, with $\{\gamma^\mu, \gamma^\nu\} = 2\, g^{\mu\nu}$	(2.9)
	$\gamma^5 = i\gamma^0\gamma^1\gamma^2\gamma^3$, with $\left\{\gamma^5, \gamma^\mu\right\} = 0$	(2.10)
	$(\gamma^0)^\dagger = \gamma^0, \quad (\gamma^i)^\dagger = -\gamma^i, \quad (\gamma^5)^\dagger = \gamma^5$	(2.11)
	$\sigma^{\mu\nu} = \frac{i}{2}\left[\gamma^\mu, \gamma^\nu\right]$	(2.12)
Feynman dagger	$\not{a} = a_\mu \gamma^\mu$	(2.13)
Quark spinor	$\psi_f^{\alpha,c}(x)$, with $x \in \mathbb{R}^4$, colour index $c = 1, 2, 3$, Dirac spinor index $\alpha = 1, 2, 3, 4$ and flavour f	(2.14)
Flavour component	$\psi_q(x) = q(x), \quad \bar{\psi}_q(x) = \bar{q}(x),$	(2.15)
Dirac adjungation	$\bar{\psi} = \psi^\dagger \gamma_0$	(2.16)
SU(3) generators	T^a, with $a = 1, \ \ldots \ , 8$	(2.17)
SU(3) structure constants	$\left[\mathrm{T}^a, \mathrm{T}^b\right] = i f^{abc} \mathrm{T}^c$	(2.18)
Four potential	$\mathrm{A}_\mu\left(x\right) = A_\mu^a\left(x\right) \mathrm{T}^a$	(2.19)
Covariant derivative	$\mathrm{D}_\mu = \partial_\mu - ig\mathrm{A}_\mu$	(2.20)
Gauge transporter	$\mathrm{U}(x, y) = \mathcal{P}\left\{\exp\left[ig \int_y^x \mathrm{d}z_\mu \, \mathrm{A}^\mu(z)\right]\right\}^1$	(2.21)
Dimensionless gauge coupling parameter	g	(2.22)
Gauge transformation	$\mathcal{G}(x) = e^{i\theta^a(x)\mathrm{T}^a}$, with $\theta^a(x) \in \mathbb{R}$	(2.23)
	$\psi(x) \to \mathcal{G}(x)\psi(x)$	(2.24)
	$\mathrm{A}_\mu(x) \to \mathcal{G}(x)(\mathrm{A}_\mu(x) + \frac{i}{g}\partial_\mu)\mathcal{G}(x)^{-1}$	(2.25)
	$\mathrm{D}_\mu(x) \to \mathcal{G}(x)\mathrm{D}(x)\mathcal{G}(x)^{-1}$	(2.26)
	$\mathrm{U}(x, y) \to \mathcal{G}(x)\mathrm{U}(x, y)\mathcal{G}(y)^{-1}$	(2.27)
Dirac operator	$K(x) = (i\not{\mathrm{D}}(x) - m)$	(2.28)

[1] $\mathcal{P}$ denotes path-ordering

Field strength tensor	$\mathrm{F}_{\mu\nu} = \frac{i}{g}\left[\mathrm{D}_\mu, \mathrm{D}_\nu\right] = \partial_\mu \mathrm{A}_\nu - \partial_\nu \mathrm{A}_\mu + ig\left[\mathrm{A}_\mu, \mathrm{A}_\nu\right]$	(2.29)
Euclidean vector	$x_\mu^{\mathrm{E}} = (x_1^{\mathrm{E}}, x_2^{\mathrm{E}}, x_3^{\mathrm{E}}, x_4^{\mathrm{E}}) = (\vec{x}, it)$	(2.30)
Euclidean covariant derivative	$\mathrm{D}_\mu^{\mathrm{E}} = \partial_\mu^{\mathrm{E}} + ig\mathrm{A}_\mu^{\mathrm{E}} = (-\vec{\mathrm{D}}, -i\mathrm{D}^0)$	(2.31)
Euclidean Dirac matrices	$\gamma_\mu^{\mathrm{E}} = (-i\vec{\gamma}, \gamma^0)$, with $\left\{\gamma_\mu^{\mathrm{E}}, \gamma_\nu^{\mathrm{E}}\right\} = 2\,\delta_{\mu\nu}$	(2.32)
	$\gamma_5^{\mathrm{E}} = \gamma_1^{\mathrm{E}}\gamma_2^{\mathrm{E}}\gamma_3^{\mathrm{E}}\gamma_4^{\mathrm{E}} = -\gamma^5$	(2.33)
Euclidean Dirac operator	$\mathrm{K}(x)^{\mathrm{E}} = \not{\mathrm{D}}_\mu^{\mathrm{E}} + m$	(2.34)
Parity projectors	$P_\pm = \frac{1 \pm \gamma_0}{2} = \frac{1 \pm \gamma_4^{\mathrm{E}}}{2},\ P_+ + P_- = \mathbb{1},\ P_\pm^2 = P_\pm$	(2.35)
Spin projectors	$P(\vec{s}) = \frac{1 + \gamma^5 \not{s}/m}{2} = \frac{1 + i\gamma_5^{\mathrm{E}} \not{s}^{\mathrm{E}}/m}{2}$	(2.36)
	$P(\vec{s}) + P(-\vec{s}) = \mathbb{1}$ and $P(\vec{s})^2 = P(\vec{s})$	(2.37)
Positive energy spinors	$u(\vec{s}, \vec{p})\bar{u}(\vec{s}, \vec{p}) = \frac{-i\not{p}^{\mathrm{E}} + m}{2m} P(\vec{s})$	(2.38)
Negative energy spinors	$v(\vec{s}, \vec{p})\bar{v}(\vec{s}, \vec{p}) = \frac{-i\not{p}^{\mathrm{E}} - m}{2m} P(\vec{s})$	(2.39)
Lattice constant	a	(2.40)
Lattice point	$x_\mu = an_\mu$ with $n_\mu \in \mathbb{N}$	(2.41)
Lattice extend	$L_\mu = aN_\mu$	(2.42)
Number of sites	$N_{\text{sites}} = N_0 N_1 N_2 N_3$	(2.43)
Transition to dimensionless lattice quantities	$m_{\mathrm{L}} = am,\ \ \psi_{\mathrm{L}}(n_\mu) = a^{3/2}\psi(x_\mu)$	(2.44)

3 Quantum chromodynamics

The strongest of the four fundamental interactions, the strong force, is described within the standard model of particle physics by the theory of quantum chromodynamics (QCD). QCD is an elegant and cleanly formulated theory.

The fundamental particles of the theory, the quarks, posses spin $1/2$ and are in the corresponding representation of the full Lorentz group (i.e. bispinor or Dirac spinor). They also are in the fundamental representation of $SU(3)_{\text{colour}}$, which means that they come in three different colour states (red, green and blue). As the colour is responsible for the basic structure of the interaction, it is also called the colour charge and the theory quantum chromodynamics (chromos, Greek: colour).

This leaves the quark operators with two indices. There exist two distinct sets of matrices that act only on their corresponding indices. Three-dimensional colour matrices from the $SU(3)_{\text{colour}}$ group or its generators acting in colour space and four-dimensional elements of the Clifford algebra, that act in Dirac spinor space. Of course, these two sets of matrices commute.

Within the standard model there exist six different types (flavours) of quarks with different masses, hence a third index that will become important later.

The free QCD Lagrangian, describing free spin-$1/2$ particles, has this form:

$$\mathcal{L}_{\text{free}}(x) = \sum_f \bar{\psi}_f^{\alpha,c}(x)(i\partial^\mu \gamma_\mu^{\alpha,\beta} - m_f)\psi_f^{\beta,c}(x) = \sum_f \bar{\psi}_f(i\partial\!\!\!/ - m_f)\psi_f \tag{3.1}$$

From now on the shorthand notation will be used for indices, sums over indices and spacetime arguments, where comprehensible.

3.1 Gauging the Free Theory

The free theory by construction possesses a global $SU(3)_{\text{colour}}$ symmetry:

$$\psi(x) \to e^{i\theta^a \mathrm{T}^a}\psi(x) = \mathcal{G}\psi(x) \text{ , with } \theta^a \in \mathbb{R} \tag{3.2}$$

$$\bar{\psi}(x) \to \bar{\psi}(x)\mathcal{G}^\dagger = \bar{\psi}(x)e^{-i\theta^a \mathrm{T}^a} = \bar{\psi}\mathcal{G}^{-1} \tag{3.3}$$

$$\mathcal{L}(x) \to \sum_f \bar{\psi}\mathcal{G}^{-1}(i\partial\!\!\!/ - m_f)\mathcal{G}\psi = \sum_f \bar{\psi}(i\partial\!\!\!/ - m_f)\psi = \mathcal{L}(x) \tag{3.4}$$

Global means, that the parameters of the symmetry transformation θ^a are constant over space and time. Only this fact lets the symmetry transformation and the derivatives commute in the crucial step of eq. (3.4).

To obtain the desired QCD interactions, the symmetry has to be gauged. Gauging a symmetry means to make the theory invariant under local gauge transformations:

$$\psi(x) \to e^{ig\theta^a(x)\mathrm{T}^a}\psi(x) = \mathcal{G}(x)\psi(x) \tag{3.5}$$

$$\bar{\psi}(x) \to \bar{\psi}(x)\mathcal{G}^\dagger(x) = \bar{\psi}(x)e^{-ig\theta^a(x)\mathrm{T}^a} = \bar{\psi}(x)\mathcal{G}^{-1}(x) \tag{3.6}$$

A local colour-contraction of two field-operators $\bar{\psi}(x)\psi(x)$ is invariant under any local transformation. Non-local contractions are not invariant, as the in general completely different transformations on the two different spacetime points do not cancel. In order to render non-local colour-contraction also invariant they have to be modified. By inserting a *gauge transporter* U with certain properties

$$\mathrm{U}(y,x) \to \mathcal{G}(y)\mathrm{U}(y,x)\mathcal{G}^\dagger(x), \tag{3.7}$$

the contraction becomes gauge invariant:

$$\bar{\psi}(y)\mathrm{U}(y,x)\psi(x) \to \bar{\psi}(y)\mathrm{U}(y,x)\psi(x) \tag{3.8}$$

The derivatives occurring in the Lagrangian density produce non-local contractions:

$$\bar{\psi}(x)\partial\!\!\!/\psi(x) = \lim_{h\to 0}\frac{1}{h}\bar{\psi}(x)\gamma^\mu\left(\psi(x+h\hat{\mu})-\psi(x)\right) \tag{3.9}$$

The invariant version would look like this:

$$\lim_{h\to 0}\frac{1}{h}\bar{\psi}(x)\gamma^\mu\left(\mathrm{U}(x,x+h\hat{\mu})\psi(x+h\hat{\mu})-\psi(x)\right) \tag{3.10}$$

By introducing a new vector field $\mathrm{A}_\mu(x) = A^a_\mu(x)\mathrm{T}^a$, called gauge field, which is made up of $SU(3)_{\text{colour}}$ generators with eight real coefficients A^a_μ, with the following behaviour under gauge transformations $\mathcal{G}$

$$\mathrm{A}_\mu \to \mathcal{G}\left(\mathrm{A}_\mu + \frac{i}{g}\partial_\mu\right)\mathcal{G}^\dagger, \tag{3.11}$$

a gauge transporter $\mathrm{U}_P(y,x)$, with the correct transformation behaviour (eq. 3.7), can be constructed:

$$\mathrm{U}_P(y,x) = \mathcal{P}\left\{\exp\left[ig\int_P \mathrm{d}z_\mu\,\mathrm{A}^\mu(z)\right]\right\} \tag{3.12}$$

The integral is taken along the path P from x to y.

Using this definition, if the gauge transporter along the shortest path that connects x and $x+h\hat{\mu}$ is considered, it can be expanded in orders of h:

$$\mathrm{U}(x,x+h\hat{\mu}) = 1 - igh\mathrm{A}_\mu(x) + \mathcal{O}(h^2) \tag{3.13}$$

If this expansion is inserted into eq. (3.10),the invariant version of the derivative part of the Lagrangian becomes

$$\bar{\psi}(x)\not{D}\psi(x) = \bar{\psi}(x)\left(\partial\!\!\!/ - ig\not{A}\right)\psi(x), \tag{3.14}$$

where the *covariant derivative*

$$\mathrm{D}^\mu(x) = \partial^\mu(x) - ig\mathrm{A}^\mu(x) \to \mathcal{G}(x)\mathrm{D}(x)\mathcal{G}^\dagger(x) \tag{3.15}$$

has been introduced, with a transformation behaviour, that leaves the product $\bar{\psi}(x)\not{D}\psi(x)$ invariant.

Using this covariant derivative the fermionic part of the gauged QCD Lagrange density becomes

$$\mathcal{L}_f(x) = \sum_f \bar{\psi}_f(i\not{D} - m_f)\psi_f \tag{3.16}$$

3.2 From Gauge Fields to Gluons

The gauge fields $A^a_\mu(x)$, that have been added to the free Lagrangian as interaction terms $g\bar{\psi}\not{\mathrm{A}}\psi$, can be made physical dynamical degrees of freedom, by adding a kinetic term to the Lagrangian that contains derivatives of A^a_μ. Then we have eight new physical particles, called gluons.

The objective is to find a gauge and Lorentz-invariant quantity that only contains the gauge fields and their derivatives. One gauge invariant quantity is the colour-trace of products of covariant derivatives:

$$\mathrm{tr}\{\mathrm{D}_\mu(x)\mathrm{D}_\nu(x)\} \to \mathrm{tr}\big\{\mathcal{G}(x)\mathrm{D}_\mu(x)\mathcal{G}^\dagger(x)\mathcal{G}(x)\mathrm{D}_\nu(x)\mathcal{G}^\dagger(x)\big\} = \mathrm{tr}\{\mathrm{D}_\mu(x)\mathrm{D}_\nu(x)\} \quad (3.17)$$

One finds that the commutator of two covariant derivatives, which are differential operators, does not contain any open derivatives acting to the right. Instead it is a simple matrix:

$$[\mathrm{D}_\mu, \mathrm{D}_\nu] = -ig\mathrm{F}_{\mu\nu} \quad (3.18)$$

where the *field strength tensor* has been introduced:

$$\mathrm{F}_{\mu\nu} = F^a_{\mu\nu}\mathrm{T}^a = \partial_\mu \mathrm{A}_\nu - \partial_\nu \mathrm{A}_\mu + ig\,[\mathrm{A}_\mu, \mathrm{A}_\nu] \quad (3.19)$$

This tensor can be used to construct the kinetic gauge part of the full QCD Lagrangian:

$$\mathcal{L}_G = -\frac{1}{2}\mathrm{tr}\{\mathrm{F}_{\mu\nu}\mathrm{F}^{\mu\nu}\} = -\frac{1}{4}F^a_{\mu\nu}F^{a\mu\nu} \quad (3.20)$$

Thus, the full QCD Lagrangian takes the form

$$\mathcal{L}_{\text{full}} = \sum_f \bar{\psi}_f(i\not{\mathrm{D}} - m_f)\psi_f - \frac{1}{4}F^a_{\mu\nu}F^{a\mu\nu} \quad (3.21)$$

and the QCD action $\mathcal{S}$, defined as the integral over the Lagrangian density:

$$\mathcal{S} = \int \mathrm{d}^4x\, \mathcal{L}(x) \quad (3.22)$$

With an eye toward lattice theory, I will point out another way to arrive at this action. Another gauge invariant quantity is the colour-trace of the gauge transporter $\mathrm{U}_S(x,x)$ along a closed square with edge length ϵ lying in the 1-2-plane:

$$\mathrm{tr}\{\mathrm{U}_S(x,x)\} \to \mathrm{tr}\big\{\mathcal{G}(x)\mathrm{U}_S(x,x)\mathcal{G}^\dagger(x)\big\} = \mathrm{tr}\{\mathrm{U}_S(x,x)\} \quad (3.23)$$

As ϵ approaches zero the transporter approaches $\mathbb{1}$, and can be expanded in terms of ϵ. The trace of U has the following expansion:

$$\mathrm{tr}\{\mathrm{U}_S(x,x)\} = 3 - \frac{1}{4}g^2F^a_{12}F^{a12}\,\epsilon^4 + \mathcal{O}(\epsilon^5) \quad (3.24)$$

One can clearly see, that the lowest non-trivial order is of the same form, as the gauge-field part of the Lagrangian density of QCD, and that the trace of the closed-path gauge transporter can in fact be used to produce the same action.

3.3 The Colour of Gluons

An interesting part of the Lagrangian density of QCD arises from the commutator in the field strength tensor in eq. (3.19) and is generated by the non-Abelian nature of the symmetry transformation. It is responsible for the self interaction of the gauge fields:

$$\mathcal{L}_{\text{G,self}} = -g f^{abc}(\partial_\mu A^a_\nu) A^{b\mu} A^{c\nu} - \frac{1}{4} g^2 f^{eab} f^{ecd} A^{a\mu} A^{b\nu} A^c_\mu A^d_\nu \tag{3.25}$$

Thus the gluons also carry colour charge (as opposed to the photons, the mediators of the electromagnetic interaction, that are called *neutral*, because they do not interact with other photons). But in contrast to the quarks (colour triplet, the fundamental representation of the $SU(3)_{\text{colour}}$), they are in the adjoint representation, that is a colour octet. The way, the gauge fields have been introduced here, as eight dimensional vectors A_μ in the real vector space of traceless, Hermitian three-dimensional matrices acting on the quark fields, makes it evident, that they can be assigned a colour-anticolour product. If the three colour states (red, blue, green) are represented by

$$r = \begin{pmatrix} 1 \\ 0 \\ 0 \end{pmatrix} , b = \begin{pmatrix} 0 \\ 1 \\ 0 \end{pmatrix} , g = \begin{pmatrix} 0 \\ 0 \\ 1 \end{pmatrix} , \tag{3.26}$$

the first $SU(3)_{\text{colour}}$ generator, i.e. the matrix corresponding to the first gluon, can be written in the following way:

$$\mathrm{T}^1 = \frac{1}{2} \begin{pmatrix} 0 & 1 & 0 \\ 1 & 0 & 0 \\ 0 & 0 & 0 \end{pmatrix} = \frac{1}{2} \left\{ \begin{pmatrix} 1 \\ 0 \\ 0 \end{pmatrix} \begin{pmatrix} 0 & 1 & 0 \end{pmatrix} + \begin{pmatrix} 0 \\ 1 \\ 0 \end{pmatrix} \begin{pmatrix} 1 & 0 & 0 \end{pmatrix} \right\} = \frac{1}{2}(r\bar{b} + b\bar{r}) \tag{3.27}$$

Another way to look at it, is to examine the quark-gluon interaction terms. The only terms that contain the field A^1_μ and quark fields are:

$$\frac{1}{2} \left(\bar{\psi}^r \not{A}^1 \psi^b + \bar{\psi}^b \not{A}^1 \psi^r \right) \tag{3.28}$$

The interpretation of these two vertices is, that the only way the A^1-gluon can decay, is with equal probability into either an blue-antired or an red-antiblue quark-antiquark pair.

3.4 Path Integral Quantization

Although many properties of the theory can already be seen by examining the classical theory, in order to really describe the strong interactions including particle creation and annihilation, the theory has to be quantized.

The two methods mainly used are the canonical quantization and the quantization using path integral. They are equivalent and lead to the same results. However, the latter will be emphasized here, because lattice QCD is founded on this formulation.

In canonical quantization, the classical measurable observables, i.e. the field values

$$\psi_f^{\alpha,a}(x), \bar{\psi}_f^{\alpha,a}(x), A_\mu^a(x) \tag{3.29}$$

are represented by operators acting in Fock-space. Operators are denoted by a hat:

$$\hat{\psi}_f^{\alpha,a}(x), \hat{\bar{\psi}}_f^{\alpha,a}(x), \hat{A}_\mu^a(x) \tag{3.30}$$

The spectrum of an operator makes up the set of possible outcomes for a measurement of the corresponding observable. The outcome of a measurement is no longer deterministic, instead it is a stochastic process and every eigenvalue of an operator can be measured with a certain probability. The probabilities are determined by the physical state, whose evolution is deterministical and can be obtained by solving the theory.

The state is described by a vector in Fock-space and the bracket notation of Dirac is employed.

The expectation value of a measurement of a quantity A in a certain physical state α is given by:

$$\langle A \rangle_\alpha = \langle \alpha | \hat{A} | \alpha \rangle \tag{3.31}$$

The vacuum state $|0\rangle$ is the state with the lowest energy.

In the path integral formulation the vacuum expectation value of any functional of the fields can be calculated by the path integral over the classical field configurations[2]:

$$\langle \mathcal{O}[\hat{\bar{\psi}}, \hat{\psi}, \hat{A}] \rangle \equiv \frac{\int \mathcal{D}\psi \mathcal{D}\bar{\psi} \mathcal{D}A \; \mathcal{O}\big[\bar{\psi}, \psi, A\big] \; e^{i\mathcal{S}[\bar{\psi},\psi,A]}}{\int \mathcal{D}\psi \mathcal{D}\bar{\psi} \mathcal{D}A \; e^{i\mathcal{S}[\bar{\psi},\psi,A]}} = \langle 0 | \mathcal{O}[\hat{\bar{\psi}}, \hat{\psi}, \hat{A}] | 0 \rangle \tag{3.32}$$

Path integration means functional integration over every possible field configuration.

It is called path integral, because, if you consider the collectivity of all field values for a time t as a point in an infinite-dimensional vector space, you could interpret the time dependence of the field as the trajectory of this point. This means that every field configuration in four-dimensional space can equally be described as a path.

If you integrate over all possible paths or configurations, this has the same effect as the single integrals over every degree of freedom, which can also be seen, by looking at the definition of the integration measures:

$$\mathcal{D}\psi = \prod_{\alpha,b,f} \prod_{x \in \mathbb{R}^4} d\psi_f^{\alpha,b}(x) \tag{3.33}$$

$$\mathcal{D}A = \prod_{a,\mu} \prod_{x \in \mathbb{R}^4} dA_\mu^a(x) \tag{3.34}$$

[2]The derivation can be found in many standard textbooks (e.g. [1]).

3.5 Asymptotic freedom

As simple as the formulas look, a convergent analytic solution of the whole theory does not exist. Still QCD has a peculiar property, that enables analytical calculations deriving results, that fit the experiments. It is called asymptotic freedom.

In order to understand this remarkable feature of QCD, I have to refer to the canonical quantization. Here, one arrives quickly at an perturbative expansion of vacuum expectation values in orders of the coupling constant. This series expansion makes it possible to calculate cross-sections order by order.

But as the coupling constant of QCD is very large, one would need to include infinitely many orders to derive a meaningful result, which makes it in many cases again impracticable.

The property of asymptotic freedom is revealed, if perturbative corrections to the quark-gluon vertex are considered. These lead to a scale dependence of the effective coupling parameter $\alpha(Q^2)$. In fact, the coupling gets smaller and smaller with increasing momentum transfer Q^2.

As a consequence, for experiments including large transferred momentum and thus small coupling constants, predictions can be derived from perturbative QCD. As higher order corrections will become smaller and smaller, the series can be truncated after a finite number of terms, more precisely, when the desired accuracy has been reached.

Asymptotic freedom has been found by David Gross, David Politzer and Frank Wilczek, who received the Nobel Prize in 2004 for their discovery.

3.6 Confinement

QCD explains the structure and properties of sub nuclear matter. It postulates, that the vast variety (hundreds) of strong interacting particles, that were regarded elementary before QCD, are made up of three new particles, that carry fractional electrical charge. These particles are called quarks.

This theory lead to the fair question, why there was and still is no experimental evidence of a free quark. Fortunately, QCD also gives the answer to this question: Confinement.

Confinement means, that at small momentum scales or equivalently large distances, the interaction is too strong to isolate single quarks. This is the opposite effect of asymptotic freedom, which occurs at large momentum scales. As a result, quarks can only be found bound together in colour-neutral hadrons. This colour neutrality can be realized e.g. by a quark antiquark pair of the same colour/anticolour (meson), or by three quarks of three different colours (baryon), which in analogy of the additive colour model yields white (i.e. colourless).

So far there was no analytical prove, that QCD exhibits confinement. On the lattice one was able to show that the quark antiquark potential grows linearly with their separation. One interpretation of this potential, lies in the fact that the gluon fields form, due to their self-interacting nature, colour strings between the quarks, that behave like rubber bands.

4 Lattice QCD

In contrast to perturbative QCD, that has produced satisfying results for decades, many non-perturbating properties of hadrons remain in the dark from a theoretic point of view.

To find the ground states of the theory, i.e. the hadrons and calculate their properties like masses, matrix elements, or decay constants, one has to look at scales, that are far away from asymptotic freedom. While physicists are still looking for analytic non-perturbative approaches to QCD, another theory is becoming more and more accepted as a method to get numbers out of QCD.

It is based on the idea to actually calculate the path integrals arising in QCD on a computer. To be able to do this, the original theory has to be changed. However, one tries to change it in a way, that the results of the original theory can be derived from the results of the modified theory, or that the two theories coincide in a certain limit.

The theory is called Lattice QCD. The name originates from the fact that the continuous spacetime is replaced by a four-dimensional hypercubic lattice of finite extend. The restriction to allow quark fields to only live on the lattice sites, makes the number of integrals finite. The minimal spatial separation also introduces a momentum cut-off and acts as a regulator of the theory. If now the phase factor $e^{i\mathcal{S}}$ is by a Wick's rotation converted into a bounded damping factor $e^{-\tilde{S}_E}$, the path integration can actually be performed using stochastical methods on a computer.

4.1 Euclidean Time

Wick's rotation is performed by switching to imaginary times. The formal procedure is to replace every occurrence of t in the action with $-i\tau$.

$$t \to -i\tau,\ \tau \in \mathbb{R} \tag{4.1}$$

Also all the fields have to be renamed:

$$\psi(t) \to \psi(\tau) \tag{4.2}$$

In order to bring the resulting action into a more compact form, the following Euclidean vectors are introduced:

$$x_\mu^{\mathrm{E}} \equiv (\vec{x}, ix^0) = (\vec{x}, \tau) \tag{4.3}$$

$$p_\mu^{\mathrm{E}} \equiv (\vec{p}, ip^0) = -i\partial_\mu^{\mathrm{E}} \tag{4.4}$$

$$A_\mu^{\mathrm{E}} \equiv (\vec{A}, iA^0) \tag{4.5}$$

$$\partial_\mu^{\mathrm{E}} \equiv \frac{\partial}{\partial x_\mu^{\mathrm{E}}} = (\vec{\nabla}, \frac{\partial}{\partial \tau}) = ip_\mu^{\mathrm{E}} \tag{4.6}$$

$$\gamma_\mu^{\mathrm{E}} \equiv (-i\vec{\gamma}, \gamma^0) \tag{4.7}$$

$$D_\mu^{\mathrm{E}} \equiv \partial_\mu^{\mathrm{E}} + igA_\mu^{\mathrm{E}} = (-\vec{D}, -iD^0) \tag{4.8}$$

$$F_{\mu\nu}^{\mathrm{E}} \equiv \frac{i}{g}\left[D_\mu^{\mathrm{E}}, D_\nu^{\mathrm{E}}\right] = \partial_\mu^{\mathrm{E}} A_\nu^{\mathrm{E}} - \partial_\nu^{\mathrm{E}} A_\mu^{\mathrm{E}} - ig\left[A_\mu^{\mathrm{E}}, A_\nu^{\mathrm{E}}\right] \tag{4.9}$$

For scalar products of Euclidean vectors the Euclidean metric is employed, yielding

$$\not{D}^{\mathrm{E}} \equiv D^{\mathrm{E}}_{\mu}\gamma^{\mathrm{E}}_{\mu} = -iD^0\gamma^0 + (-i\vec{\gamma})(-\vec{D}) = -i\not{D} \tag{4.10}$$

$$D^{\mathrm{E}}_{\mu}D^{\mathrm{E}}_{\mu} = -D^0D^0 + \vec{D}^2 = -D^{\mu}D_{\mu} \tag{4.11}$$

$$F^{\mathrm{E}}_{\mu\nu}F^{\mathrm{E}}_{\mu\nu} = \frac{-1}{g^2}\left[D^{\mathrm{E}}_{\mu}, D^{\mathrm{E}}_{\nu}\right]\left[D^{\mathrm{E}}_{\mu}, D^{\mathrm{E}}_{\nu}\right] = \frac{-1}{g^2}\left[D^{\mu}, D^{\nu}\right]\left[D\mu, D_{\nu}\right] = F_{\mu\nu}F^{\mu\nu} \tag{4.12}$$

Using these equalities, we can express the Lagranian density by:s

$$\mathcal{L} = \sum_f \bar{\psi}_f(i\not{D} - m_f)\psi_f - \frac{1}{4}F^a_{\mu\nu}F^{a\mu\nu} \tag{4.13}$$

$$= -\left(\sum_f \bar{\psi}_f(\not{D}^{\mathrm{E}} + m_f)\psi_f + \frac{1}{4}F^{\mathrm{E}a}_{\mu\nu}F^{a\mu\nu}_{\mathrm{E}}\right) \tag{4.14}$$

$$\equiv -\mathcal{L}^{\mathrm{E}} \tag{4.15}$$

The actions $\mathcal{S}$, after the replacements from eqs. (4.1) and (4.2) have been performed, will have this form:

$$i\mathcal{S} = i\int \mathrm{d}^4x\, \mathcal{L}(x) = i\int \mathrm{d}^3\vec{x}\mathrm{d}(-i\tau)\,(-\mathcal{L}^{\mathrm{E}}(\tau,\vec{x})) = -\int \mathrm{d}^4x^{\mathrm{E}}\, \mathcal{L}^{\mathrm{E}}(x^{\mathrm{E}}) \equiv -\mathcal{S}^{\mathrm{E}}, \tag{4.16}$$

where we introduced $\mathcal{S}^{\mathrm{E}}$, called the Euclidean action.

In this Euclidean field theory the vacuum expectation value of a an operator $\mathcal{O}[\hat{\bar{\psi}}, \hat{\psi}, \hat{A}^{\mathrm{E}}]$ has the following value:

$$\langle 0|\mathcal{O}[\hat{\bar{\psi}}, \hat{\psi}, \hat{A}^{\mathrm{E}}]|0\rangle = \frac{\int \mathcal{D}\psi\mathcal{D}\bar{\psi}\mathcal{D}A^{\mathrm{E}}\, \mathcal{O}\left[\bar{\psi}, \psi, A^{\mathrm{E}}\right]\, e^{-\mathcal{S}^{\mathrm{E}}[\bar{\psi},\psi,A^{\mathrm{E}}]}}{\int \mathcal{D}\psi\mathcal{D}\bar{\psi}\mathcal{D}A^{\mathrm{E}}\, e^{-\mathcal{S}^{\mathrm{E}}[\bar{\psi},\psi,A^{\mathrm{E}}]}} \tag{4.17}$$

The effect of the transition to Euclidean time is two-fold:

- Firstly, the time evolution operator now has the form

  $$e^{-\tau\mathcal{H}}. \tag{4.18}$$

  This is helpful, for the time evolution of any state will be dominated for large τ by the lowest contributing energy-state:

  $$|\alpha(\tau)\rangle = \sum_E |E(\tau)\rangle\langle E|\alpha\rangle = \sum_E e^{-\tau E}|E\rangle\langle E|\alpha\rangle \approx e^{-\tau E_0}|E_0\rangle\langle E_0|\alpha\rangle \tag{4.19}$$

  All other contributions will be exponentially damped with time.

  This will be used to isolate the ground state of certain hadrons, by simply creating some state, with a simple wave-function that will actually be a complex superposition of hadron states and waiting long enough for higher state components to fall off.

- The second effect is that the pure phase $e^{i\mathcal{S}}$ has become a damping factor due to the negative real part of the exponent in $e^{-\mathcal{S}^{\mathrm{E}}}$. This makes it possible to actually calculate the integral using statistical methods.

From now on we will work in Euclidean spacetime and all labels E will be dropped, unless stated differently. Also instead of τ the variable t will be used. τ is freed from its meaning.

For the basics of Euclidean field theory we refer to [2], for a treatment within the framework of lattice field theory see [3], for mathematical considerations refer to [4] and [5].

4.2 Discretizing Spacetime

The continuous spacetime, $x \in \mathbb{R}^4$, is replaced by a four-dimensional hypercubical lattice. The number of lattice sites in μ-direction is N_μ. The total number of sites is

$$N_{\text{sites}} = N_1 N_2 N_3 N_4 \tag{4.20}$$

By numbering the lattice sites in every spacetime direction, starting by 0 in the origin, every lattice site can be assigned a four-vector of integers:

$$n_\mu = (n_1, n_2, n_3, n_4), \text{ with } n_\mu \in \{0, \ldots, N_\mu - 1\} \tag{4.21}$$

By imposing a distance between two sites, the lattice spacing a, usually in the order of 0.1 femtometers for QCD, every site now represents a point in physical spacetime:

$$x_\mu = a n_\mu = (n_1, n_2, n_3, n_4) \tag{4.22}$$

The physical lattice extend becomes:

$$L_\mu = a N_\mu = (L_t, L_x, L_y, L_z) \tag{4.23}$$

To every lattice site a fermion field gets attached:

$$\psi(n_\mu) \tag{4.24}$$

In order to understand how gauge fields are handled, one has to recall eq. (3.10):

$$\lim_{h \to 0} \frac{1}{h} \bar{\psi}(x) \gamma^\mu \left(\mathrm{U}(x, x + h\hat{\mu}) \psi(x + h\hat{\mu}) - \psi(x) \right) \tag{4.25}$$

In the continuum theory, the limit will isolate the generator of the gauge transporter A_μ. However, on the lattice this limit will stop at a finite $h = a$. Thus, it is sufficient to regard the elemental gauge transporters between neighbouring sites as the gluon field, making the use of A^a_μ obsolete. These gauge fields are said to live on the lattice links and called link variables:

$$\mathrm{U}_\mu(x) \equiv \mathrm{U}(x, x + a\hat{\mu}) \in SU(3)_{\text{colour}} \tag{4.26}$$

The four link variables attached to every lattice site are $SU(3)$ matrices, that of course have eight real degrees of freedom (corresponding to the eight vector fields A^a_μ).

A general gauge transporter along a path P from x to y can be constructed by the path ordered multiplication of link variables along the path:

$$\mathrm{U}_P(y, x) = \mathrm{U}_{\mu_n}(y - \mu_n) \ldots \mathrm{U}_{\mu_2}(x + \mu_1) \mathrm{U}_{\mu_1}(x) \tag{4.27}$$

4.3 Transfer Matrix Formalism

The derivation of the path integral formulation of quantum field theory, especially eq. (3.32), uses the fact, that spacetime, especially time, is infinite. If time is limited, as in the case of the finite lattice spacetime volume, the path integral has the value:

$$\int \mathcal{D}\psi\mathcal{D}\bar{\psi}\mathcal{D}A\ \mathcal{O}\big[\bar{\psi},\psi,A\big]\ \ e^{-\mathcal{S}[\bar{\psi},\psi,A]} = \mathrm{tr}\Big\{e^{-L_t\mathcal{H}}\mathcal{O}[\hat{\bar{\psi}},\hat{\psi},\hat{A}]\Big\} \tag{4.28}$$

This means, that eq. (3.32) is not valid any more. Instead, if for example the basis of energy states is used to calculate the traces, it takes this form:[3]

$$\big\langle \mathcal{O}\big[\bar{\psi},\psi\,A\big]\big\rangle = \mathcal{Z}^{-1}\sum_E e^{-EL_t}\langle E|\mathcal{O}\Big[\hat{\bar{\psi}},\hat{\psi},\hat{A}\Big]\,|E\rangle \tag{4.29}$$

$\mathcal{Z}$ is the partition function with

$$\mathcal{Z} = \sum_E e^{-EL_t} \tag{4.30}$$

Eq. (4.29) will be used to determine, *what* is calculated by the evaluation of the path integral.

If the temporal lattice extend $L_t = aN_0$ is much larger than the inverse energy gap between the vacuum and the first excited state, due to the Euclidean formulation, only the vacuum state will survive, as higher energy contributions are suppressed exponentially. Thus, the limit of a large L_t corresponds to the zero-temperature limit.

This is also why in typical lattice QCD calculations the temporal extend is much larger than the spatial one (e.g. 32 and 16^3)

4.4 Fermions on the Lattice

In the framework of canonical quantization the fermionic field operators have to obey anti-commutator relations:

$$\Big\{\hat{\psi}_\alpha(\vec{x},t),\hat{\psi}^\dagger_\beta(\vec{y},t)\Big\} = \delta_{\alpha\beta}\delta^3(\vec{x}-\vec{y}) \tag{4.31}$$

$$\Big\{\hat{\psi}_\alpha(\vec{x},t),\hat{\psi}_\beta(\vec{y},t)\Big\} = \Big\{\hat{\psi}^\dagger_\alpha(\vec{x},t),\hat{\psi}^\dagger_\beta(\vec{y},t)\Big\} = 0 \tag{4.32}$$

There exist profound reasons why anti-commutator relations have to be used instead of commutator relations as in quantum mechanics or bosonic field theories. The use of commutator relations would violate micro-causality and destroy the positive-definiteness of the Hamiltonian, which is only guaranteed by the applicability of Dirac statistics, which in turn can only be imposed by anti-commutator relations. [2]

The necessity to preserve this anti-commuting character of the field operators, prevents from using complex numbers as the allowed classical field values in the

[3] Lattice normalization is employed: $\langle E|E\rangle = 1$

path-integral formalism. Instead, they have to be Grassmann valued. Grassmann variables are anti-commuting c-numbers. [3]

Periodic boundary conditions are taken in spatial direction:

$$\psi(n_1 + N_1, n_2, n_3, n_4) = \psi(n_1, n_2, n_3, n_4) \tag{4.33}$$

In time direction anti-periodic boundary conditions are chosen, which are necessary for the validity of the transfer matrix formalism. [5]

$$\psi(n_1, n_2, n_3, n_4 + N_4) = -\psi(n_1, n_2, n_3, n_4) \tag{4.34}$$

For fermion fields on the lattice dimensionless versions of the continuum fields are used:

$$\psi_{\text{lattice}} = a^{3/2}\psi_{\text{cont}} \tag{4.35}$$

To describe fermions on the lattice, a fermion action has to be constructed, which has the correct continuum limit:

$$\mathcal{S}_{\text{F}} = \sum_{n,m} \bar{\psi}(n)\text{K}(n,m)\psi(m) \to \int \text{d}^4x\, \bar{\psi}(x)(\not{\partial} + m)\psi(x) \tag{4.36}$$

The kernel $\text{K}(n,m)$ is called lattice Dirac operator. (Sometimes Dirac operator referrers only to the massless part of it.)

4.4.1 Naive Implementation

The naive version of the Dirac operator is the direct implementation of a symmetrisation of eq. (3.10):[4]

$$\begin{aligned}\bar{\psi}(n)\text{K}(n,n')\psi(n') =& \frac{1}{2}\bar{\psi}(n)\gamma_\mu \left(\text{U}_\mu(n)\psi(n+\hat{\mu}) - \text{U}_{-\mu}(n)\psi(n-\hat{\mu})\right) \\ &+ \bar{\psi}(n)m\psi(n)\end{aligned} \tag{4.37}$$

$$\Rightarrow \text{K}(n,n') = \frac{1}{2}\left(\text{U}_\mu(n)\delta_{n',n+\hat{\mu}} - \text{U}_{-\mu}(n)\delta_{n',n-\hat{\mu}}\right) + m\delta_{x,y} \tag{4.38}$$

Although the mathematical expression possesses the correct limit $a \to 0$, there will occur problems in the continuum limit of the whole theory.

It can be seen quite easily by calculating the Fourier transform[5] of the free operator:

$$\tilde{\text{K}}(k,l) = \sum_{n,n'} e^{-ikn}\text{K}(n,n')e^{iln'} = \left(\frac{1}{2}\gamma_\mu\left(e^{il_\mu} - e^{-il\mu}\right) + m\right)\sum_{n,n'} e^{i(l-k)n} \tag{4.39}$$

$$= N_{\text{sites}}\delta_{k,l}\left(i\gamma_\mu \sin l_\mu + m\right) \tag{4.40}$$

[4] The mass has also been replaced by its dimensionless equivalent: $m_{\text{lattice}} = a\, m_{\text{cont}}$

[5] k and l are dimensionless wave numbers or momenta with $k_\mu = a\, p_\mu$

As the operator is block-diagonal in this representation, we can easily derive the inverse operator by inverting the block matrices:[6]

$$\left(i\gamma_\mu \sin l_\mu + m\right)^{-1} = \frac{m - i\gamma_\mu \sin l_\mu}{m^2 + \sum_\mu \sin^2 l_\mu} \tag{4.41}$$

Of course it has the correct limit:

$$\lim_{a\to 0} a\frac{m - i\gamma_\mu \sin ap_\mu}{m^2 + \sum_\mu \sin^2 ap_\mu} = \frac{m_{\text{cont}} - i\not{p}}{m_{\text{cont}}^2 + p^2} \tag{4.42}$$

The problem is however, that for finite but sufficiently small a, there exist 16 disjunct regions in the first Brillouin zone, where the corresponding operator in Minkowsky-space is singular. Responsible for that is the sine function in the denominator. One of these regions is the pole of the continuum theory in the vicinity of $p_\mu = (0,0,0,0)$. The others are located at the corners of the first Brillouin zone:

$$p_\mu \in \left\{ \left(\frac{\pi}{a},0,0,0\right), \ldots \left(\frac{\pi}{a},\frac{\pi}{a},0,0\right), \ldots, \left(\frac{\pi}{a},\frac{\pi}{a},\frac{\pi}{a},0\right), \ldots, \left(\frac{\pi}{a},\frac{\pi}{a},\frac{\pi}{a},\frac{\pi}{a}\right) \right\} \tag{4.43}$$

The poles of course are shifted to infinity for $a \to 0$, but in order to obtain the inverse of the Dirac operator in configuration space, the Fourier integral (sum) has to be taken over the whole first Brillouin zone, which in the limit will also expand and always contain the unphysical poles. Therefore, in the continuum limit, there will remain contributions that resemble 15 fermion-like excitations. These are lattice/discretization artefacts making it impossible to use the *naive operator* for lattice QCD predictions of continuum QCD.

As the number of poles (including the physical one) doubles with every space-time dimension ($2^4 = 16$) the unphysical excitations are called *doublers*, and this problem the *fermion doubling problem*.

For a closer look on fermion doubling we refer to [3].

4.4.2 Nielsen-Ninomiya No-Go theorem

Many different fermion actions have the correct $a \to 0$ limit. This freedom was used to specifically develop numerous actions that have certain properties and circumvent certain problems. (For a small overview see [6])

However, no action was found that combines all properties of the continuum operator. In fact Nielsen and Ninomiya provided mathematical prove that such an action does not exist. Their statement, which describes a major obstacle to lattice

[6] Using:

$$\begin{aligned}\left(i\gamma_\mu \sin l_\mu + m\right)^{-1} &= \left(i\gamma_\mu \sin l_\mu + m\right)^{-1}\left(-i\gamma_\mu \sin l_\mu + m\right)^{-1}\left(-i\gamma_\mu \sin l_\mu + m\right)\\ &= \left(-(\gamma_\mu \sin l_\mu)^2 + m^2\right)^{-1}\left(-i\gamma_\mu \sin l_\mu + m\right)\end{aligned}$$

and

$$(\gamma_\mu \sin l_\mu)^2 = \frac{1}{2}\left(\gamma_\mu\gamma_\nu \sin l_\mu \sin l_\nu + \gamma_\nu\gamma_\mu \sin l_\nu \sin l_\mu\right)) = \frac{1}{2}\left[\gamma_\mu,\gamma_\nu\right]\sin l_\mu \sin l_\nu \overset{(2.32)}{=} \sin^2 l_\mu$$

QCD, has been called the Nielsen-Ninomiya No-Go theorem [7, 8]. The content of the theorem is the following [6]:

On the lattice there exists no massless Dirac operator that possesses all of the following properties simultaneously:

a) Correct continuum limit

b) No doublers

c) Exact chiral symmetry, i.e. $\{\mathrm{K}, \gamma_5\} = 0$

d) Locality, i.e. $|K(x,y)| < \mathcal{C}e^{-\gamma|x-y|}$

4.4.3 Chirally Improved Fermions

Ginsparg and Wilson [9] proposed a weaker chiral symmetry condition:

$$\left\{\mathrm{K}^{-1}, \gamma_5\right\} = a\gamma_5 \tag{4.44}$$

Fermions described by this Dirac operator break the symmetry in a controlled way, the symmetry is restored within the continuum limit very smoothly and the symmetry condition also suffices to show that there are no doublers. [10]

In 2000, Gattringer, Hip and Lang [11, 12] suggested to use an approximate solution to this equation, which has been called the *chirally improved (CI) Dirac operator*. The results presented in this work have been obtained using CI-fermions. They represent a good compromise between all the aspects of the No-Go theorem and require a lot less computational effort than known exact solutions to the Ginsparg-Wilson relation.

To derive the CI-Dirac operator, one starts with a very general ansatz. Keeping in mind that $\mathrm{K}(x,y)$ is an element of the Clifford-algebra and needs to transform like a gauge transporter (cp. eq. 3.7), a general form of a lattice Dirac operator is a linear combination of all products formed of a Clifford algebra generator Γ^α and gauge transporters $\mathrm{U}_P(x,y)$ that connect x and y via the path P:

$$\mathrm{K}(x,y) = \sum_{\alpha}^{16} \sum_{p \in \mathcal{P}_{x,y}} c_\alpha^P \, \Gamma^\alpha \, \mathrm{U}_P(x,y) \tag{4.45}$$

$\mathcal{P}_{x,y}$ denote all possible paths from x to y. The next step is to translate all the requirements, that the Dirac operator should fulfil, into equations for the coefficients. (Ginsparg-Wilson relation; invariance under translation, rotation, charge conjugation and parity transformation; γ_5-hermiticity; correct continuum limit)

This system of equations for infinitely many coefficients can be solved numerically, if only paths up to a certain length and correspondingly only leading contributions are considered (The structure of the Ginsparg-Wilson equation imposes exponential suppression of longer paths [11]).

This method allows to construct arbitrarily precise solutions to the Ginsparg-Wilson equation with the correct continuum limit. The result is an operator with

a good chiral behaviour and no doublers. As mentioned earlier, the exponential suppression of longer paths ensures a certain degree of locality. The CI-fermions are a promising approach to master the constraints imposed by the No-Go theorem.

The CI-Dirac operator used in this work contains paths consisting of a maximum length of four links. In four space time dimensions, these paths connect every lattice site with its closest 128 neighbours, i.e. connecting points with a maximum separation of $\sqrt{5}a$. The coefficients that were used can be found in Appendix D of [6].

4.5 Gluons on the Lattice

In continuum QCD, after the free theory was made gauge invariant, another action containing only the gauge fields and its first derivatives is constructed. On the lattice the gauge fields are the link variables. A vector field A^a_μ or a covariant derivative D_μ is not available to form the field strength tensor (or it is at least an unnecessary detour).

Instead, we have to resort to the alternative way of constructing the gauge action, presented in section 3.2. It uses only the gauge transporter $\mathrm{U}_P(x, y)$. More precisely the trace of a gauge transporter along a closed path, which is called Wilson loop.

$$\mathrm{tr}\{\mathrm{U}_\mathcal{C}(x, x)\} \tag{4.46}$$

The simplest closed path on the lattice is the *plaquette* (a square of edge length a). If the square lies in the $\mu\nu$-plane at position n, the corresponding Wilson loop is the trace of this newly defined operator:

$$\mathrm{U}_{\mu\nu}(n) \equiv \mathrm{U}_{\text{plaquette}}(n, n) = \mathrm{U}_{-\nu}(n + \hat{\nu})\mathrm{U}_{-\mu}(n + \hat{\mu} + \hat{\nu})\mathrm{U}_\nu(n + \hat{\mu})\mathrm{U}_\mu(n) \tag{4.47}$$

Wilson constructed the *Wilson action* [13] by summing over all lattice sites and any possible orientation of the plaquette [6]:

$$\mathcal{S}_{\text{Wilson,G}} = \beta \sum_n \sum_{\mu<\nu} \left(1 - \frac{1}{3}\mathrm{Re\ tr}\mathrm{U}_{\mu\nu}(n)\right) \tag{4.48}$$

β is defined as

$$\beta \equiv \frac{6}{g^2}. \tag{4.49}$$

It can be shown, in fashion of eq. (3.24), that the limit $a \to 0$ for this action is indeed the continuum Yang-Mills action (eq. 3.20).

To reduce the discretization effects of this simple gauge action, Lüscher and Weisz [14, 15] proposed to take additional loops into account.

The Lüscher-Weisz gauge action, in addition to the squares $\mathcal{S}$, also includes 2×1 rectangles $\mathcal{R}$ and $1 \times 1 \times 1$ three-dimensional parallelograms $\mathcal{P}$[6]:

$$\mathcal{S}_{\text{LW,G}} = \beta_0 \sum_\mathcal{S} \left(1 - \frac{1}{3}\mathrm{Re\ tr}\mathrm{U}_\mathcal{S}\right) + \beta_1 \sum_\mathcal{R} \left(1 - \frac{1}{3}\mathrm{Re\ tr}\mathrm{U}_\mathcal{R}\right) + \beta_2 \sum_\mathcal{P} \left(1 - \frac{1}{3}\mathrm{Re\ tr}\mathrm{U}_\mathcal{P}\right)$$

(4.50)

The sums run over all squares,rectangles or parallelograms, respectively that exist on the lattice. $\mathrm{U}_{\mathcal{S},\mathcal{R},\mathcal{P}}$ denote the corresponding gauge transporters:

$$\mathrm{U}_{\mathcal{S}} \equiv \mathrm{U}_{\mu\nu}(n) \tag{4.51}$$

$$\mathrm{U}_{\mathcal{R}} \equiv \mathrm{U}_{-\nu}(n+\hat{\nu})\mathrm{U}_{-\mu}(n+\hat{\mu}+\hat{\nu})\mathrm{U}_{-\mu}(n+2\hat{\mu}+\hat{\nu})\times \\ \mathrm{U}_{\nu}(n+2\hat{\mu})\mathrm{U}_{\mu}(n+\hat{\mu})\mathrm{U}_{\mu}(n) \tag{4.52}$$

$$\mathrm{U}_{\mathcal{P}} \equiv \mathrm{U}_{-\kappa}(n+\hat{\kappa})\mathrm{U}_{-\nu}(n+\hat{\nu}+\hat{\kappa})\mathrm{U}_{-\mu}(n+\hat{\nu}+\hat{\mu}+\hat{\kappa})\times \\ \mathrm{U}_{\kappa}(n+\hat{\nu}+\hat{\mu})\mathrm{U}_{\nu}(n+\hat{\mu})\mathrm{U}_{\mu}(n) \tag{4.53}$$

The coupling constant β_0 is equivalent to β in Wilson's action:

$$\beta_0 = \frac{6}{g^2} \tag{4.54}$$

β_1 and β_2 are chosen such that the leading discretization errors vanish. Within the framework of tadpole improved perturbation theory they can be determined and states in terms of the expectation value of the plaquette variable, u^2 [16, 17]:

$$u^2 = \frac{1}{3}\mathrm{Re\ tr}\left\langle \mathrm{U}_{\text{plaquette}} \right\rangle, \tag{4.55}$$

$$\alpha = -\frac{\ln u^2}{3.06839}, \tag{4.56}$$

$$\beta_1 = -\frac{\beta_0}{20u}(1+0.4805\alpha), \tag{4.57}$$

$$\beta_2 = -\frac{\beta_0}{u}0.03325\alpha \tag{4.58}$$

All results of this work were obtained from calculations using the Lüscher-Weisz gauge action with these coefficients.

4.6 Evaluation of the Path Integral

Lattice QCD is the numerical calculation of expectation values related to path integrals in continuum QCD. However eq. (4.17) is not the place to start the numerical integration, because fermionic integrations can be performed analytically.

The fermionic Lagrange density is a bilinear form in the fields. By following the rules for integration over Grassmann variables, the following integrals can be solved:[7]

$$\int \mathcal{D}\psi\mathcal{D}\bar{\psi}\; e^{-\bar{\psi}\mathrm{K}[A]\psi} = \det \mathrm{K}[A] \tag{4.59}$$

[7] As the spacetime coordinates can also understood as indices, all indices (spacetime, $SU(3)_{\text{colour}}$ and Dirac) can symbolically be merged into one. For this index summation convention will be used.

$$\int \mathcal{D}\psi\mathcal{D}\bar{\psi}\ \psi^{\alpha_1}\cdots\psi^{\alpha_j}\bar{\psi}^{\beta_1}\cdots\bar{\psi}^{\beta_j}\ e^{-\bar{\psi}\mathrm{K}[A]\psi} = \xi_j\,(\det \mathrm{K}[A])\sum_P (-1)^{\sigma_P}\mathrm{K}[A]^{-1}_{\alpha_1\beta_{P_1}}\cdots\mathrm{K}[A]^{-1}_{\alpha_j\beta_{P_j}} \tag{4.60}$$

where $\xi_j = (-1)^{j(j-1)/2}$, α symbolically stands for all parameters of the fermion field (Dirac, colour, spacetime coordinate), the sum extends over all permutations and $(-1)^{\sigma_P}$ is the signum of the permutation:

$$P : \begin{pmatrix} \beta_1 & \beta_2 & \cdots & \beta_j \\ \beta_{P_1} & \beta_{P_2} & \cdots & \beta_{P_j} \end{pmatrix} \tag{4.61}$$

Now consider a theory of fermions on a fixed gauge field background without back reaction of the gauge fields (i.e. gluons). In this case the path integral representation of n-point functions contains no integration over gauge fields and only the fermionic action is used:

$$\begin{aligned} \left\langle \psi^{\alpha_1}\cdots\psi^{\alpha_j}\bar{\psi}^{\beta_1}\cdots\bar{\psi}^{\beta_j}\right\rangle_A &= \frac{\int \mathcal{D}\psi\mathcal{D}\bar{\psi}\ \psi^{\alpha_1}\cdots\psi^{\alpha_j}\bar{\psi}^{\beta_1}\cdots\bar{\psi}^{\beta_j} e^{-\mathcal{S}_F[\bar{\psi},\psi,A]}}{\int \mathcal{D}\psi\mathcal{D}\bar{\psi}\ e^{-\mathcal{S}_F[\bar{\psi},\psi,A]}} \\ &\overset{(4.59)(4.60)}{=} \xi_j \sum_P (-1)^{\sigma_P}\mathrm{K}[A]^{-1}_{\alpha_1\beta_{P_1}}\cdots\mathrm{K}[A]^{-1}_{\alpha_j\beta_{P_j}} \qquad (4.62) \\ &= \xi_j \sum_P (-1)^{\sigma_P}\left\langle \psi^{\alpha_1}\bar{\psi}^{\beta_{P_1}}\right\rangle_A\cdots\left\langle \psi^{\alpha_j}\bar{\psi}^{\beta_{P_j}}\right\rangle_A \qquad (4.63) \end{aligned}$$

Eq. (4.63) is nothing else than the path integral derivation of Wick's theorem and the fact that n-point functions of fermions on a fixed gauge background can be expressed in terms of 2-point functions.

A 2-point function is also called propagator G, because it is the amplitude for particle to propagate from y to x:

$$\mathrm{G}(x,y) \equiv \langle\psi(y)\bar{\psi}(x)\rangle_A = \mathrm{K}[A](x,y)^{-1} \tag{4.64}$$

It is the solution to the Dirac equation an a fixed gauge-background:

$$\sum_x \mathrm{K}[A](z,x)G(x,y) = \delta_{z,y} \tag{4.65}$$

The result for the non back reacting theory can be used to evaluate further the integrals of the full interacting theory. First it should be mentioned that in the following it is sufficient to treat operators of the form

$$\mathcal{O}[\hat{\bar{\psi}},\hat{\psi},\hat{A}] = \hat{\psi}^{\alpha_1}\cdots\hat{\psi}^{\alpha_j}\hat{\bar{\psi}}^{\beta_1}\cdots\hat{\bar{\psi}}^{\beta_j}\ \mathcal{O}_G[\hat{A}], \tag{4.66}$$

as they can be used to construct any operator, i.e. a general functional in the fermion fields.

Starting from the definition in eq. (4.17), the path integral expression of this operator can be expressed in the following way

$$\left\langle \psi^{\alpha_1} \cdots \psi^{\alpha_j} \bar{\psi}^{\beta_1} \cdots \bar{\psi}^{\beta_j} \; \mathcal{O}_G[A] \right\rangle \tag{4.67}$$

$$= \frac{\int \mathcal{D}A \, \mathcal{O}_G[A] \; e^{-\mathcal{S}_G[A]} \left(\int \mathcal{D}\psi \mathcal{D}\bar{\psi} \; \psi^{\alpha_1} \cdots \psi^{\alpha_j} \bar{\psi}^{\beta_1} \cdots \bar{\psi}^{\beta_j} \; e^{-\mathcal{S}_F[\bar{\psi},\psi,A]} \right)}{\int \mathcal{D}A \, e^{-\mathcal{S}_G[A]} \left(\int \mathcal{D}\psi \mathcal{D}\bar{\psi} \, e^{i\mathcal{S}_F[\bar{\psi},\psi,A]} \right)} \tag{4.68}$$

$$= \frac{\int \mathcal{D}A \, \mathcal{O}_G[A] \; e^{-\mathcal{S}_G[A]} \left\langle \psi^{\alpha_1} \cdots \psi^{\alpha_j} \bar{\psi}^{\beta_1} \cdots \bar{\psi}^{\beta_j} \right\rangle_A \det \mathrm{K}[A]}{\int \mathcal{D}A \, e^{-\mathcal{S}_G[A]} \det \mathrm{K}[A]} \tag{4.69}$$

Lattice calculations that evaluate the occurring determinants are called dynamic calculations. But as the numerical cost of the evaluation of the determinant of a $12N \times 12N$ matrix is extremely high, it is sometimes useful to use the *quenched approximation*:

$$\det \mathrm{K}[A] = \text{const.} \tag{4.70}$$

This simplification of QCD has the effect of an infinite sea quark mass and neglecting the internal quark loops.

To actually numerically evaluate the integrals in eq. (4.69), Monte-Carlo methods are employed. Basically, instead of performing the sum over all possible field configurations, a sample of configurations is generated with a certain probability distribution and the integral simply becomes the average over the sample.

Within the quenched approximation eq. (4.69) with the use of eq. (4.63) becomes after statistical sampling with sample $\{A_i\}_{1 \le i \le n}$ and probability distribution $\sim e^{-S_G[A]}$:

$$\begin{aligned} \left\langle \psi^{\alpha_1} \cdots \psi^{\alpha_j} \bar{\psi}^{\beta_1} \cdots \bar{\psi}^{\beta_j} \; \mathcal{O}_G[A] \right\rangle &= \frac{1}{n} \sum_i^n \; \mathcal{O}_G[A_i] \left\langle \psi^{\alpha_1} \cdots \psi^{\alpha_j} \bar{\psi}^{\beta_1} \cdots \bar{\psi}^{\beta_j} \right\rangle_A \\ &= \frac{1}{n} \sum_i^n \; \mathcal{O}_G[A_i] \, \xi_j \sum_P (-1)^{\sigma_P} \mathrm{K}[A_i]^{-1}_{\alpha_1 \beta_{P_1}} \cdots \mathrm{K}[A_i]^{-1}_{\alpha_j \beta_{P_j}} \end{aligned} \tag{4.71}$$

This equation gives a recipe, of how to evaluate the path integral. Eq. (4.29) is the counterpart, that helps to understand, what has been measured (calculated).

All the results of this work were obtained in the quenched approximation using formula (4.71).

4.7 Setting the scale

The theory formulated so far is scale invariant. The parameters, gauge coupling g or β, and the quark lattice masses, which are products of the lattice constant and the physical mass, are all dimensionless. Hence all results obtained from calculations are dimensionless. But we know that QCD possesses a scale that amounts to the typical size and mass of bound quark states, what is known as conformal anomaly.

The fact that the plain SU(3) Yang-Mills theory is already an interacting theory results in an interesting situation. Once the dimensionless gauge coupling parameter

is specified, the regulator of the theory (e.g. the lattice constant a) is also implicitly specified.

'Setting the scale' denotes the process of determining this value. On the lattice this is in general done by selecting a quantity that has been measured in experiments and whose lattice equivalent only depends on the gauge coupling. Then the value of a can be determined by matching the dimensionless lattice result to agree with a dimensionless combination of a and the experimental value.

For example, the string tension σ of the static quark-quark potential can be used:

$$a^2\sigma_{\text{experiment}} \stackrel{!}{=} \sigma_{\text{lattice}} \rightarrow a \tag{4.72}$$

Sommer introduced a method that uses the characteristic length scale r_0 of the static quark potential to set the scale. On typically uses a value $r_0 < 0.5\,\text{fm}$.

For a more detailed introduction and references see [6] and [3].

The quantities, that have been calculated in this work, are dimensionless. The derivation of the continuum value from the lattice results does not require a scale. However this section is included for the sake of completeness and for the curious reader.

4.8 Chiral and continuum extrapolation

To obtain results that can be compared to continuum calculations or experiments, a so called continuum extrapolation needs to be performed. For this purpose lattice results for different values of a (i.e. different values of β) are necessary.

Another problem is the huge amount of computer time that is needed to perform simulations at realistic quark masses. To circumvent this, one performs several simulations for higher masses. These are used to fit predictions of chiral perturbation theory, in order to make an extrapolation to the physical or zero mass.

For a more detailed introduction and references see [6].

The calculations in this work were performed for one value of β (i.e. a) and ten quark masses, permitting no continuum, but a chiral extrapolation.

5 Deriving Hadron Properties from Lattice QCD

Among the properties of hadrons, that can be calculated on the lattice, there are four interesting topics, I will introduce within this short overview. What these properties have in common, is that they originate from the formation of bound quark states, which is especially for light quarks a highly non-perturbative process and predestined for lattice QCD calculations.

- Firstly, the mass spectrum: For some years now, the community is able to reproduce the lower end of the hadronic spectrum within a tolerance of a few percent.
- Secondly, the decay constants: More precisely, semi-leptonic decays of mesons. The decay constant contains the unknown part of the decay matrix element. Its value is determined by the particular structure of the particle state (i.e. there is so far no analytical way to derive it). For example the weak pion decay constant is given by:[8]

$$\langle 0|\bar{u}\gamma_\mu\gamma_5 d|\pi^+(\vec{p})\rangle = f_\pi p_\mu \tag{5.1}$$

- Thirdly, form factors: The matrix element of the elastic scattering of a hadron and a neutrino or an electron, including the exchange of one gauge boson, is known except for the unknown hadron vertices. They are forward matrix elements of local operators like $\bar{q}(x)\Gamma q(x)$ with some Clifford algebra generator Γ. Again, their value is not analytically accessible. Instead, we express its value in terms of *form factors*, that contain the missing information, i.e. the remaining freedoms taking into account the Lorentz structure of the matrix element. For example, the *electric form factor* occurring in electron-proton scattering:

$$\langle p(\vec{p}_f)|J_\mu(\vec{q})|p(\vec{p}_i)\rangle = \bar{u}_p(\vec{p}_f)\left[\gamma_\mu F_1(q^2) + i\sigma_{\mu\nu}\frac{q_\nu}{2m_p}F_2(q^2)\right]u_p(\vec{p}_i) \tag{5.2}$$

  J_μ is the quark electric current:

$$J_\mu(\vec{q}) = \sum_f Q_f\bar{\psi}\gamma_\mu\psi = \frac{2}{3}\bar{u}\gamma_\mu u - \frac{1}{3}\bar{d}\gamma_\mu d + \dots \tag{5.3}$$

  Or the axial form factors, that occur in neutrino-neutron scattering:

$$\langle p(\vec{p}_f)|\bar{u}\gamma_\mu(1-\gamma_5)d|n(\vec{p}_i)\rangle = \bar{u}_p(\vec{p}_f)\left[\gamma_\mu\gamma_5 g_A(q^2) + \gamma_5\frac{q_\nu}{2m_n}h_A(q^2)\right]u_n(\vec{p}_i) \tag{5.4}$$

  For zero momentum transfer $q^2 = 0$, these quantities are also called charges. The vector charge $g_V = F(0)$, and the axial charge $g_A = g_A(0)$. Current conservation of J_μ leads to

$$g_V = 1 \tag{5.5}$$

[8] We use the flavour component notation of eq. (2.15)

end experiments give [18]:

$$\frac{g_A}{g_V} = 1.2694(28) \tag{5.6}$$

- Fourthly, structure functions: More information about the inner structure of the nucleon can be obtained in *deep inelastic scattering* (DIS) of electrons and protons. The cross section, can be decomposed into the leptonic scattering tensor $L_{\mu\nu}$, which is easily derived by Feynman rules and the hadronic scattering tensor $W^{\mu\nu}$ [19]:

$$W_{\mu\nu} = \frac{1}{4}\int \mathrm{d}^4x e^{-iq\cdot x}\langle p(\vec{p})|\left[J_\mu(x), J_\nu(0)\right]|p(\vec{p})\rangle \tag{5.7}$$

$$\equiv W_S^{\mu\nu} + iW_A^{\mu\nu} \tag{5.8}$$

Eq. (5.8) is the decomposition in symmetric and anti-symmetric parts. For the same reason stated above, this tensor cannot be derived analytically. *Structure functions* are the Lorentz invariant freedoms of a general Lorentz decomposition of these tensors. As the symmetric tensor determines the unpolarized contribution to the cross section, the occurring structure functions are called the *unpolarized structure functions* F_1 and F_2:

$$W_S^{\mu\nu} = \left(-g^{\mu\nu} + \frac{q^\mu q^\nu}{q^2}\right)F_1(x,Q^2) + \left(\frac{p^\mu}{p\cdot q} - \frac{q^\mu}{q^2}\right)\left(\frac{p^\nu}{p\cdot q} - \frac{q^\nu}{q^2}\right)F_2(x,Q^2) \tag{5.9}$$

In an analogous manner anti-symmetric contains the *polarized structure functions* g_1 and g_2:

$$W_A^{\mu\nu} = \frac{e^{\mu\nu\rho\sigma}q_\rho}{p\cdot q}\left(s_\sigma g_1(x,Q^2) + \left(s_\sigma - \frac{s\cdot q}{p\cdot q}p_\sigma\right)g_2(x,Q^2)\right) \tag{5.10}$$

Another highly inelastic processes is the *Drell-Yan* process. The collision of a transversely polarized proton with an anti-proton, leading to an annihilation of a quark with an anti-quark and subsequent creation of an e^+e^- pair, reveals another aspect of the inner structure of the nucleon, which is described by the transversity structure function $h_1(x,Q^2)$.

In contrast to masses, decay constants and form factors, structure functions are not directly calculated on the lattice. Instead, the *operator product expansion* is employed. It is an expansion of the non-local operator product $J^\mu(x)J^\nu(0)$ in terms of quasi local operators: [9]

$$\mathcal{O}^{\mu_1\cdots\mu_n}_{\Gamma,q} = i^{n-1}\bar{q}\Gamma^{\mu_1\ldots\mu_i}\overleftrightarrow{\mathrm{D}}^{\mu_i}\cdots\overleftrightarrow{\mathrm{D}}^{\mu_n}q \tag{5.11}$$

[9] $\overleftrightarrow{\mathrm{D}}^\mu = \frac{1}{2}\left(\overrightarrow{\mathrm{D}}^\mu - \overleftarrow{\mathrm{D}}^\mu\right)$

If this expansion is inserted into eq. (5.7), we obtain relations between moments of structure functions and nucleon forward matrix elements of local operators, that can be calculated on the lattice [20]:[10]

$$\left\langle N_{\vec{p}} \left| \mathcal{O}_{\gamma q}^{\{\mu_1 \cdots \mu_n\}} \right| N_{\vec{p}} \right\rangle = 2 v_n^{(q)} \left[p^{\mu_1} \dots p^{\mu_n} - \text{tr} \right] \tag{5.12}$$

$$\left\langle N_{\vec{s},\vec{p}} \left| \mathcal{O}_{\gamma\gamma_5 q}^{\{\mu_1 \cdots \mu_n\}} \right| N_{\vec{s},\vec{p}} \right\rangle = a_n^{(q)} \left[s^{\{\mu_1} p^{\mu_2} \dots p^{\mu_n\}} - \text{tr} \right] \tag{5.13}$$

$$\left\langle N_{\vec{s},\vec{p}} \left| \mathcal{O}_{\sigma q}^{\mu_1 \{\mu_2 \cdots \mu_n\}} \right| N_{\vec{s},\vec{p}} \right\rangle = \frac{t_n^{(q)}}{m_N} \left[\left(s^{\mu_1} p^{\{\mu_2} - p^{\mu_1} s^{\{\mu_2} \right) p^{\mu_3} \dots p^{\mu_n\}} - \text{tr} \right] \tag{5.14}$$

Using the parton model interpretation of structure functions, the moments can be expressed in terms of quark distribution functions:[11]

$$v_n^{(q)}(\mu) = \int_0^1 \mathrm{d}x x^{n-1} [q(x,\mu) + (-1)^n \bar{q}(x,\mu)] \tag{5.15}$$

$$a_n^{(q)}(\mu) = 2 \int_0^1 \mathrm{d}x x^{n} [\Delta q(x,\mu) + (-1)^n \Delta \bar{q}(x,\mu)] \tag{5.16}$$

$$t_n^{(q)}(\mu) = 2 \int_0^1 \mathrm{d}x x^{n-1} [\delta q(x,\mu) - (-1)^{n-1} \delta \bar{q}(x,\mu)] \tag{5.17}$$

5.1 Choosing a Baryon Operator and Deriving its Overlap

As already pointed out in section 4.1, it is possible to derive properties of hadron states without knowing the corresponding wave function. It is sufficient to create a state, that generally will be a superposition of energy states and whose lowest contribution is the desired hadron state. Of course, the larger the overlap with the desired particle, the better will be its isolation during the lattice calculations.

As the aim of this work was to calculate g_A for the lightest negative parity baryon states, the following *baryon operator* has been used:

$$\hat{B}_\alpha(t,\vec{p}) = \sum_{\vec{x}} e^{-i\vec{p}\vec{x}} \epsilon^{abc} \hat{u}_\alpha^a(\vec{x},t) \left[\hat{u}^b(\vec{x},t)^T C \gamma_5 \hat{d}^c(\vec{x},t) \right] \tag{5.18}$$

$$\hat{\bar{B}}_\alpha(t,\vec{p}) \equiv \hat{B}_\alpha(t,\vec{p})^\dagger \gamma_0 = \sum_{\vec{x}} e^{i\vec{p}\vec{x}} \epsilon^{abc} \hat{\bar{u}}_\alpha^a(\vec{x},t) \left[\hat{\bar{d}}^b(\vec{x},t) \gamma_5 C^{-1} \hat{\bar{u}}^c(\vec{x},t)^T \right] \tag{5.19}$$

where $C = \gamma_4\gamma_2$ is the charge conjugation matrix, that is defined via

$$\begin{aligned} &C\gamma_\mu C^{-1} = -\gamma_\mu^T, \text{ and has the properties} \\ &- C = C^\dagger = C^T = C^{-1} \end{aligned} \tag{5.20}$$

[10] The braces around Lorentz indices state that the expression has to be symmetrised with respect to the Lorentz indices.

[11] Quark distribution functions $q_\sigma(x)$ give the probability to find a quark in the nucleon that carries the momentum fraction x of the nucleon in the infinite momentum frame: $\vec{p}_{\text{quark}} = x\,\vec{p}_{\text{nucleon}}$. σ refers to the relative spin of quark and nucleon. $\sigma = \uparrow / \downarrow$ denotes a parallel or anti-parallel relative orientation for longitudinal nucleon polarization and $\sigma = \perp / \top$ the same for transversal polarization. On top of these, one defines the following combinations: $q(x) \equiv q_\uparrow(x) + q_\downarrow(x)$, $\Delta q(x) \equiv q_\uparrow(x) - q_\downarrow(x)$ and $\delta q(x) \equiv q_\perp(x) - q_\top(x)$

This operator creates a state with three valence quarks uud forming a colour singlet and transforms like a spin-1/2 particle. These properties ensure that an overlap with the desired state is in principle permitted.

The operator still has one open index α, which actually gives four operators. They are constructed such that they transform like the components of a Dirac spinor:

- Charge conjugation:

$$\hat{\mathcal{C}}\hat{q}(x)\hat{\mathcal{C}}^\dagger = C\hat{\bar{q}}(x)^T \rightarrow \hat{\mathcal{C}}\hat{B}(\vec{p})\hat{\mathcal{C}}^\dagger = C\hat{\bar{B}}(-\vec{p})^T \tag{5.21}$$

- Parity transformation:

$$\hat{\mathcal{P}}\hat{q}(\vec{x})\hat{\mathcal{P}}^\dagger = \gamma_0\hat{q}(-\vec{x}) \rightarrow \hat{\mathcal{P}}\hat{B}(\vec{p})\hat{\mathcal{P}}^\dagger = \gamma_0\hat{B}(-\vec{p}) \tag{5.22}$$

- Spatial rotation ($\boldsymbol{R} = \exp(\boldsymbol{\omega}), S = \exp(-\frac{i}{4}\sigma_{ij}\omega_{ij})$):

$$\hat{\mathcal{R}}\hat{q}(\vec{x}\,)\hat{\mathcal{R}}^\dagger = S\hat{q}(\boldsymbol{R}\vec{x}) \rightarrow \hat{\mathcal{R}}\hat{B}(\vec{p})\hat{\mathcal{R}}^\dagger = S\hat{B}(\boldsymbol{R}\vec{p}) \tag{5.23}$$

The last two relations can be checked quite easily, because the expression $\hat{B}(t, \vec{p}\,)$ within square brackets is invariant under Lorentz transformations and as the sum extends over all spatial lattice sites, the summation variable can be renamed. The Lorentz invariance of the square bracket can be seen by application of the definition of charge conjugation C (eq. 5.20):

$$\gamma_0^T\, C\gamma_5 = C\gamma_5\, \gamma_0 \tag{5.24}$$

$$S^T\, C\gamma_5 = C\gamma_5\, S^\dagger \tag{5.25}$$

The following conclusion can be drawn: By projecting out a certain component of $\hat{B}(\vec{p}\,)$ in the basis of energy-spinors ($u_m(\vec{p}, \vec{s}\,)$ or $v_m(\vec{p}, \vec{s}\,)$), we obtain one operator, that will, when acting on the vacuum, create a state with spin-direction $\vec{s}$ and positive or negative parity. For example the operator

$$\bar{v}(0, \vec{s})\hat{B}(0) \left(= \sum_\alpha \bar{v}_\alpha(0, \vec{s})\hat{B}_\alpha(0) \right) \tag{5.26}$$

produces a state with negative parity and spin $\vec{s}$. This can be seen by applying for example a Fock space parity transformation $\hat{\mathcal{P}}$:

$$\langle 0|\bar{v}(0, \vec{s})\hat{B}(0) \rightarrow \Big(\langle 0|\bar{v}(0, \vec{s})\hat{B}(0)\Big)\,\hat{\mathcal{P}}^\dagger \overset{(5.22)}{=} \langle 0|\bar{v}(0, \vec{s})\gamma_0\hat{B}(0) = -\Big(\langle 0|\bar{v}(0, \vec{s})\hat{B}(0)\Big) \tag{5.27}$$

In the last step one defining property of the negative energy spinor v was used.

This conclusion can be used to derive an expression for the overlap of $\langle 0|\hat{B}(0)$ with a particle ν (mass m, spin $\vec{s}$ and parity η_ν):[12]

$$\langle 0|\hat{B}(0)|\nu,\vec{s}\,\rangle = \cdots = Z_\nu \begin{cases} u(0,\vec{s}) & \text{if } \eta_\nu = 1 \\ v(0,\vec{s}) & \text{if } \eta_\nu = -1 \end{cases} \text{, with } Z_\nu \in \mathbb{C}. \tag{5.29}$$

Lorentz boosts

The behaviour under Lorentz boosts has not been discussed so far, because it is not that trivial, for there is no Lorentz-invariant summation over the time variable in $\hat{B}(t,\vec{p}\,)$. Instead, all field operators act on a plain of equal-time. A boost will rotate this plain, so that at every lattice point in the sum a different time parameter will occur. Field operators transform in the following way:

$$\mathcal{K}q(x)\mathcal{K}^\dagger = S(\vec{v}\,)q(x')\,, \tag{5.30}$$

where $\vec{v}$ is the velocity of the boost, $(\vec{p}\,',E') = L(\vec{p},m)$, $(\vec{x}\,',t') = L(\vec{x},0)$, $L = \exp(w)$ and $S(\vec{v}\,) = \exp(-\frac{i}{4}\sigma_{\mu\nu}\omega^{\mu\nu})$. This is used to derive the transformation behaviour of $\hat{B}(t,\vec{p}\,)$:

$$\hat{\mathcal{K}}\hat{B}(0,\vec{p}\,)\hat{\mathcal{K}}^\dagger = S(\vec{v}\,)\sum_{\vec{x}} e^{-i\vec{p}\vec{x}}\epsilon^{abc}u^a(\vec{x}',t')\left[u^b(\vec{x}',t')^T C\gamma_5 d^c(\vec{x}',t')\right] \tag{5.31}$$

This expression is not of much use, as there is no way to relate it to $\hat{B}(0,\vec{p}\,)$, i.e. no equivalent to eqs. (5.21-5.23). However, within the overlap, all time arguments can be shifted to zero using the time-evolution operator $\mathcal{S}^{t'} = e^{-\mathcal{H}t'}$:

$$\langle 0|\hat{B}(0)|\nu,\vec{s}\,\rangle = \langle 0|\hat{\mathcal{K}}^\dagger\hat{\mathcal{K}}\hat{B}(0)\hat{\mathcal{K}}^\dagger\hat{\mathcal{K}}|\nu,\vec{s}\,\rangle = \langle 0|\hat{\mathcal{K}}\hat{B}(0)\hat{\mathcal{K}}^\dagger|\nu,\vec{s},\vec{p}\,\rangle \tag{5.32}$$

$$= \langle 0|S(\vec{v})\sum_{\vec{x}}\left(e^{\mathcal{H}t'}e^{-i\vec{p}\vec{x}}\epsilon^{abc}\hat{u}^a(\vec{x}',0)\left[\hat{u}^b(\vec{x}',0)^T C\gamma_5\hat{d}^c(\vec{x}',0)\right]e^{-\mathcal{H}t'}\right)|\nu,\vec{s},\vec{p}\,\rangle \tag{5.33}$$

$$= \langle 0|S(\vec{v})\sum_{\vec{x}}\left(e^{-i\vec{p}\vec{x}-E't'}\epsilon^{abc}\hat{u}^a(\vec{x}',0)\left[\hat{u}^b(\vec{x}',0)^T C\gamma_5\hat{d}^c(\vec{x}',0)\right]\right)|\nu,\vec{s},\vec{p}\,\rangle \tag{5.34}$$

In the last step, the vacuum energy was assumed to be zero. Now a Lorentz invariant is used to rewrite the exponent:

$$-i\vec{p}\cdot\vec{x} = -i\vec{p}\cdot\vec{x} + m\cdot(t=0) = ix_\mu p_\mu = -i\vec{x}\,'\cdot\vec{p}\,' + E't' \tag{5.35}$$

[12] The completeness relation for energy-spinors is inserted

$$\sum_s u(0,\vec{s})\bar{u}(0,\vec{s}) - v(0,\vec{s})\bar{v}(0,\vec{s}) = 2m\mathbb{1}_{\text{Dirac}} \tag{5.28}$$

and the fact is used, that states of opposite spin or parity are orthogonal.

And the sum variable $\vec{x}$, which does not appear directly anymore, is changed to $\vec{x}\,'$:

$$\langle 0|\hat{B}(0)|\nu,\vec{s}\,\rangle = \langle 0|\sum_{\vec{x}\,'}\left(e^{-i\vec{p}'\vec{x}'}\epsilon^{abc}\hat{u}^a(\vec{x}',0)\left[\hat{u}^b(\vec{x}',0)^T C\gamma_5\hat{d}^c(\vec{x}',0)\right]\right)|\nu,\vec{s},\vec{p}\,\rangle \tag{5.36}$$

$$= S(\vec{v})\langle 0|\hat{B}(0,\vec{p}\,)|\nu,\vec{s},\vec{p}\,\rangle \tag{5.37}$$

With use of eq. (5.29), one obtains the final expression for the overlap with arbitrary momentum:

$$\langle 0|B(0,\vec{p})|\nu,\vec{p},\vec{s}\,\rangle = Z_\nu \begin{cases} S(-\vec{v})u(0,\vec{s}\,) = u_{m_\nu}(\vec{p},\vec{s}\,) & \text{if } \eta_\nu = 1 \\ S(-\vec{v})v(0,\vec{s}\,) = v_{m_\nu}(\vec{p},\vec{s}\,) & \text{if } \eta_\nu = -1 \end{cases} \tag{5.38}$$

5.2 Quark Smearing

Improving the overlap will enhance the accuracy of the calculation. One way to achieve a larger $|Z_\nu|^2$, is to spatially smear the quarks. This is motivated by the fact, that the nucleon is not point like, but rather an extended object. Its extend can be measured in using the root mean square (rms) radius of the charge density:

$$r = \sqrt{\langle r^2\rangle}. \tag{5.39}$$

The idea is to spatially smear the point like quark operators in the baryon operator (eq. 5.18). The best overlap is expected, if the smeared quarks have the radius of the nucleon. Spatial smearing in general has this form [21, 22]:

$${}^S\psi(\vec{x},t) = \sum_{\vec{y}} H(\vec{x},\vec{y};t)\psi(\vec{y},t) \tag{5.40}$$

$${}^S\bar{\psi}(\vec{x},t) = \sum_{\vec{y}} \psi(\vec{y},t)H(\vec{y},\vec{x};t) \tag{5.41}$$

The superscript S stands for smearing. L will be used for local operators (${}^L\psi = \psi$). The smearing operator H should be diagonal in Dirac space, to not mess up the spinor structure of the baryon operator, and of course Hermitian. It also should be gauge covariant. In this work, Jacobi smearing is used. It is defined by

$$H = (\mathbb{1} - \kappa_S D)^{-1}\,, \tag{5.42}$$

where D is defined as

$$D(\vec{x},\vec{y},t) = \mathbb{1}_{\text{Dirac}}\sum_i^3 (\mathrm{U}_i(\,\vec{x},t)\delta_{\vec{x}+\vec{i},\vec{y}} + \mathrm{U}_{-i}(\vec{x},t)\delta_{\vec{x}-\vec{i},\vec{y}}) \tag{5.43}$$

The actual operator that is used in the calculations, H^*, is defined as the N_s-th Jacobi iteration of the solution to eq. (5.42).

$$H^* = H^{(N_s)}, \text{with } H^{(n)} = \mathbb{1} + \kappa_s D H^{(n-1)} \tag{5.44}$$

The rms radius of the smeared quark is

$$r = \sqrt{\frac{\sum_{\vec{x}} \vec{x}^{\,2} |S(\vec{x},0)|^2}{\sum_{\vec{x}} |S(\vec{x},0)|^2}} \tag{5.45}$$

and depends on κ_s and N_s. The requirement of a specific quark radius only fixes one parameter. The other one can be used to regulate the computational effort required by smearing operation. In this work the radius was

$$r = 0.354\,\mathrm{fm} = 2.39a \tag{5.46}$$

and the smearing parameters were

$$\begin{aligned} \kappa_s &= 0.21 \\ N_s &= 18 \end{aligned} \tag{5.47}$$

which represented a good trade-off between coarseness ($\sim \kappa_S$) and computation time ($\sim N_S$).

At this point, the smeared propagators are introduced in analogy to eq. (4.64):

$$^{SS}\mathrm{G}(x,y) \equiv \langle {}^{S}\psi(y)\,{}^{S}\bar{\psi}(x)\rangle_A \tag{5.48}$$

$$^{LS}\mathrm{G}(x,y) \equiv \langle {}^{L}\psi(y)\,{}^{S}\bar{\psi}(x)\rangle_A \tag{5.49}$$

$$^{SL}\mathrm{G}(x,y) \equiv \langle {}^{S}\psi(y)\,{}^{L}\bar{\psi}(x)\rangle_A \tag{5.50}$$

$$^{LL}\mathrm{G}(x,y) \equiv G(x,y) \tag{5.51}$$

5.3 Correlators and Matrix Elements

Without the knowledge of the nucleon wave function, a direct lattice evaluation of nucleon matrix elements is not possible. Instead, one calculates the so called *two- and three-point correlation functions*. In this section, the transfer matrix formalism is used to understand what is actually measured by these calculations and how to obtain the nucleon matrix elements from them.

5.3.1 Two-point Correlation Function

The baryon two-point correlator is the amplitude of the following process: A baryon[13] is created at time $t_1 = 0$ (source time) and propagates to time $t_2 = t$ (sink time), where it gets destroyed. The baryon is created by the operator

$$\hat{\bar{B}}(0,\vec{p}\,)w \tag{5.52}$$

where w is some Dirac spinor, that will determine the parity and spin properties of the state, as worked out in section 5.1, especially at eq. (5.26). The amplitude has this form:

$$\langle \bar{w}\hat{B}(t,\vec{p}\,)\;\hat{\bar{B}}(0,\vec{p}\,)w\rangle = \mathrm{tr}\Big\{\Gamma\langle \hat{B}(t,\vec{p}\,)\hat{\bar{B}}(0,\vec{p}\,)\rangle\Big\} \equiv C_\Gamma(\vec{p},t) \tag{5.53}$$

[13] More correct, it is a linear combination of all hadron states with the same quantum numbers, with unknown coefficients.

with $\Gamma = w\bar{w}$.

Following eq. (4.29) the correlator takes the form:

$$C_\Gamma(t,\vec{p}) = \mathcal{Z}^{-1}\mathrm{tr}\Big[\Gamma e^{-\mathcal{H}(L_t-t)}\hat{B}(0,\vec{p})e^{-\mathcal{H}t}\hat{\bar{B}}(0,\vec{p})\Big] \tag{5.54}$$

This can be further evaluated by insertion of energy state identities

$$\mathbb{1} = \sum_\nu |\nu\rangle\langle\nu| \quad \text{with} \quad \mathcal{H}|\nu\rangle = E_\nu|\nu\rangle \quad \text{and} \quad \langle\nu|\eta\rangle = \delta_{\nu\eta}, \tag{5.55}$$

where lattice normalization has been used. Further:

$$\begin{aligned} C_\Gamma(t,\vec{p}) &= \mathcal{Z}^{-1}\sum_{E_1,\dots,E_4}\mathrm{tr}\Big[\Gamma\langle E_1|e^{-\mathcal{H}(L_t-t)}|E_2\rangle\langle E_2|\hat{B}(\vec{p})|E_3\rangle\langle E_3|e^{-\mathcal{H}t}|E_4\rangle\langle E_4|\hat{\bar{B}}(\vec{p})|E_1\rangle\Big] \\ &= \mathcal{Z}^{-1}\sum_{E_1,E_4} e^{-(L_t-t)E_1}e^{-tE_4}\langle E_4|\hat{\bar{B}}(\vec{p})|E_1\rangle\Gamma\langle E_1|\hat{B}(\vec{p})|E_4\rangle \end{aligned} \tag{5.56}$$

Now the sum is expanded to be further simplified:

$$\begin{aligned} \mathcal{Z}C_\Gamma(t,\vec{p}) &= \langle 0|\hat{\bar{B}}(\vec{p})|0\rangle\Gamma\langle 0|\hat{B}(\vec{p})|0\rangle \\ &\quad + \sum_E e^{-tE}\langle E|\hat{\bar{B}}(\vec{p})|0\rangle\Gamma\langle 0|\hat{B}(\vec{p})|E\rangle \\ &\quad + \sum_E e^{-(L_t-t)E}\langle 0|\hat{\bar{B}}(\vec{p})|E\rangle\Gamma\langle E|\hat{B}(\vec{p})|0\rangle \\ &\quad + \sum_{\substack{E_1\neq 0\\ E_2\neq 0}} e^{-(L_t-t)E_1}e^{-tE_2}\langle E_2|\hat{\bar{B}}(\vec{p})|E_1\rangle\Gamma\langle E_1|\hat{B}(\vec{p})|E_2\rangle \end{aligned} \tag{5.57}$$

If t is far away from 0 and L_t

$$0 \ll t \ll L_t, \tag{5.58}$$

the forth term is exponentially suppressed relative to the second and third term. The first term is identically zero.

The sum over all energy states is a sum over all mass states, momenta and spin orientations. The sum over momenta is easily reduced, because the operator produces a state with definite momentum $\vec{p}$. The sum over mass states can be interpreted as the sum over every particle and its anti-particle. So it is possible to write the correlator as a sum over particle states ν with spin projection $\sigma = \pm$:[14]

$$\begin{aligned} C_\Gamma(t,\vec{p}) = \mathcal{Z}^{-1}\sum_{\nu,\sigma} & e^{-tE_\nu}\langle\nu,\sigma,\vec{p}|\hat{\bar{B}}(\vec{p})|0\rangle\Gamma\langle 0|\hat{B}(\vec{p})|\nu,\sigma,\vec{p}\rangle + \\ & e^{-(L_t-t)E_{\bar{\nu}}}\langle 0|\hat{\bar{B}}(\vec{p})|\bar{\nu},\sigma,-\vec{p}\rangle\Gamma\langle\bar{\nu},\sigma,-\vec{p}|\hat{B}(\vec{p})|0\rangle \end{aligned} \tag{5.59}$$

[14] In the rest frame: $\vec{s} = \sigma\vec{n}$ and $\vec{n}/m$ is the quantization axis that is considered fixed throughout this work.

This equation actually shows the consequence of a finite-size periodic spacetime: The contributions of anti-particles is not suppressed. The operator B creates an anti-particle. Although this happens at time t, it can nevertheless arrive at an earlier time 0 by using the periodicity of the lattice and travelling once around the whole lattice in temporal direction. In the limit of infinite spacetime, these contribution will however vanish, as $\lim_{L_t\to\infty} e^{-L_t E_{\bar{\nu}}} = 0$. (A complementary interpretation: The negative energy quarks, are created at 0 an can although travelling backwards in time arrive at later time t by going once around the lattice.)

With help of the transformation properties of $\hat{B}$, the anti-particle overlap can be transformed into the particle overlap:

$$\begin{aligned}\langle\bar{\nu},-\vec{p},\sigma|\hat{B}(\vec{p})|0\rangle &\overset{(5.21)}{=} C\langle\bar{\nu},-\vec{p},\sigma|\mathcal{C}^\dagger\hat{\bar{B}}(-\vec{p})^T\mathcal{C}|0\rangle = C\langle\nu,-\vec{p},\sigma|\hat{\bar{B}}(-\vec{p})^T|0\rangle \\ &\overset{(5.22)}{=} C\gamma_0^T\langle\nu,-\vec{p},\sigma|\mathcal{P}^\dagger\hat{\bar{B}}(\vec{p})^T\mathcal{P}|0\rangle = \eta_\nu C\gamma_0^T\langle\nu,\vec{p},\sigma|\hat{\bar{B}}(\vec{p})^T|0\rangle\end{aligned} \tag{5.60}$$

η_ν is the parity eigenvalue of the state ν:

$$\mathcal{P}|\nu,\vec{p},\sigma\rangle = \eta_\nu|\nu,-\vec{p},\sigma\rangle, \text{ with } \eta_\nu^2 = 1 \tag{5.61}$$

Analogously:

$$\langle 0|\hat{\bar{B}}(\vec{p})|\bar{\nu},-\vec{p},\sigma\rangle = \eta_\nu\langle 0|\hat{B}(\vec{p})^T|\nu,\vec{p},\sigma\rangle\gamma_0^T C \tag{5.62}$$

And finally one finds:

$$\begin{aligned}\langle 0|\hat{\bar{B}}(\vec{p})|\bar{\nu},-\vec{p},\sigma\rangle\Gamma\langle\bar{\nu},-\vec{p},\sigma|\hat{B}(\vec{p})|0\rangle &= \eta_\nu^2\langle 0|\hat{B}(\vec{p})^T|\nu,\vec{p},\sigma\rangle\gamma_0^T C\,\Gamma C\gamma_0^T\langle\nu,\vec{p},\sigma|\hat{\bar{B}}(\vec{p})^T|0\rangle \\ &= \langle\nu,\vec{p},\sigma|\hat{\bar{B}}(\vec{p})|0\rangle\gamma_0 C\,\Gamma^T C\gamma_0\langle 0|\hat{B}(\vec{p})|\nu,\vec{p},\sigma\rangle\end{aligned} \tag{5.63}$$

Using this result, the expression for the overlap (eq. 5.38), the normalization of energy spinors (eq. 2.38) and after performing the spin sum, we can write

$$C_\Gamma(t,\vec{p}) = \mathcal{Z}^{-1}\sum_\nu |Z_\nu|^2\ \mathrm{tr}\left\{\frac{-i\not{p}+\eta_\nu m}{2m_\nu}\left(\Gamma\, e^{-tE_\nu} + \tilde{\Gamma}\, e^{-(L_t-t)E_{\bar{\nu}}}\right)\right\} \tag{5.64}$$

where a tilde notation has been introduced:

$$\tilde{\Gamma} \equiv \gamma_0 C\,\Gamma^T C\gamma_0 \tag{5.65}$$

One useful example is

$$\tilde{P_a} = \gamma_0 C\,P_a C\gamma_0 \overset{(5.20)}{=} -P_{-a} \tag{5.66}$$

Now consider the case $\vec{p} = 0$:

$$\frac{-i\not{p}+\eta_\nu m}{2m} = \eta_\nu P_{\eta_\nu} \tag{5.67}$$

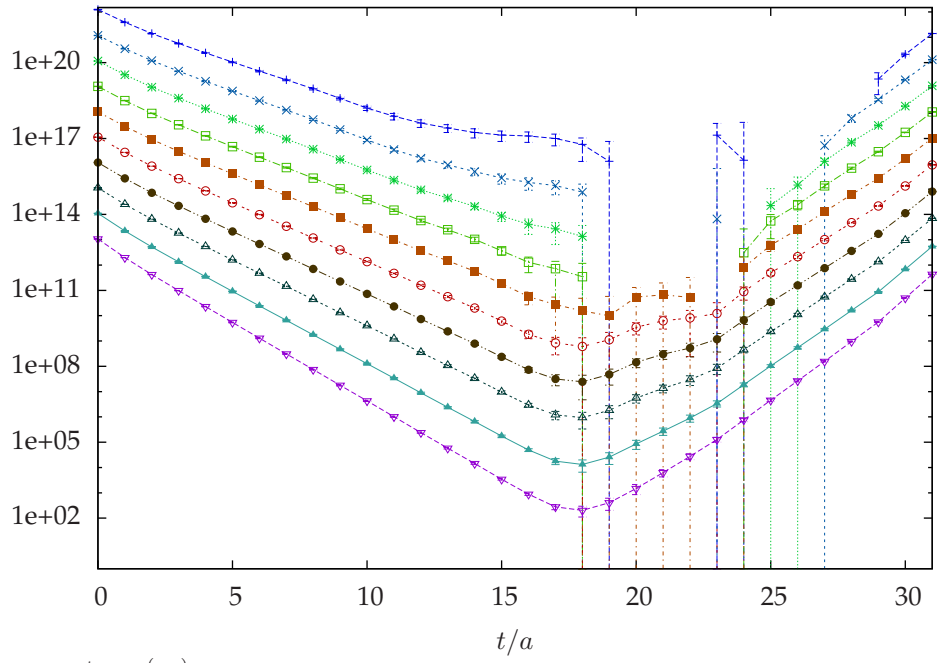

Fig. 1: $10^i \times C_{P_+}^{(m_i)}(t,0)$. The positive parity correlators for ten different quark masses m_i, scaled with a factor 10^i. If points are missing, the calculated value was negative, which is possible within statistical errors.

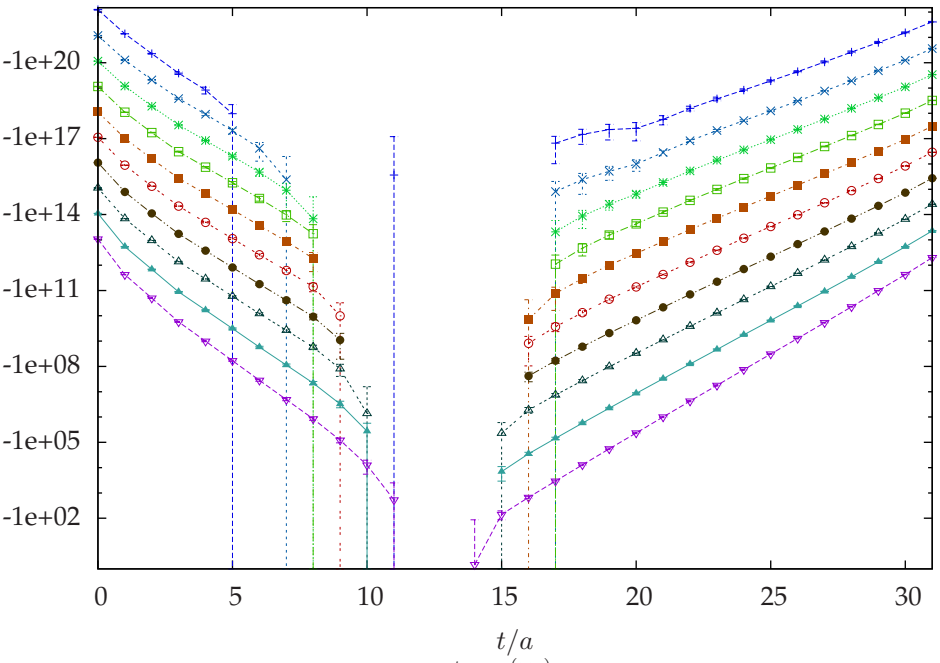

Fig. 2: $10^i \times C_{P_-}^{(m_i)}(t,0)$

If $\Gamma = P_a$ (the parity projector with parity a), the correlator becomes:[15]

$$C_{P_a}(t,0) = \mathcal{Z}^{-1} \sum_\nu \eta_\nu |Z_\nu|^2 \ \mathrm{tr}\Big\{ P_{\eta_\nu} \left(P_a \, e^{-tE_\nu} - P_{-a} \, e^{-(L_t - t)E_\nu} \right) \Big\} \tag{5.68}$$

$$= \mathcal{Z}^{-1} \sum_\nu 2a |Z_\nu|^2 \ \left(\delta_{\eta_\nu, a} \, e^{-tE_\nu} + \delta_{\eta_\nu, -a} \, e^{-(L_t - t)E_\nu} \right) \tag{5.69}$$

For $0 \ll t \ll L_t$,, the terms are dominated by the lowest energy contributions and all higher contributions are exponentially suppressed. The lowest state with positive parity is the nucleon n and the lowest states with negative parity are the two resonances $N^*(1535)$ and $N^*(1650)$:

$$C_{P_+}(t,0) = 2\mathcal{Z}^{-1} \left(|Z_n|^2 e^{-tE_n} + \sum_{N^*} |Z_{N^*}|^2 e^{-(L_t - t)E_{N^*}} \right) \tag{5.70}$$

$$C_{P_-}(t,0) = -2\mathcal{Z}^{-1} \left(|Z_n|^2 e^{-(L_t - t)E_n} + \sum_{N^*} |Z_{N^*}|^2 e^{-tE_{N^*}} \right) \tag{5.71}$$

$$= -C_{P_+}(L_t - t, 0) \tag{5.72}$$

The two-point correlators can be used to derive the mass of the lowest energy state. The mass m equals the absolute value of the derivative of the logarithm of the correlator:

$$m = \left| \frac{d \ln C(t)}{dt} \right| \tag{5.73}$$

Figure 1 and 2 show the results of lattice calculations for these correlators. The expected t dependence can be observed.

In figure 1 (2), the slope for $t < 15$ ($t > 17$) can be used to determine the mass of the nucleon and the slope for $t > 20$ ($t < 12$) for the mass of the lightest particle with negative parity (or of a linear combination of the two lightest).

5.3.2 Three-point Correlation Function

The three-point function describes another process: A baryon is created at $t_1 = 0$ (source time), propagates to time $t_2 = \tau$ (insertion time), where the operator $\hat{\mathcal{O}}$ is inserted and then gets destroyed at $t_3 = t$ (sink time). In this work $\hat{\mathcal{O}}$ is chosen to have zero momentum.

The corresponding expression is:

$$\left\langle \mathrm{T}\Big\{ \bar{w} \hat{B}(t, \vec{p}\,) \hat{\mathcal{O}}(\tau) \hat{\bar{B}}(0, \vec{p}\,) w \Big\} \right\rangle = \mathrm{tr}\Big\{ \Gamma \left\langle \mathrm{T}\Big\{ \hat{B}(t, \vec{p}\,) \hat{\mathcal{O}}(\tau) \hat{\bar{B}}(0, \vec{p}\,) \Big\} \right\rangle \Big\} \equiv C_\Gamma^{\hat{\mathcal{O}}}(\vec{p}, t, \tau) \tag{5.74}$$

T is the time ordered product. It commutes the contained operators until they are ordered by their time arguments, with the earliest time operator being the first on

[15] The second step used: $P_a P_b = \delta_{ab} P_a$ and $\mathrm{tr}\{P\} = 2$

the right. For every commutation of fermion fields a minus sign is included, which ensures that for space-like distances after a relative time sign-changing Lorentz-transformation the time-ordering operator has the same effect as regular anti-commutation which is allowed for space-like separations (cp. eq. 4.31).

Time ordering means that one has to differentiate between two cases described, before applying the transfer matrix formalism:

- $\tau < t$: Using eq. (4.29) one can write:

$$C_\Gamma^{\hat{\mathcal{O}}}(\vec{p},t,\tau) = \mathcal{Z}^{-1}\mathrm{tr}\Big[\Gamma e^{-\mathcal{H}(L_t-t)}\hat{B}(0,\vec{p})e^{-\mathcal{H}(t-\tau)}\hat{\mathcal{O}}e^{-\mathcal{H}\tau}\hat{\bar{B}}(0,\vec{p})\Big] \tag{5.75}$$

Again energy state identities are inserted:

$$\begin{aligned} C_\Gamma^{\hat{\mathcal{O}}}(\vec{p},t,\tau) = \mathcal{Z}^{-1}\sum_{E_1,E_2,E_3}\mathrm{tr}\Big[\Gamma\times \\ e^{-(L_t-t)E_1}\langle E_1|\hat{B}|E_2\rangle e^{-(t-\tau)E_2}\langle E_2|\hat{\mathcal{O}}|E_3\rangle e^{-\tau E_3}\langle E_3|\hat{\bar{B}}|E_1\rangle\Big] \end{aligned} \tag{5.76}$$

It is sufficient to examine this expression for fixed t and concentrate on its τ dependence. To isolate the ground state contributions and exclude the anti-particles travelling around the lattice, t is fixed within

$$0 \ll t \ll L_t/2 \tag{5.77}$$

Due to the first exponential function only the contribution with energy $E_1 = 0$ will survive and the remaining sum can be rewritten:

$$\begin{aligned} C_\Gamma^{\hat{\mathcal{O}}}(\vec{p},t,\tau) = \mathcal{Z}^{-1}\sum_{E_2}e^{-tE_2}\Big[&\langle E_2|\hat{\bar{B}}|0\rangle\Gamma\langle 0|\hat{B}|E_2\rangle\langle E_2|\hat{\mathcal{O}}|E_2\rangle \\ &+\sum_{E_3>E_2}\Big(\langle E_3|\hat{\bar{B}}|0\rangle\Gamma\langle 0|\hat{B}|E_2\rangle\langle E_2|\hat{\mathcal{O}}|E_3\rangle e^{-\tau\Delta E} \\ &\quad+\langle E_2|\hat{\bar{B}}|0\rangle\Gamma\langle 0|\hat{B}|E_3\rangle\langle E_3|\hat{\mathcal{O}}|E_2\rangle e^{-(t-\tau)\Delta E}\Big)\Big] \end{aligned} \tag{5.78}$$

With $\Delta E = E_3 - E_2$. The value of t, restricted by eq. (5.77), will lead to a suppression of high energies E_2. As the surviving contribution to this sum still depends on the choice of Γ, the general sum will be kept until Γ is further specified. Eq. (5.78) now clearly reveals the τ dependence of the three-point correlator. For

$$0 \ll \tau \ll t, \tag{5.79}$$

i.e. the region where the exponential functions are both strongly damped, a plateau is expected, with the following value:

$$C_\Gamma^{\hat{\mathcal{O}}}(\vec{p},t)_{\text{plat}} = \mathcal{Z}^{-1}\sum_{\nu,\sigma}e^{-tE_\nu}|Z_\nu|^2\mathrm{tr}\Big\{\frac{-i\not{p}+\eta_\nu m_\nu}{2m_\nu}P(\sigma\vec{n}\,)\Gamma\Big\}\langle\nu,\vec{p},\sigma|\hat{\mathcal{O}}|\nu,\vec{p},\sigma\rangle$$

(5.80)

The sum extends over all particles ν with momentum $\vec{p}$, parity η_ν and spin orientation σ (see footnote 14 and page 33). Other momenta, or anti-particles have zero overlap and thus are excluded. The overlap definitions (eq. 5.38) and spinor normalization (eq. 2.38) also have been used.

To obtain polarized (cp. footnote 17) matrix elements of negative parity particles, Γ is chosen to be the negative parity and the anti-symmetric combination of spin projectors:

$$\Gamma = P_- \left(P(\sigma\vec{n}\,) - P(-\sigma\vec{n}\,)\right) = \frac{1-\gamma_4}{2} i\gamma_5 \not{n}/m \tag{5.81}$$

For $\vec{p} = 0$ this gives (using eq 5.67):

$$C^{\hat{\mathcal{O}}}_{-,\text{pol}}(0,t)_{\text{plat}} = \mathcal{Z}^{-1} \sum_{\nu,\sigma} e^{-tE_\nu} |Z_\nu|^2 \eta_\nu \text{tr}\{P_{\eta_\nu} P(\sigma\vec{n}) P_- i\gamma_5 \not{n}/m\} \langle \nu,\sigma|\hat{\mathcal{O}}|\nu,\sigma\rangle \tag{5.82}$$

With the general properties of projectors[16] and gamma matrices the trace is found to be:

$$\text{tr}\{P_{\eta_\nu} P(\sigma\vec{n}) P_- i\gamma_5 \not{n}/m\} = \sigma\delta_{\eta_\nu,-1} \tag{5.83}$$

This eliminated all positive parity states from the sum and the exponential function with time $0 \ll t$ isolates the two lowest negative parity states $N^*(1535)$ and $N^*(1650)$, yielding:[17]

$$C^{\hat{\mathcal{O}}}_{-,\text{pol}}(0,t)_{\text{plat}} = -\mathcal{Z}^{-1} \sum_{N^*} e^{-tE_{N^*}} \, |Z_{N^*}|^2 \langle N^*|\hat{\mathcal{O}}|N^*\rangle_{\text{pol}} \tag{5.84}$$

- $\tau > t$:

$$C^{\hat{\mathcal{O}}}_\Gamma(\vec{p},t',\tau) = \mathcal{Z}^{-1}\text{tr}\Big[\Gamma e^{-\mathcal{H}(L_t-\tau)} \hat{\mathcal{O}} e^{-\mathcal{H}(\tau-t')} \hat{B}(0,\vec{p}) e^{-\mathcal{H}t'} \hat{\bar{B}}(0,\vec{p})\Big] \tag{5.85}$$

In this case, the particle and anti-particle roles are interchanged. If still the same process is to be measured, but this time using the anti-particle contributions, the time t' has to be fixed to the value $L_t - t$, where t denotes the time for the first case. This means

$$L_t/2 \ll t' \ll L_t \tag{5.86}$$

and the third exponential function will suppress all states other than vacuum,

[16] $P_a P_b = \delta_{ab} P_a$

[17] The polarized matrix element is defined as $\langle N^*|\hat{\mathcal{O}}|N^*\rangle_{\text{pol}} = \langle N^*,\sigma|\hat{\mathcal{O}}|N^*,\sigma\rangle - \langle N^*,-\sigma|\hat{\mathcal{O}}|N^*,-\sigma\rangle$

yielding an expression analogously to eq. (5.78):

$$C_{\Gamma}^{\hat{\mathcal{O}}}(\vec{p}, t' = L_t - t, \tau) = \mathcal{Z}^{-1} \sum_{E_2} e^{-tE_2} \Big[\langle 0|\hat{\bar{B}}|E_2\rangle \Gamma \langle E_2|\hat{B}|0\rangle \langle E_2|\hat{\mathcal{O}}|E_2\rangle + \sum_{E_1 > E_2} \Big(\langle 0|\hat{\bar{B}}|E_1\rangle \Gamma \langle E_2|\hat{B}|0\rangle \langle E_1|\hat{\mathcal{O}}|E_2\rangle e^{-(L_t-\tau)\Delta E} + \langle 0|\hat{\bar{B}}|E_2\rangle \Gamma \langle E_1|\hat{B}|0\rangle \langle E_2|\hat{\mathcal{O}}|E_1\rangle e^{-(\tau-t')\Delta E} \Big) \Big] \tag{5.87}$$

$\Delta E = E_1 - E_2$. For

$$t' \ll \tau \ll L_t \tag{5.88}$$

again a plateau is expected. Using the anti-particle overlap relation (eq. 5.63) with the sum carried out as far as possible, its value is

$$C_{\Gamma}^{\hat{\mathcal{O}}}(\vec{p}, L_t - t)_{\text{plat}} = \mathcal{Z}^{-1} \sum_{\nu,\sigma} e^{-tE_\nu} |Z_\nu|^2 \text{tr}\left\{ \frac{-i\not{p} + \eta_\nu m_\nu}{m_\nu} P(\sigma\vec{n}) \tilde{\Gamma} \right\} \times \langle \bar{\nu}, \vec{p}, \sigma|\hat{\mathcal{O}}|\bar{\nu}, \vec{p}, \sigma\rangle \tag{5.89}$$

To extract the polarized matrix elements of the lightest negative parity particles, in this case the positive parity projector has to be chosen, for is contains only anti-particle contributions, which have the opposite parity:

$$\Gamma = P_+ \left(P(\sigma\vec{n}) - P(-\sigma\vec{n})\right) = \frac{1+\gamma_4}{2} i\gamma_5 \not{n}/m \tag{5.90}$$

For $\vec{p} = 0$ the following applies:

$$\tilde{\Gamma} = P_- i\gamma_5 \not{n}/m \tag{5.91}$$

$$\frac{-i\not{p} + \eta_\nu m}{2m} = \eta_\nu P_{\eta_\nu} \tag{5.92}$$

$$\text{tr}\left\{ \frac{-i\not{p} + \eta_\nu m_\nu}{2m} P(\vec{s}) \tilde{\Gamma} \right\} = \eta_\nu \sigma \delta_{\eta_\nu, -1} \tag{5.93}$$

after evaluation of the trace using eq. (5.83), after the spin sum has been performed:

$$C_{+,\text{pol}}^{\hat{\mathcal{O}}}(0, L_t - t)_{\text{plat}} = \mathcal{Z}^{-1} \sum_{N^*} e^{-tE_{N^*}} \ |Z_{N^*}|^2 \langle N^*|\hat{C}\hat{\mathcal{O}}\hat{C}^\dagger|N^*\rangle_{\text{pol}} \tag{5.94}$$

The anti-particle matrix element was transformed into the particle matrix element with the charge conjugation operator $\hat{C}$.

For comparison eq. (5.84) from the case $\tau < t$ read:

$$C_{-,\text{pol}}^{\hat{\mathcal{O}}}(0, t)_{\text{plat}} = -\mathcal{Z}^{-1} \sum_{N^*} e^{-tE_{N^*}} \ |Z_{N^*}|^2 \langle N^*|\hat{\mathcal{O}}|N^*\rangle_{\text{pol}} \tag{5.95}$$

5.4 Calculation of Two- and Three-Point Functions

The last section showed, how to obtain baryon matrix elements from lattice calculations of two- and three-point functions. This section demonstrates in detail the derivation of the corresponding Green's functions in terms of quark propagators, that are needed for eq. (4.71), i.e. the actual lattice calculation.

5.4.1 Two-point Correlation Function

In the case of the two-point correlator, eq. (4.71) takes the following form:

$$C_\Gamma(\vec{p},t) \equiv \mathrm{tr}\Big\{\Gamma\langle\hat{B}(t,\vec{p})\hat{\bar{B}}(0,\vec{p})\rangle\Big\} = \frac{1}{n}\sum_i^n \mathcal{O}_G[A_i]\, C_\Gamma^{\hat{\mathcal{O}}}[A](\vec{p},t,\tau) \tag{5.96}$$

where the two-point correlator on fixed gauge background A was introduced:

$$C_\Gamma[A](\vec{p},t) \equiv \mathrm{tr}\Big\{\Gamma\langle\hat{B}(t,\vec{p})\hat{\bar{B}}(0,\vec{p})\rangle_A\Big\} \tag{5.97}$$

This quantity can be expressed using propagators in the fashion of eq. (4.63). First the definitions of the operators (eq. 5.18) are inserted:

$$\begin{aligned} C_\Gamma^{\hat{\mathcal{O}}}[A](\vec{p},t,\tau) = \mathrm{tr}\Big\{\Gamma \sum_{\vec{x},\vec{y}} e^{-i\vec{p}(\vec{x}-\vec{y})}\epsilon^{abc}\epsilon^{a'b'c'}\times \\ \Big\langle \hat{u}^a(\vec{x},t)\Big[\hat{u}^b(\vec{x},t)^T C\gamma_5 \hat{d}^c(\vec{x},t)\Big]\hat{\bar{u}}^{a'}(\vec{y},0)\Big[\hat{\bar{d}}^{b'}(\vec{y},0)\gamma_5 C^{-1}\hat{\bar{u}}^{c'}(\vec{y},0)^T\Big]\Big\rangle_A\Big\} \end{aligned} \tag{5.98}$$

The translational invariance is broken by the fixed gauge background, but it will be recovered in the full ensemble average. Thus, if the expression is meant to be ensemble averaged, the symmetry can be exploited even at this stage. This can be used to shift all spatial coordinates by $-\vec{y}$:

$$\begin{aligned} &\vec{x} \to \vec{x} - \vec{y} \\ &\vec{y} \to 0 \end{aligned}$$

The summation variable $(\vec{x}-\vec{y})$ of the first sum can be relabeled as it extends over all spatial sites, leaving an expression that does not depend on $\vec{y}$ anymore. The second sum then only yields a factor $N_S = N_1N_2N_3$:

$$\begin{aligned} C_\Gamma^{\hat{\mathcal{O}}}[A](\vec{p},t,\tau) = N_S \sum_{\vec{x}} e^{-i\vec{p}\vec{x}}\epsilon^{abc}\epsilon^{a'b'c'}\Gamma_{\alpha\beta}\times \\ \Big\langle \hat{u}^a_\beta(\vec{x},t)\Big[\hat{u}^b_\mu(\vec{x},t)(C\gamma_5)_{\mu\nu}\hat{d}^c_\nu(\vec{x},t)\Big]\hat{\bar{u}}^{a'}_\alpha(0,0)\Big[\hat{\bar{d}}^{b'}_\kappa(0,0)(\gamma_5 C^{-1})_{\kappa\eta}\hat{\bar{u}}^{c'}_\eta(0,0)\Big]\Big\rangle_A \end{aligned} \tag{5.99}$$

Two contractions contribute to this amplitude:

- Figure 3(a):

$$\begin{aligned} \langle\hat{u}^a_\beta(x)\hat{u}^b_\mu(x)\hat{d}^c_\nu(x)\hat{\bar{u}}^{a'}_\alpha(0)\hat{\bar{d}}^{b'}_\kappa(0)\hat{\bar{u}}^{c'}_\eta(0)\rangle_A = \\ {}_u\mathrm{G}[A]^{aa'}_{\beta\alpha}(x,0)\ {}_u\mathrm{G}[A]^{bc'}_{\mu\eta}(x,0)\ {}_d\mathrm{G}[A]^{cb'}_{\nu\kappa}(x,0) \end{aligned} \tag{5.100}$$

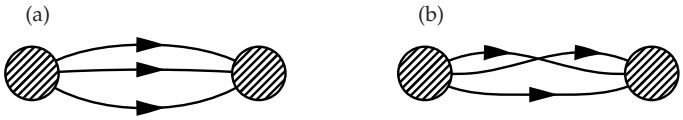

Fig. 3: The two graphs corresponding to the two contractions that contribute to eq. (5.102)

- Figure 3(b):

$$\langle \hat{u}^a_\beta(x)\hat{u}^b_\mu(x)\hat{d}^c_\nu(x)\hat{\bar{u}}^{a'}_\alpha(0)\hat{\bar{d}}^{b'}_\kappa(0)\hat{\bar{u}}^{c'}_\eta(0)\rangle_A = \\ - \ {}_u\mathrm{G}[A]^{ac'}_{\beta\eta}(x,0)\ {}_u\mathrm{G}[A]^{ba'}_{\mu\alpha}(x,0)\ {}_d\mathrm{G}[A]^{cb'}_{\nu\kappa}(x,0) \quad (5.101)$$

The final result is

$$C^{\hat{\mathcal{O}}}_\Gamma[A](\vec{p},t,\tau) = N_S \sum_{\vec{x}} e^{-i\vec{p}\vec{x}}\epsilon^{abc}\epsilon^{a'b'c'} \times \\ \Big(\mathrm{tr}\Big\{\Gamma\ {}^{SS}_{u}\mathrm{G}[A]^{aa'}(x,0)\Big\}\,\mathrm{tr}\Big\{\ {}^{SS}_{d}\tilde{\mathrm{G}}[A]^{bb'}(x,0)\ {}^{SS}_{u}\mathrm{G}[A]^{cc'}(x,0)\Big\} \\ + \mathrm{tr}\Big\{\Gamma\ {}^{SS}_{u}\mathrm{G}[A]^{aa'}(x,0)\ {}^{SS}_{d}\tilde{\mathrm{G}}[A]^{bb'}(x,0)\ {}^{SS}_{u}\mathrm{G}[A]^{cc'}(x,0)\Big\}\Big) \quad (5.102)$$

where some indices have been relabeled and a new tilde notation has been introduced:

$$\tilde{\mathrm{G}} \equiv \gamma_5 C \mathrm{G}^T C \gamma_5 \quad (5.103)$$

Also the smearing is indicated explicitly. For reasons explained in section 5.2, the quarks in the operators $\hat{B}$ and $\hat{\bar{B}}$ are smeared, leading to smeared sink and source propagators.

Now it is evident, why the exploitation of the translational symmetry was crucial. To the two-point correlator on the lattice, only one spacetime row of the Dirac matrix is required. If the expression included so called all-to-all propagators (i.e. $G(x,y)$ for $x,y \in \mathbb{R}^4$), the computational effort to obtain the required propagators by direct inversion of the Dirac matrix would be N_{sites}-times higher (e.g. on a 32×16^3 lattice: $N_{\text{sites}} = 131072$).

5.4.2 Three-point Correlation Function

The three-point correlator is defined as

$$C^{\hat{\mathcal{O}}}_\Gamma(\vec{p},t,\tau) \equiv \mathrm{tr}\Big[\Gamma\Big\langle \mathrm{T}\Big\{\hat{B}(t,\vec{p})\hat{\mathcal{O}}(\tau)\hat{\bar{B}}(0,\vec{p})\Big\}\Big\rangle\Big] = \frac{1}{n}\sum_i^n \mathcal{O}_G[A_i]\, C^{\hat{\mathcal{O}}}_\Gamma[A](\vec{p},t,\tau) \quad (5.104)$$

where the definition of the fixed gauge background three-point-correlator has been employed:

$$C^{\hat{\mathcal{O}}}_\Gamma[A](\vec{p},t,\tau) \equiv \mathrm{tr}\Big[\Gamma\Big\langle \mathrm{T}\Big\{{}^{S}\hat{B}(t,\vec{p})\,{}^{L}\hat{\mathcal{O}}(\tau)\,{}^{S}\hat{\bar{B}}(0,\vec{p})\Big\}\Big\rangle_A\Big] \quad (5.105)$$

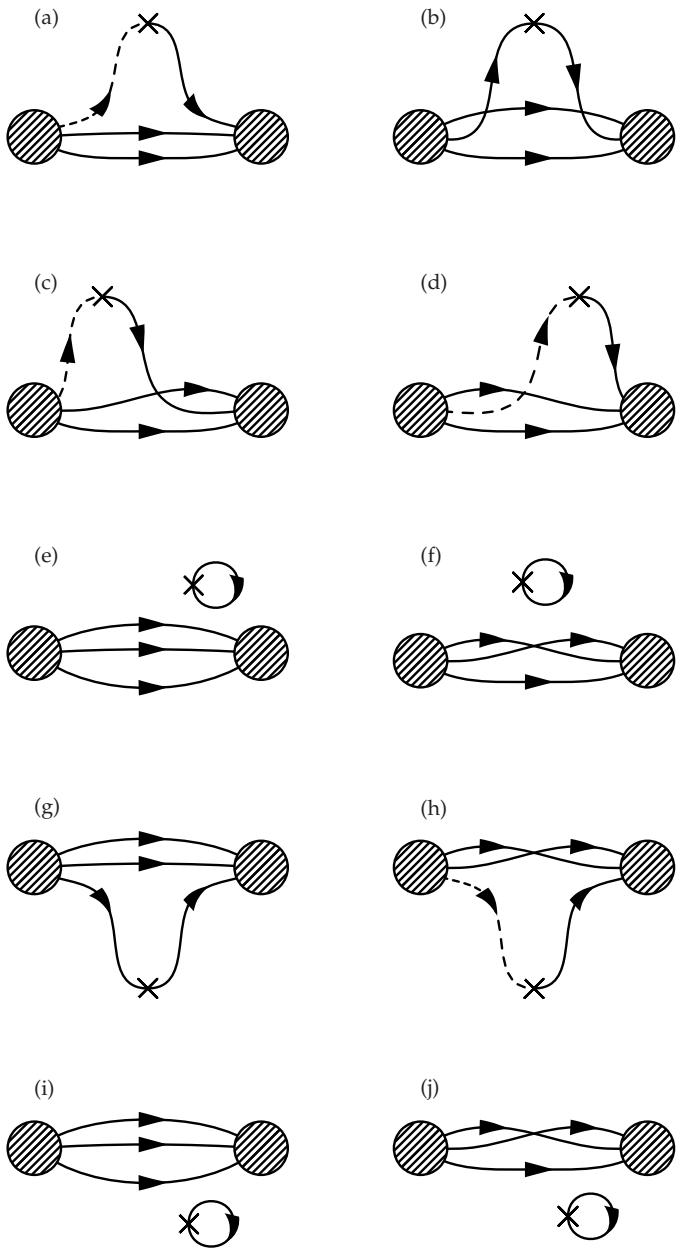

Fig. 4: All possible contractions from u-quark insertion ((a) through (f)) and d-quark insertion ((g) through (j)). The dashed lines correspond to the $G(w,0)$ part of eq. (5.119), the solid lines to the sequential propagators $\Sigma(0,v)$ and the cross to the operator insertion

Smearing is indicated. The insertion operators are not smeared, as it would make no sense to smear a point-like interaction. The general structure of $\mathcal{O}$ has to be made clear. The operator is not strictly local, as it can contain a certain number of derivatives. Furthermore, it is restricted to possesses zero momentum, as the results of this work only require zero momentum. Its general form is

$$\hat{\mathcal{O}}(\tau) = \sum_{\vec{y},v,w} \hat{\bar{q}}(\vec{y},\tau)\mathrm{O}(\vec{y},\tau;v,w)\hat{q}(\vec{y},\tau) \tag{5.106}$$

Now the definitions (5.18) are inserted and again the position argument of the source operators are shifted to zero and all others are relabelled correspondingly:

$$\begin{aligned} C_\Gamma^{\hat{\mathcal{O}}}[A](\vec{p},t,\tau) = N_S \sum_{\vec{x},\vec{y},v,w} e^{-i\vec{p}\vec{x}} \epsilon^{abc}\epsilon^{a'b'c'} \Gamma_{\alpha\beta}(C\gamma_5)_{\mu\nu}\mathrm{O}^{de}(\vec{y},\tau;v,w)_{\rho\eta}(\gamma_5 C^{-1})_{\kappa\chi} \\ \times \left\langle {}^S\hat{u}^a_\beta(x)\,{}^S\hat{u}^b_\mu(x)\,{}^S\hat{d}^c_\nu(x)\,{}^L\hat{\bar{q}}^d_\rho(v)\,{}^L\hat{q}^e_\eta(w)\,{}^S\hat{\bar{u}}^{a'}_\alpha(0)\,{}^S\hat{\bar{d}}^{b'}_\kappa(0)\,{}^S\hat{\bar{u}}^{c'}_\chi(0)\right\rangle_A \end{aligned} \tag{5.107}$$

The indication of the gauge field dependence of the propagators ($[A]$) is omitted from now on. For an up-quark insertion there are six contractions:

- Figure 4(a):

$$\begin{aligned} \langle {}^S\hat{u}^a_\beta(x)\,{}^S\hat{u}^b_\mu(x)\,{}^S\hat{d}^c_\nu(x)\,{}^L\hat{\bar{u}}^d_\rho(v)\,{}^L\hat{u}^e_\eta(w)\,{}^S\hat{\bar{u}}^{a'}_\alpha(0)\,{}^S\hat{\bar{d}}^{b'}_\kappa(0)\,{}^S\hat{\bar{u}}^{c'}_\chi(0)\rangle_A = \\ {}^{SL}_{u}\mathrm{G}^{ad}_{\beta\rho}(x,v)\,{}^{SS}_{u}\mathrm{G}^{bc'}_{\mu\chi}(x,0)\,{}^{SS}_{d}\mathrm{G}^{cb'}_{\nu\kappa}(x,0)\,{}^{LS}_{u}\mathrm{G}^{ea'}_{\eta\alpha}(w,0) \end{aligned} \tag{5.108}$$

- Figure 4(b):

$$\begin{aligned} \langle {}^S\hat{u}^a_\beta(x)\,{}^S\hat{u}^b_\mu(x)\,{}^S\hat{d}^c_\nu(x)\,{}^L\hat{\bar{u}}^d_\rho(v)\,{}^L\hat{u}^e_\eta(w)\,{}^S\hat{\bar{u}}^{a'}_\alpha(0)\,{}^S\hat{\bar{d}}^{b'}_\kappa(0)\,{}^S\hat{\bar{u}}^{c'}_\chi(0)\rangle_A = \\ {}^{SS}_{u}\mathrm{G}^{aa'}_{\beta\alpha}(x,0)\,{}^{SL}_{u}\mathrm{G}^{bd}_{\mu\rho}(x,v)\,{}^{SS}_{d}\mathrm{G}^{cb'}_{\nu\kappa}(x,0)\,{}^{LS}_{u}\mathrm{G}^{ec'}_{\eta\chi}(w,0) \end{aligned} \tag{5.109}$$

- Figure 4(c):

$$\begin{aligned} \langle {}^S\hat{u}^a_\beta(x)\,{}^S\hat{u}^b_\mu(x)\,{}^S\hat{d}^c_\nu(x)\,{}^L\hat{\bar{u}}^d_\rho(v)\,{}^L\hat{u}^e_\eta(w)\,{}^S\hat{\bar{u}}^{a'}_\alpha(0)\,{}^S\hat{\bar{d}}^{b'}_\kappa(0)\,{}^S\hat{\bar{u}}^{c'}_\chi(0)\rangle_A = \\ -\,{}^{SL}_{u}\mathrm{G}^{ad}_{\beta\rho}(x,v)\,{}^{SS}_{u}\mathrm{G}^{ba'}_{\mu\alpha}(x,0)\,{}^{SS}_{d}\mathrm{G}^{cb'}_{\nu\kappa}(x,0)\,{}^{LS}_{u}\mathrm{G}^{ec'}_{\eta\chi}(w,0) \end{aligned} \tag{5.110}$$

- Figure 4(d):

$$\begin{aligned} \langle {}^S\hat{u}^a_\beta(x)\,{}^S\hat{u}^b_\mu(x)\,{}^S\hat{d}^c_\nu(x)\,{}^L\hat{\bar{u}}^d_\rho(v)\,{}^L\hat{u}^e_\eta(w)\,{}^S\hat{\bar{u}}^{a'}_\alpha(0)\,{}^S\hat{\bar{d}}^{b'}_\kappa(0)\,{}^S\hat{\bar{u}}^{c'}_\chi(0)\rangle_A = \\ -\,{}^{SS}_{u}\mathrm{G}^{ac'}_{\beta\chi}(x,0)\,{}^{SL}_{u}\mathrm{G}^{bd}_{\mu\rho}(x,v)\,{}^{SS}_{d}\mathrm{G}^{cb'}_{\nu\kappa}(x,0)\,{}^{LS}_{u}\mathrm{G}^{ea'}_{\eta\alpha}(w,0) \end{aligned} \tag{5.111}$$

- Figure 4(e):

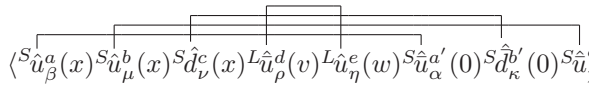

$$\begin{aligned}\langle {}^{S}\hat{u}^{a}_{\beta}(x)\,{}^{S}\hat{u}^{b}_{\mu}(x)\,{}^{S}\hat{d}^{c}_{\nu}(x)\,{}^{L}\hat{\bar{u}}^{d}_{\rho}(v)\,{}^{L}\hat{u}^{e}_{\eta}(w)\,{}^{S}\hat{\bar{u}}^{a'}_{\alpha}(0)\,{}^{S}\hat{\bar{d}}^{b'}_{\kappa}(0)\,{}^{S}\hat{\bar{u}}^{c'}_{\chi}(0)\rangle_{A} = \\ {}^{SS}_{u}\mathrm{G}^{aa'}_{\beta\alpha}(x,0)\,{}^{SS}_{u}\mathrm{G}^{bc'}_{\mu\chi}(x,0)\,{}^{SS}_{d}\mathrm{G}^{cb'}_{\nu\kappa}(x,0)\,{}^{LL}_{u}\mathrm{G}^{de}_{\rho\eta}(v,w) \quad (5.112)\end{aligned}$$

- Figure 4(f):

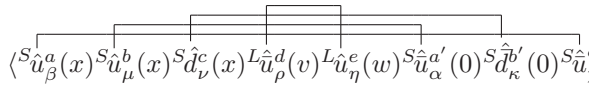

$$\begin{aligned}\langle {}^{S}\hat{u}^{a}_{\beta}(x)\,{}^{S}\hat{u}^{b}_{\mu}(x)\,{}^{S}\hat{d}^{c}_{\nu}(x)\,{}^{L}\hat{\bar{u}}^{d}_{\rho}(v)\,{}^{L}\hat{u}^{e}_{\eta}(w)\,{}^{S}\hat{\bar{u}}^{a'}_{\alpha}(0)\,{}^{S}\hat{\bar{d}}^{b'}_{\kappa}(0)\,{}^{S}\hat{\bar{u}}^{c'}_{\chi}(0)\rangle_{A} = \\ -\ {}^{SS}_{u}\mathrm{G}^{ac'}_{\beta\chi}(x,0)\,{}^{SS}_{u}\mathrm{G}^{ba'}_{\mu\alpha}(x,0)\,{}^{SS}_{d}\mathrm{G}^{cb'}_{\nu\kappa}(x,0)\,{}^{LL}_{u}\mathrm{G}^{de}_{\rho\eta}(v,w) \quad (5.113)\end{aligned}$$

For a down-quark insertion there are four contractions:

- Figure 4(g):

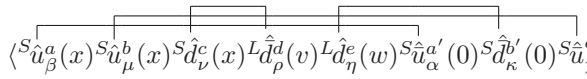

$$\begin{aligned}\langle {}^{S}\hat{u}^{a}_{\beta}(x)\,{}^{S}\hat{u}^{b}_{\mu}(x)\,{}^{S}\hat{d}^{c}_{\nu}(x)\,{}^{L}\hat{\bar{d}}^{d}_{\rho}(v)\,{}^{L}\hat{d}^{e}_{\eta}(w)\,{}^{S}\hat{\bar{u}}^{a'}_{\alpha}(0)\,{}^{S}\hat{\bar{d}}^{b'}_{\kappa}(0)\,{}^{S}\hat{\bar{u}}^{c'}_{\chi}(0)\rangle_{A} = \\ {}^{SS}_{u}\mathrm{G}^{aa'}_{\beta\alpha}(x,0)\,{}^{SS}_{u}\mathrm{G}^{bc'}_{\mu\chi}(x,0)\,{}^{SL}_{d}\mathrm{G}^{cd}_{\nu\rho}(x,v)\,{}^{LS}_{d}\mathrm{G}^{eb'}_{\eta\kappa}(w,0) \quad (5.114)\end{aligned}$$

- Figure 4(h):

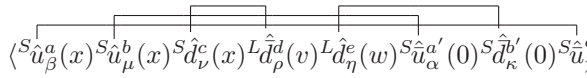

$$\begin{aligned}\langle {}^{S}\hat{u}^{a}_{\beta}(x)\,{}^{S}\hat{u}^{b}_{\mu}(x)\,{}^{S}\hat{d}^{c}_{\nu}(x)\,{}^{L}\hat{\bar{d}}^{d}_{\rho}(v)\,{}^{L}\hat{d}^{e}_{\eta}(w)\,{}^{S}\hat{\bar{u}}^{a'}_{\alpha}(0)\,{}^{S}\hat{\bar{d}}^{b'}_{\kappa}(0)\,{}^{S}\hat{\bar{u}}^{c'}_{\chi}(0)\rangle_{A} = \\ -\ {}^{SS}_{u}\mathrm{G}^{ac'}_{\beta\chi}(x,0)\,{}^{SS}_{u}\mathrm{G}^{ba'}_{\mu\alpha}(x,0)\,{}^{SL}_{d}\mathrm{G}^{cd}_{\nu\rho}(x,v)\,{}^{LS}_{d}\mathrm{G}^{eb'}_{\eta\kappa}(w,0) \quad (5.115)\end{aligned}$$

- Figure 4(i):

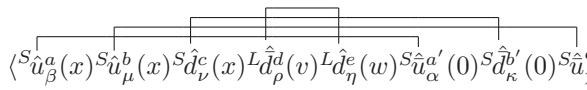

$$\begin{aligned}\langle {}^{S}\hat{u}^{a}_{\beta}(x)\,{}^{S}\hat{u}^{b}_{\mu}(x)\,{}^{S}\hat{d}^{c}_{\nu}(x)\,{}^{L}\hat{\bar{d}}^{d}_{\rho}(v)\,{}^{L}\hat{d}^{e}_{\eta}(w)\,{}^{S}\hat{\bar{u}}^{a'}_{\alpha}(0)\,{}^{S}\hat{\bar{d}}^{b'}_{\kappa}(0)\,{}^{S}\hat{\bar{u}}^{c'}_{\chi}(0)\rangle_{A} = \\ {}^{SS}_{u}\mathrm{G}^{aa'}_{\beta\alpha}(x,0)\,{}^{SS}_{u}\mathrm{G}^{bc'}_{\mu\chi}(x,0)\,{}^{SS}_{d}\mathrm{G}^{cb'}_{\nu\kappa}(x,0)\,{}^{LL}_{d}\mathrm{G}^{de}_{\rho\eta}(v,w) \quad (5.116)\end{aligned}$$

- Figure 4(j):

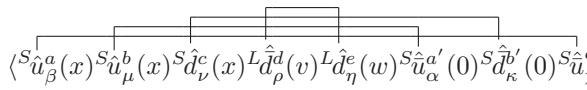

$$\begin{aligned}\langle {}^{S}\hat{u}^{a}_{\beta}(x)\,{}^{S}\hat{u}^{b}_{\mu}(x)\,{}^{S}\hat{d}^{c}_{\nu}(x)\,{}^{L}\hat{\bar{d}}^{d}_{\rho}(v)\,{}^{L}\hat{d}^{e}_{\eta}(w)\,{}^{S}\hat{\bar{u}}^{a'}_{\alpha}(0)\,{}^{S}\hat{\bar{d}}^{b'}_{\kappa}(0)\,{}^{S}\hat{\bar{u}}^{c'}_{\chi}(0)\rangle_{A} = \\ -\ {}^{SS}_{u}\mathrm{G}^{ac'}_{\beta\chi}(x,0)\,{}^{SS}_{u}\mathrm{G}^{ba'}_{\mu\alpha}(x,0)\,{}^{SS}_{d}\mathrm{G}^{cb'}_{\nu\kappa}(x,0)\,{}^{LL}_{d}\mathrm{G}^{de}_{\rho\eta}(v,w) \quad (5.117)\end{aligned}$$

If the calculation is performed using degenerate quark masses (i.e. $m_d = m_u$), there occur three contributions for the u insertion, that have the exact value as three contribution from the d insertion. Most obvious are the two quark line disconnected

terms. The u insertion contributions from eqs. (5.112), fig 4(f) and (5.113), fig. 4(e) have the same value as eqs. (5.116), fig. 4(i) and (5.117), fig. 4(j) form the d insertion, if degenerate quark masses and thus identical propagators are used.

The third pair of contributions, only becomes evident, if the sum over colour and Dirac indices is considered. Taking into account the anti-symmetry of ϵ^{abc} and the symmetry of $\gamma_5 C^{-1}$ and $C\gamma_5$, the following indices can be interchanged in eq. (5.109) without altering the sum:

$$\begin{aligned} b &\longleftrightarrow c \\ b' &\longleftrightarrow c' \\ \nu &\longleftrightarrow \mu \\ \kappa &\longleftrightarrow \chi \end{aligned} \tag{5.118}$$

After this transformation, the equality of eqs. (5.109) or fig. 4(b) and (5.114) or fig. 4(g) for degenerate quarks becomes obvious.

As explained in the last section, all-to-all propagators are prohibitively expensive. If a flavour non-singlet matrix element , i.e. insertion $u-d$, is calculated, the six equal contractions, including the four disconnected terms, will cancel. The remaining contributions (4(a), (c), (d), (g)) can be brought into the following form:

$$C_\Gamma^{\hat{\mathcal{O}}_q}[A](\vec{p},t,\tau) = N_S \sum_{\vec{y},v,w} \mathrm{tr}\Big\{ \left(\sum_{\vec{x}} {}_q\mathrm{S}_\Gamma(x,\vec{p})\, {}^{SL}_{q}\mathrm{G}(x,v) \right) \times \mathrm{O}(\vec{y},\tau;v,w)\, {}^{LS}_{q}\mathrm{G}(w,0) \Big\} \tag{5.119}$$

with

$${}_u\mathrm{S}_\Gamma(x,\vec{p}) = e^{-i\vec{p}\vec{x}} \epsilon^{abc}\epsilon^{a'b'c'} \Big(\Gamma \mathrm{tr}\Big\{ {}^{SS}_{u}\mathrm{G}^{bb'}(x,0)\, {}^{SS}_{d}\tilde{\mathrm{G}}^{cc'}(x,0) \Big\} \tag{5.120}$$

$$+\Gamma\, {}^{SS}_{u}\mathrm{G}^{bb'}(x,0)\, {}^{SS}_{d}\tilde{\mathrm{G}}^{cc'}(x,0) + {}^{SS}_{d}\tilde{\mathrm{G}}^{cc'}(x,0)\, {}^{SS}_{u}\mathrm{G}^{bb'}(x,0)\Gamma \Big) \tag{5.121}$$

and

$${}_d\mathrm{S}_\Gamma(x,\vec{p}) = e^{-i\vec{p}\vec{x}} \epsilon^{abc}\epsilon^{a'b'c'} \Big({}^{SS}_{u}\tilde{\mathrm{G}}^{cc'}(x,0)\tilde{\Gamma}\, {}^{SS}_{u}\tilde{\mathrm{G}}^{bb'}(x,0) \Big) \tag{5.122}$$

Eq. (5.119) can be interpreted graphically: The right-most propagator in the trace ($\mathrm{G}(w,0)$) corresponds to quark propagation from the source 0 to the insertion w (depicted by the dashed line in figure 4). The curved bracket contains the propagation from the source 0 to the insertion point v via the sink x (solid lines in figure 4). It consists of two parts. The first part is the propagation of the two remaining quarks of the baryon, that did not interact, from source 0 to sink x. The second part is the propagation from the insertion v to the sink x. As the sink position $\vec{x}$ is summed over, this curved bracket can be understood as the propagation of source with the non-trivial spatial distribution $\mathrm{S}(x)$ to the point v. This source shall be called *sequential source* and its propagator *sequential propagator*:

$$\Sigma(v,\vec{p},t) \equiv \sum_{\vec{x}} {}_q\mathrm{S}_\Gamma(x,\vec{p})\, {}^{SL}_{q}\mathrm{G}(x,v) \tag{5.123}$$

Σ in fact is a propagator, for it can be obtained by solving the Dirac equation. In distinction from the propagator G, instead of the delta-function, the special source $\mathrm{S}(\vec{x}, x_0)\delta_{x_0,t}$ is used.

However, to derive an expression analogous to eq. (4.65), several steps are needed. Firstly, because eq. (5.123) includes a smeared propagator and secondly, the direction specified in the sequential propagator (from source to insertion via the sink) actually includes a reverse quark propagator, while the original expression only included a propagator from the insertion to the sink. The last detail will be responsible for the occurrence of γ_5 and hermitian conjugation, which can be used to revert the Dirac operator:

$$\gamma_5^\dagger \mathrm{K}^\dagger(y,x) = \mathrm{K}(x,y)\gamma_5 \tag{5.124}$$

Multiplying eq. (5.123) from the right with the Dirac operator and inserting smearing yields:

$$\sum_v \Sigma(v,\vec{p},t)\mathrm{K}(v,v') = \sum_{\vec{x},\vec{y},v} {}_q\mathrm{S}_\Gamma(x,\vec{p})H(\vec{x},\vec{y};t)\,{}^{LL}_{q}\mathrm{G}(\vec{y},t;v)\mathrm{K}(v,v') \tag{5.125}$$

$$= \sum_{\vec{x}} {}_q\mathrm{S}_\Gamma(x,\vec{p})H(\vec{x},\vec{v}';t)\delta_{v_0',t} \tag{5.126}$$

Hermitian conjugation, insertion of eq. (5.124) and multiplication of γ_5 from the left yields the final equation for the sequential propagator:

$$\sum_v \mathrm{K}(v',v)\Big(\Sigma(v,\vec{p},t)\gamma_5\Big)^\dagger = \sum_{\vec{x}} H(\vec{v}',\vec{x};t)\Big({}_q\mathrm{S}_\Gamma(x,\vec{p})\gamma_5\Big)^\dagger \delta_{v_0',t} \quad \text{for all } v' \tag{5.127}$$

What has been won by the introduction of this new propagator? The curved bracket in eq. (5.119) involves the propagator $\mathrm{G}(x,v)$ and the sum over $\vec{x}$. The direct evaluation of this expression requires $N_1N_2N_3 = 4096$ inversions of the Dirac matrix in addition to the inversion that is needed to obtain $\mathrm{G}(w,0)$.

This bracket has been found to be expressible as the sequential propagator. The evaluation of the sequential propagator as a solution to equation (5.127) requires only one additional inversion, if $\mathrm{G}(x,0)$ is already known. The crucial part is that the sequential source $\mathrm{S}(x)$ is made up solely from propagators $\mathrm{G}(x,0)$.

The specific form of eq. (5.127) also allows to use the exact same code for its solution, that has been used for the point propagator $\mathrm{G}(x,0)$.

6 Numerical Calculation

The computation of lattice QCD quantities can be split up in four distinctive steps, that largely differ in their requirements of computation time and resources.

The first step is the generation of an ensemble of gauge configurations with a certain probability distribution (cp. eq. 4.71). These are usually stored for later use, for example in the computation of matrix elements that involve gauge field operators or for the computation of propagators, which is the second step of the computation. If possible only propagators from the origin and sequential propagators are calculated, by inversion of the Dirac matrix and the corresponding sources. If there is sufficient storage available, i.e. for small enough lattices, propagators are also stored. The third step is the computation of the fermion Green's functions on each configuration by summing up the contributing contractions which are multiplications of propagators. The final step is the actual integration, which is basically the statistical averaging over the configurations.

If several different quantities are to be calculated, only the third and fourth step have to be repeated, the propagators and gauge configurations can be reused. As their production also accounts for the major part of the computational effort, the generation of gauge configurations and propagators can be regarded as the actual work that has to be done. Part three and four are merely seen as the evaluation of results.(This is not true, if sequential propagators are employed. Depending on the desired matrix element or e.g. the projection matrix Γ, they might have to be recalculated as well)

6.1 Generating Samples of Gauge Configurations

As explained in section (4.6), the integration over the fermion fields can always be carried out analytically due to the quadratic action in the Grassmann fermionic fields variables. The remaining integrals are of the following form:

$$\langle \mathcal{O}[A] \rangle = \mathcal{Z} \int \mathcal{D}A \, \mathcal{O}[A] \, e^{-\mathcal{S}_G[A]} \tag{6.1}$$

If a sample of gauge configurations $\{A_i\}_{1 \leq i \leq N}$ is generated such that the probability to include a certain gauge configuration A_i in the sample is

$$p(A_i) \sim e^{-\mathcal{S}_G[A]}, \tag{6.2}$$

the integral can be approximated by the average over the sample:

$$\langle \mathcal{O}[A] \rangle \approx \frac{1}{N} \sum_{i}^{N} \mathcal{O}[A_i] \tag{6.3}$$

This technique is called *importance sampling*, because important configurations with large weight factors $e^{-\mathcal{S}}$ are favored and minimal computation time is wasted on configurations that will contribute only little to the integral.

The samples are usually generated by a Markov chain. A Markov chain is a sequence of configurations, where the probability distribution for a new configuration only depends on the last configuration in the sequence. The details of this process have to be chosen such that the generated sample will have the desired probability distribution eq. (6.2).

A well known algorithm for the Markov process is the Metropolis-Algorithm. The probability of accepting a new candidate configuration is given by

$$p(A_{i+1} \leftarrow A_i) = \min(1, e^{-(\mathcal{S}[A_{i+1}]-\mathcal{S}[A_i])}) \tag{6.4}$$

The configurations used in this work have been obtained using the *Hybrid Monte-Carlo algorithm*, which is designed especially to meet the difficulties of dynamical calculations. [23]

The quality of the approximation (6.3) and the validity of the calculated errors strongly depend on the quality of the sample. The configurations in the sample have to be representative and statistically independent. To minimize correlation between different configurations in the sample not every configuration generated by the Markov chain is used. Instead a considerable number of Markov steps has to be performed before a new configuration is added to the sample. The number of required steps between two configurations shows critical behaviour in the continuum limit, which is called *critical slowing down*.

The generation of the sample is the part of lattice QCD, that profits from the quenched approximation. The presence of the fermion determinant dramatically increases the amount of computer time that is needed to calculate new configurations or transition probabilities required in the Markov process.

6.2 Inverting the Dirac Matrix

Once the sample of gauge configurations has been obtained, the propagators can be calculated. This is done by inversion of the lattice Dirac operator on a local source or a sequential source (to obtain sequential propagators). The total task of obtaining the propagators for all the different quark masses, configurations, different momenta, sink times or projections (of the sequential source) requires a huge amount of computation time, making it inevitable to parallize the computation.

The parallelization, at first sight seems quite easy, because the number of independent inversions with separate data that have to be done is very large. In this work case, inversions for each out of 100 configurations, 10 different quark masses, two different parity projections and sink times, the four Dirac and three colour indices had to be performed. This multiplies to a total of 24,000 independent inversions. So unless there are more than 24,000 processor cores available, the most efficient method would be to use sequential code, that can perform one inversion using exactly one core and run it 24,000 times using all the processors. This way linear speed-up is achieved, as the parallelization produced no overhead and if t_{seq} is the time one core needs for one inversion, the total time needed per inversion is

$$t_{\text{par}} = \frac{t_{\text{seq}}}{n_{\text{cores}}}.$$

The problem however usually is caused by the required amount of memory. On the 32×16^3 lattice, about 24 GiB were needed for one inversion, and as the RAM per core was not higher than 4 GiB on any node, the inversion algorithm had in fact to be parallized to run on up to 16 cores from two nodes in parallel.

If several processes on different cores, processors and nodes actually have to work on the same inversion at a time using an iterative algorithm, they need to be synchronized and be able to communicate and exchange data. There are of course several ways this can be realized, but as basic functionalities coincide for many areas of application, some parallel programming standards emerged over the last two decades. They can be split up roughly in two complementary programming approaches: Threaded shared memory programming and parallel message passing systems.

6.2.1 MPI

The message passing interface (MPI) has been used in our case. It is a very popular specification for an application programming interface(API) that implements a parallel message passing system. MPI provides source-code portability across a variety of architectures through its C and Fortran language bindings. There exist several implementations in form of libraries containing a set of routines that provide MPI functionalities to a variety of programming languages.

As the name suggest, communication within MPI is done by sending and receiving messages. A message is an array of one particular data type. Every MPI routine possesses the three arguments `buf`, `count`, `type` characterizing the message and `comm`, which specifies the communicator. `buf` contains the memory address of the data, `count` specifies the number of elements of the type `type` that the message should contain. The communicator handles the communication among processes and provides for example the rank of a process, which will be used to identify the process.

The communication functions provided by MPI can be classified in two types:

Point-to-Point communication
One process sends a message that is received by another process. Both processes have to share a communicator and each other's rank within the communicator has to be known to them. There are different versions of the send and receive commands that differ in their communication mode. The communication mode determines mainly whether the program halts until the send or receive is completed or continues regardless of the completion. This difference is also named blocking or non-blocking communication.

```
MPI_SEND(buf,count,type,dest,tag,comm)
```

is the standard blocking send. This call will return only after the data has been moved to the receiver. `comm` contains the communicator, `dest` the rank of the destination process and `tag` is an integer value that can be used by the programmer to mark different types of messages.

```
MPI_RECV(buf,count,type,source,tag,comm,status)
```

This is the standard blocking receive, which will return when a message has been received. `buf` specifies the address where the received data should be stored, `source` contains the rank of the source process and `status` will contain some information about the message after it has been received.

Collective communication
Collective communication always involves every process in the specified communicator. Consequently, every process in the communicator has to call the routine. As the inversion algorithm will exclusively use collective communication, the important functions are explained in more detail:

Broadcast: `MPI_BCAST(buf,count,type,root,comm)`

All processes must specify the same `root` and `comm`. This function acts like a send on the root process and a receive on all other processes. After completion every process will hold the same data in `buf`.

Scatter:
```
MPI_SCATTER(sendbuf,sendcount,sendtype,
recvbuf,recvcount,recvtype,root,comm)
```

The root process scatters the data in portions specified by `sendcount` and `sendtype` to each process in the given communicator, including itself. This routine explicitly gives the possibility, as opposed to `MPI_BCAST`, to specify different send and receive types. These only have to match if primitive data types are used. When using derived data types, this restriction is loosened, but one still has to ensure via the variables `sendcount` and `recvcount`, that the amount of data is identical.

Gather:
```
MPI_GATHER(sendbuf,sendcount,sendtype,
recvbuf,recvcount,recvtype,root,comm)
```

The root process gathers data specified by `sendcount` and `sendtype` by each process in the given communicator, including itself and stores it in portions specified by `recvcount` and `recvtype` sorted by process rank in the `recvbuf`.

```
MPI_ALLGATHER(sendbuf,sendcount,sendtype,
recvbuf,recvcount,recvtype,comm)
```

While the `MPI_GATHER` command stored the gathered data only in the root process' memory, this command will provide every process in the communicator with a copy of the gathered data.

Reduce: `MPI_REDUCE(sendbuf,recvbuf,count,type,op,root,comm)`

This routine will take the i-th element of the `sendbuf` of every process within the communicator, reduce it using some reduction operation `op` and store it in the i-th element of the root process in `recvbuf`. This is done for $i = 1...$`count`.
For primitive data types there exists a number of predefined operators: Maximum, minimum, sum, product, bitwise/logical and/or/xor, rank of the process holding the maximum or minimum value. It is also possible to create user-defined operands.

`MPI_ALLREDUCE(sendbuf,recvbuf,count,type,op,comm)`

While the `MPI_REDUCE` command stored the reduced data only in the root process' memory, this command will provide every process in the communicator with a copy of the reduced data.

6.2.2 Parallelization

In order to make programming and the notation a little easier, all lattice sites are numbered using the following mapping:

$$x_\mu = an_\mu \longmapsto i = n_0 + n_1 N_0 + n_2 N_0 N_1 + n_3 N_0 N_1 N_2 \,, \quad \text{with } 0 \leq i < N_{\text{sites}} \tag{6.5}$$

This way all quantities can be defines using only one index for the spacetime coordinate and the equation that has to be solved is:

$$\sum_j^{N_{\text{sites}}} D(i,j)G(j) = S(i) \tag{6.6}$$

G is one row of the propagator, S the source vector, and D the Dirac operator. Dirac and colour indices have been dropped as they play no role in the construction of the algorithm or the parallelization. All expressions can be easily generalized to Dirac and colour matrices.

The crucial part of the parallelization is to let every process handle just a subset of lattice sites. Requiring that the number of processes involved in the calculation is a divisor of N_{sites}, the workload can be equally distributed, if every process handles N_{sub} sites, with

$$N_{\text{sub}} = N_{\text{sites}}/n_{\text{cores}}. \tag{6.7}$$

In this manner *local* quantities are defined, that will satisfy the following relations:

$$S^r_{\text{loc}}(i) = S(r \cdot N_{\text{sub}} + i) \tag{6.8}$$
$$G^r_{\text{loc}}(i) = G(r \cdot N_{\text{sub}} + i) \tag{6.9}$$
$$D^r_{\text{loc}}(i,j) = D(r \cdot N_{\text{sub}} + i, j) \tag{6.10}$$

$0 \leq i < N_{\text{sub}}$ and $0 \leq j < N_{\text{sites}}$. r is the rank of the process with $0 \leq r < n_{\text{cores}}$.
Every process *knows* only his part of the complete vector or matrix. This knowledge

is sufficient for vector addition, as the i-th component of the resulting vector only involves the i-th components of the operands. But operations that involve the complete set of sites, need to be emulated using MPI. Operations of this kind, that will be used in this algorithm, are calculation of a scalar product of two vectors and matrix on vector multiplication.

Vector on vector

The dot product of two vectors A, B with N_{sites} entries that are distributed over all processes is calculated in the following way:

$$c = A \cdot B = \sum_{r}^{n_{\text{cores}}} c^r_{\text{loc}} = \sum_{r}^{n_{\text{cores}}} \left(\sum_{i}^{N_{\text{sub}}} A^r_{\text{loc}}(i) B^r_{\text{loc}}(i) \right) \tag{6.11}$$

In FORTRAN-code:

```
c_loc=dot_product(A_loc,B_loc)

call MPI_ALLREDUCE(c_loc,c,1,MPI_DOUBLE_PRECISION,&
MPI_SUM,MPI_COMM_WORLD,ierr)
```

The sum over i in eq. (6.11) is performed in the routine `dot_product`, the sum over r is performed by the MPI reduction routine, that provides every process with the result of the full dot product in variable `c`.

Matrix on vector

In this case, a square matrix D with N_{sites} rows that are distributed over all processes, has to be multiplied on a column vector A with N_{sites} entries that are also distributed over all processes. The local parts of the resulting vector B are calculated:

$$B^r_{\text{loc}}(i) = \sum_{j}^{N_{\text{sites}}} D^r_{\text{loc}}(i,j) A(j) \text{ , for all } 0 < i < N_{\text{sub}} \tag{6.12}$$

To perform this calculation every process has to have the complete vector A in its memory. So the different parts of the vector A have to be gathered, which is done by the corresponding MPI routine:

```
call MPI_ALLGATHER(                                  &
      A_loc,N_dirac*N_colour*N_sub,MPI_DOUBLE_COMPLEX, &
      A,    N_dirac*N_colour*N_sub,MPI_DOUBLE_COMPLEX, &
    MPI_COMM_WORLD,ierr)

do i=0,n_sub-1
  B_loc(i)=dot_product(D_loc(i,:),A)
enddo
```

As a result of this operation, every process will have only his local part of the result vector B.

6.2.3 The sparse Dirac operator

The ultra-local nature of the Dirac operator is reflected in the fact that the Dirac matrix in configuration space is a sparse matrix . In the case of the chirally improved Dirac operator used in this work, only one in 1016 entries was non-zero. These entries only connect points with a physical distance of less than $2.3a$. This means that every point is only connected to 128 neighbours.
Of course internally the Dirac matrix is not handled as a sparse two-dimensional array, but instead only non-zero entries are stored. If N_{neigh} is the number of neighbouring sites that are connected via the Dirac matrix to every single site (this might also include the site itself), the matrix is stored in a $N_{\text{sites}} \times N_{\text{neigh}}$ two-dimensional array with one spacetime and a neighbour index:

$$D^r_{\text{loc,sparse}}(i,j) \text{ , with } 0 \leq i < N_{\text{sub}}, 0 \leq j < N_{\text{neigh}} \tag{6.13}$$

In order to be able to reconstruct the full matrix, another two-dimensional array is needed. It contains the addresses of every neighbour of all local lattice sites:

$$a^r_{\text{loc,neigh}}(i,j) \in \{0,\ldots,N_{\text{sites}}-1\} \text{ , with } 0 \leq i < N_{\text{sub}} \text{ and } 0 \leq j < N_{\text{neigh}} \tag{6.14}$$

It returns the global site index of the j-th neighbor of the i-th site handled by the process with rank r.
With this new definition of D the matrix on vector multiplication of eq. (6.12) can be performed in the following way:

$$B^r_{\text{loc}}(i) = \sum_j^{N_{\text{neigh}}} D^r_{\text{loc,sparse}}(i, a^r_{\text{loc,neigh}}(i,j)) A(a^r_{\text{loc,neigh}}(i,j)) \tag{6.15}$$

6.2.4 BiCG-stab

Using the methods described so far, the parallelization of an inversion algorithm of a sparse Dirac matrix is straight forward. First an algorithm is chosen that is suited best for the kind of problem: Sparse matrix, non-symmetric, etc. For this work the Biconjugate gradient stabilized (BiCG-stab) algorithm was chosen, which is an iterative method that takes an arbitrary starting vector and transforms it iteratively into the solution vector after a finite number of steps. For more information on conjugate gradient inverters and especially the BiCG-stab refer to [24].

Usually the algorithm terminates before the exact solution is reached, e.g. when the estimated distance of the intermediate vector from the solution vector is smaller than the specified tolerance.

The next step is the parallelization of the inversion routine. This is done by replacing the vector operations of the sequential routine by the corresponding parallel versions for local quantities as described above. For the BiCG-stab this includes only vector addition, vector on vector multiplication and Dirac matrix on vector multiplication, which also proves the implementation of the sparse version of the Dirac matrix, as described above, to be quite easy.

If, as in the case with the free quark propagators, one has to do a whole set of inversions, where the sources are identical and the Dirac matrices only differ by a constant (i.e. the different quark masses)

$$\sum_{j}^{N_{\text{sites}}} \left(D_{\text{massless}}(i,j) + m_{\text{quark}} \right) G(j) = \delta(i,k), \tag{6.16}$$

a modified version of the algorithm is used. The so called BiCGstab-M [25] can perform these different inversions using only as many matrix-vector operations as the solution of the most difficult single system requires.

This is however not possible for the calculation of sequential propagators, because the sources are also mass dependent.

6.3 Calculating Green's functions

This step basically is the numerical realization of the formulas described in section 5.4. For every configuration A the correlator $C[A]$ is calculated. The computation is simply the multiplications of propagators and sequential propagators and the sum over lattice sites, spinor and colour indices and the sum over the different contractions.

In this step one has to be aware of the desired quark smearing. The two-point correlator from eq. (5.102) is made up solely from smeared sink and smeared source propagators.

$$^{SS}\mathrm{G}[A] \tag{6.17}$$

The three-point correlator (eq. 5.119) is made up from the sequential propagator and local sink, smeared source propagator.

$$^{LS}\mathrm{G}[A] \tag{6.18}$$

The sequential sources (eqs. 5.120 and 5.122), which are required for the production of the sequential propagators, also only contains smeared sink and smeared source propagators.

This motivates a strategy, where in step 2 (section 6.2) only the local sink, smeared source propagators are calculated and stored. Then the sinks get smeared, where needed, for example in the calculation of the sequential sources or in two point correlators, i.e. in this step.

6.4 Performing the Integration

The value of the lattice path integral is approximated with use of Monte-Carlo methods. In this framework it is the ensemble average:

$$\left\langle \psi^{\alpha_1} \cdots \psi^{\alpha_j} \bar{\psi}^{\beta_1} \cdots \bar{\psi}^{\beta_j} \, \mathcal{O}_G[A] \right\rangle = \frac{1}{n} \sum_{i}^{n} \mathcal{O}_G[A_i] \left\langle \psi^{\alpha_1} \cdots \psi^{\alpha_j} \bar{\psi}^{\beta_1} \cdots \bar{\psi}^{\beta_j} \right\rangle_A \tag{6.19}$$

The errors of this approximation can be estimated by the statistical uncertainties.

As will become clear later, one is often interested in the ratio of three- and two-point functions. These two quantities are not statistically independend and their errors are correlated. In order to obtain most sensitive error bars and unbiased estimates for the ensemble quantities, jack-knife methods are employed as described in [6].

Consequently, the integration is reduced to jack-knifing. All errors given in this work are pure jackknife errors.

7 The Hypothesis of Chiral Symmetry Restauration

7.1 Chiral Symmetry

In one flavour QCD the quark Lagrangian density takes the following form:

$$\mathcal{L} = \bar{\psi}(i\not{D} + m)\psi \tag{7.1}$$

This Lagrangian is invariant under a global $U(1)$ transformation

$$\psi \to e^{i\theta_V}\psi. \tag{7.2}$$

The conserved Noether current implied by this symmetry is

$$\bar{\psi}\gamma_\mu\psi, \tag{7.3}$$

which transforms like a Lorentz vector. The transformation eq. (7.2) is thus called *vectorial transformation* and the symmetry *vector symmetry*.

If the quark mass is neglected, an additional symmetry will arise. To unveil it, and provide the basics for further discussion about chirality the attention is drawn to an operator and its properties: γ_5 is called the *chirally operator* (for reasons that will become clear later) and possesses two eigenvalues $+1$ and -1 that are two-fold degenerate each, with the two eigenspace projectors

$$\begin{aligned} P_R &= \frac{1}{2}(1+\gamma_5) \\ P_L &= \frac{1}{2}(1-\gamma_5) \end{aligned} \tag{7.4}$$

with the following properties:

$$\gamma_5 P_R = +P_R \text{ and } \gamma_5 P_L = -P_L$$
$$P_R^2 = P_R \text{ and } P_L^2 = P_L$$
$$P_L P_R = P_R P_L = 0$$
$$\gamma_\mu P_{R/L} = P_{L/R}\gamma_\mu \tag{7.5}$$
$$\bar{P}_{R/L} = P_{L/R} \tag{7.6}$$
$$P_L + P_R = 1 \tag{7.7}$$
$$P_R^2 + P_L^2 = 1 \tag{7.8}$$

R stands for right-handed and L for left-handed (for reasons that also will become clear later).

Property (7.7) can be used to decompose every spinor in its left- and right-handed parts:

$$\psi = \psi_R + \psi_L = P_R\psi + P_L\psi \tag{7.9}$$

If identities (7.8) are inserted into the Lagrangian density one obtains:

$$\begin{aligned}\mathcal{L} &= \bar{\psi}(i\mathrm{D}^{\mu}\gamma_{\mu} + m)(P_R^2 + P_L^2)\psi \\ &= i\bar{\psi}_R \not{\mathrm{D}}\psi_R + i\bar{\psi}_L \not{\mathrm{D}}\psi_L + \bar{\psi}_R m\psi_L + \bar{\psi}_L m\psi_R \end{aligned} \tag{7.10}$$

Eqs. (7.5) and (7.6) have been used in the last step.

If the quark mass is neglected (which is called the *chiral limit*), the left- and right handed fields decouple and the Lagrangian could be interpreted as describing two independent particles. The particles possess two complex-valued degrees of freedom and by looking at the corresponding free one-particle equation they can be identified with positive and negative energy components of the wave function.

The chirality operator γ_5, that commutes in the chiral limit with the free one-particle Hamilton operator, also commutes with the helicity operator

$$\vec{\Sigma} \cdot \vec{p}/p, \tag{7.11}$$

which is the projection of the spin-operator on the momentum of the particle. Consequently there exists a basis of plane wave solutions that are simultaneously chirality and helicity eigenstates. A closer examination yields the following mapping of eigenvalues:

Energy	Helicity	Chirality
$\gamma_0\vec{\gamma}\cdot\vec{p}$	$\vec{\Sigma}\cdot\vec{p}/p$	γ_5
$+E_{\vec{p}}$	$+1$	$+1$
$-E_{\vec{p}}$	-1	$+1$
$+E_{\vec{p}}$	-1	-1
$-E_{\vec{p}}$	$+1$	-1

Table 2: Eigenvalues of simultaneous eigenvectors

Massless particles travel at the speed of light, making the definition of the spin in the rest frame impossible. Instead they can be characterized by their helicity, which for a massless particle cannot be changed by a Lorentz transformation.

Now it becomes evident, why the γ_5 eigenvalue is called chirality ("screw-sense"). A massless Dirac-particle comes in two versions. A particle with spin parallel to the direction of motion (this also applies for the negative energy solution, as it travels in reversed momentum direction $\vec{v} = -\vec{p}$), which is called a *right-handed* particle. Together with its left-handed anti-particle they both carry $+1$ as γ_5 eigenvalue. Analogously, the solutions with negative chirality represent a left-handed particle (and right-handed anti-particle).

In the chiral limit the form of the Lagrange density (7.10) explicitly shows the invariance under two independent $U(1)$ transformations for right- and left-handed fields:

$$\begin{aligned}\psi_R &\to e^{i\theta_R}\psi_R \\ \psi_L &\to e^{i\theta_L}\psi_L \end{aligned} \tag{7.12}$$

$$\mathcal{L} \to \mathcal{L} \tag{7.13}$$

If the action of a simultaneous transformation of right- and left-handed parts with the same angle $\theta_R = \theta_L = \theta_V$ on the composed field ψ is considered

$$\psi \to \left(e^{i\theta} \frac{1}{2}(1+\gamma_5) + e^{i\theta} \frac{1}{2}(1-\gamma_5) \right) \psi = e^{i\theta_V} \psi, \tag{7.14}$$

one finds the vector symmetry, which also existed in the case with non-zero mass (cp. eq. 7.2). The newly achieved symmetry can be obtained by regarding a transformation with $\theta_R = -\theta_L = \theta_A$:[18]

$$\begin{aligned} \psi \to & \left(e^{i\theta_A}(1+\gamma_5)/2 + e^{-i\theta_A}(1-\gamma_5)/2 \right) \psi = \\ & \left((e^{i\theta_A} + e^{-i\theta_A})/2 + \gamma_5 (e^{i\theta_A} - e^{-i\theta_A})/2 \right) \psi = \\ & (\cos(\theta_A) + i \sin(\theta_A)\gamma_5)\, \psi \end{aligned} \tag{7.15}$$

$$\psi \to \exp(i\theta_A \gamma_5)\, \psi \tag{7.16}$$

The conserved Noether current implied by this symmetry is

$$A_\mu(x) \equiv \bar{\psi} \gamma_\mu \gamma_5 \psi, \tag{7.17}$$

which transforms like an axial vector under parity transformation. The transformation eq. (7.16) is thus called *axial transformation* and the symmetry *axial symmetry*.

All in all, the classical Lagrangian with zero quark mass possesses the following symmetry group:

$$U(1)_R \times U(1)_L = U(1)_V \times U(1)_A \tag{7.18}$$

If the theory should allow for quarks of different flavour, and the quarks are considered mass-degenerate, the Lagrangian density takes the form

$$\mathcal{L} = \bar{\Psi}(i\not{\partial} + m)\Psi, \tag{7.19}$$

where Ψ is the N-dimensional vector of the different flavour quarks:

$$\Psi = \begin{pmatrix} u \\ d \\ s \\ \vdots \end{pmatrix} \tag{7.20}$$

The flavour independent form of the bracket leads in addition to the $U(1)_V$ symmetry to a $SU(N)_V$ symmetry:

$$\Psi \to \exp(i\theta_V^a \tau^a)\, \Psi \tag{7.21}$$

τ^a (for $1 \leq a \leq N$) are the $SU(N)$ generators. This symmetry is called *isospin*-symmetry for $N = 2$ or *flavour*-symmetry in general.

[18] The last step uses $\gamma_5^{2n} = 1$ and $\gamma_5^{2n+1} = \gamma_5$

The corresponding vectorial current is

$$V_\mu^a(x) \equiv \bar{\Psi}\gamma_\mu\tau^a\Psi, \tag{7.22}$$

and the charge is defined as the spatial integral over the $\mu = 0$ component:

$$Q_V^a \equiv \int d^3\vec{x}\, V_0^a(t,\vec{x}) \tag{7.23}$$

In the chiral limit, the Lagrangian can again be written in terms of right- and left-handed fields:

$$\mathcal{L} = i\bar{\Psi}_R \not{\partial}\Psi_R + i\bar{\Psi}_L \not{\partial}\Psi_L \tag{7.24}$$

It is invariant under independent $SU(N)$ transformations of the right- and left-handed fields (in addition to the $U(1)_R$ and $U(1)_L$ symmetries from above):

$$\begin{aligned} \Psi_R &\to \exp(i\theta_R^a\tau^a)\ \Psi_R \\ \Psi_L &\to \exp(i\theta_L^a\tau^a)\ \Psi_L \end{aligned} \tag{7.25}$$

Again the complete group contains already the vectorial flavour transformations. The additional transformations are the *axial* transformations, which are simultaneous rotations with opposing angles $\theta_R = -\theta_L = \theta_A$:

$$\Psi \to \exp(i\theta_A^a\tau^a\gamma_5)\ \Psi \tag{7.26}$$

which do not form a group. The set of axial transformations will still be named $SU(N)_A$ for simplicity.

The corresponding axial current is:

$$A_\mu^a(x) \equiv \bar{\Psi}\gamma_\mu\gamma_5\tau^a\Psi \tag{7.27}$$

The vector charge and the axial current fulfil the following useful current algebra relation:

$$\left[\hat{Q}_V^a, \hat{A}_\mu^b\right] = i\epsilon^{abc}\hat{A}_\mu^c \tag{7.28}$$

7.2 Chiral Symmetry Breaking

The complete symmetry group of the QCD Lagrangian with neglected quark masses is:

$$\begin{aligned} U(1)_R \times U(1)_L \times SU(N)_L \times SU(N)_R = \\ U(1)_V \times U(1)_A \times SU(N)_V \times \text{“}SU(N)_A\text{”} \end{aligned} \tag{7.29}$$

The masses of quarks other than u and d (cp. Table 3) are far from zero and far from being equal. This breaks the $SU(N)_L \times SU(N)_R$ symmetry down to $SU(2)_L \times SU(2)_R$ for u and d flavour. Compared to the QCD scale $\Lambda_{\text{QCD}} \approx 217\,\text{MeV}$ the masses of the u

Flavour	m/Mev
u	1.5 to 3.3
d	3.5 to 6.0
s	104^{+26}_{-34}
c	$1,270^{+\ 70}_{-110}$
b	$4,200^{+170}_{-\ 70}$
t	$171,200 \pm 2,100$

Table 3: Estimated current quark masses from [18]

and d quarks are very small and of comparable size, leaving the following symmetry groups only as approximate symmetries:

$$SU(2)_L \times SU(2)_R \times U(1)_A \tag{7.30}$$

However, even in the chiral limit, the axial symmetries are broken. The $U(1)_A$ symmetry is explicitly broken on the quantum level, which is called axial anomaly [26]. The origin can be found for example in the non-invariance of the path-integral measure under axial rotations. As a consequence the axial current (eq. 7.17) is no longer conserved:

$$\partial^\mu A_\mu(x) = \frac{\alpha_S N_f}{4\pi} \mathrm{tr}\Big\{\tilde{\mathrm{F}}^{\mu\nu}\mathrm{F}_{\mu\nu}\Big\} \tag{7.31}$$

F is the gluon field strength tensor, $\tilde{\mathrm{F}}$ the dual tensor, N_f the number of flavours, α_S the strong coupling constant.

Also $SU(2)_A$, which is in the chiral limit a symmetry of the classical theory, is broken. In contrast to the $U(1)_A$ symmetry it is not anomalously, but instead spontaneously broken. The three massless Goldstone bosons are the three pions, which are massless in the chiral limit. The order parameters of spontaneous symmetry breaking are the non-zero values of the quark condensates [27]:

$$\langle \bar{u}u \rangle \approx \langle \bar{d}d \rangle \approx -(240 \pm 10\,\mathrm{MeV})^3 \tag{7.32}$$

These expectation values are not invariant under axial transformations and their finite value directly shows the symmetry violation.

As $SU(2)_A$ is only an approximate symmetry the pions are pseudo-Goldstone bosons with finite mass. The mass of the pions can be expressed in terms of the explicit symmetry breaking parameter, i.e. the quark masses [28]:

$$m_\pi^2 = -\frac{m_u + m_d}{2} \frac{\langle \bar{u}u \rangle + \langle \bar{d}d \rangle}{f_\pi^2} + \mathcal{O}(m_{u,d}^2) \tag{7.33}$$

The surviving symmetry group of QCD is:

$$SU(2)_I \times U(1)_V \tag{7.34}$$

The $U(1)_V$ symmetry remains untouched on the quantum level and is responsible for baryon number conservation.

The approximate isospin symmetry $SU(2)_I$ manifests itself for example in the existence of almost degenerate isospin multiplets in the baryon spectrum. In table 4 some multiplets are given.

7.3 Chiral Symmetry Restauration

The occurrence of parity doublets in the upper light baryon spectrum has been the motivation to suggest an effective restauration of chiral symmetry in high lying hadrons [29]. Table 5 shows how close the parity doublets are located in the baryon spectrum.

For the nucleon no chiral partner can be identified, indicating that the symmetry breaking still plays a major role in its mass generation. A significant part of the nucleons mass can be shown to come from the quark condensate, i.e. the symmetry breaking parameter [30, 31]. Moreover, the nucleon's coupling to the Goldstone bosons (pions) can be connected via the Goldberger-Treiman relation to the axial charge and mass of the nucleon [27]

$$g_{\pi NN} = \frac{g_A m_N}{f_\pi}, \tag{7.35}$$

which is experimentally confirmed ($g_{\pi NN} = 13.4$ and $\frac{g_A m_N}{f_\pi} = 12.7$). The coupling to the pion, which is nothing else then the decay constant of the nucleon in the nucleon-pion channel, is induced by the spontaneous breaking of chiral symmetry and is for the nucleon quite large.

The only other well established excited nucleon for which no chiral partner could be identified is $N(1520)$. Its decay constant into the $N\pi$ channel is comparable with that of the nucleon. On the other hand, the decay of recognized members of parity doublets was found to be suppressed by a factor of ten [32]. Why this is further indication for the hypothesis, that parity doublets occur due to an effective restauration of chiral symmetry at higher baryon masses, will be explained in the next section.

Parity doubling in the spectrum is a testable prediction [29]. The required smallness of the pion coupling and axial charge for parity doublets and largeness baryons without chiral partner provides a test for the hypothesis of restauration [32].

7.4 Parity-Chiral Multiplets

[33] suggests, that the observed parity doubling can be explained via the formation of chiral multiplets.

If chiral symmetry is restored, all states fall into irreducible representations of the chiral group

$$SU(2)_L \times SU(2)_R. \tag{7.36}$$

If one state of a certain irreducible representation is rotated by a symmetry transformation, it does only mix with other states within its representation. Consequently all states that belong to a representation have the same mass. States of the same representation are called to form a *multiplet*.

If the symmetry is effectively restored, the multiplets will only be approximately degenerate, meaning that the spectrum will consist of multiplets, with mass splittings within the multiplet, that are far smaller than the difference between two multiplets in the spectrum.

Name	Isospin	$\text{Spin}^{\text{Parity}}$	Strangeness	Charm	Charge	mass/MeV
p	$1/2$	$1/2^+$	0	0	1	0,938.3
n	$1/2$	$1/2^+$	0	0	0	0,939.6
Σ^+	1	$1/2^+$	-1	0	1	1,189.4
Σ^0	1	$1/2^+$	-1	0	0	1,192.6
Σ^-	1	$1/2^+$	-1	0	-1	1,197.4
Σ_c^{++}	1	$1/2^+$	0	1	2	2,454.0
Σ_c^+	1	$1/2^+$	0	1	1	2,452.9
Σ_c^0	1	$1/2^+$	0	1	0	2,453.8
Ξ^0	$1/2$	$1/2^+$	-2	0	0	1,314.9
Ξ^-	$1/2$	$1/2^+$	-2	0	-1	1,321.7
Δ^{++}	$3/2$	$3/2^+$	0	0	2	1,232
Δ^+	$3/2$	$3/2^+$	0	0	1	1,232
Δ^0	$3/2$	$3/2^+$	0	0	0	1,232
Δ^-	$3/2$	$3/2^+$	0	0	-1	1,232
Σ^{*-}	1	$3/2^+$	-1	0	1	1,382.8
Σ^{*-}	1	$3/2^+$	-1	0	0	1,383.7
Σ^{*-}	1	$3/2^+$	-1	0	-1	1,387.2

Table 4: Masses of the isospin multiplets in the baryon spectrum. [18]

Spin	Type	$m(+)/\text{MeV}$	$m(-)/\text{MeV}$	$\frac{\lvert m(+)-m(-)\rvert}{m(+)+m(-)}$
$1/2$	N	1710	1650	1.79%
$3/2$	N	1720	1700	0.58%
$5/2$	N	1680	1675	0.15%
$1/2$	Δ	1910	1900	0.26%
$1/2$	N	2100	2090	0.24%
$3/2$	Δ	1,920	1,940	0.52%
$3/2$	N	1,900	2,080	4.52%
$5/2$	Δ	1,905	1,930	0.65%
$5/2$	N	2,000	2,200	4.76%
$7/2$	Δ	1,950	2,200	6.02%
$7/2$	N	1,990	2,190	4.78%
$9/2$	Δ	2,300	2,400	2.13%
$9/2$	N	2,220	2,250	0.67%

Table 5: Masses of parity doublets in the baryon spectrum [29, 27]. States with $m < 1.9\,\text{GeV}$ can clearly be attributed to the $\left(\frac{1}{2},0\right)\oplus\left(0,\frac{1}{2}\right)$ representation of the parity-chiral group. States above $1.9\,\text{GeV}$ could either belong to the multiplet $\left(1,\frac{1}{2}\right)\oplus\left(\frac{1}{2},1\right)$ or to the two different multiplets $\left(\frac{3}{2},0\right)\oplus\left(0,\frac{3}{2}\right)$ and $\left(\frac{1}{2},0\right)\oplus\left(0,\frac{1}{2}\right)$

The irreducible representations of the product (eq. 7.36) can be easily constructed from the representations of the group $SU(2)$, which is the well known spin group. Representations of this group are characterized by the eigenvalue of the Casimir operator of the group:

$$\hat{J}^2 \equiv \hat{J}_1^2 + \hat{J}_2^2 + \hat{J}_3^2 \tag{7.37}$$

Here $\hat{J}_i$ are the three generators of $SU(2)$. Possible eigenvalues of the Casimir operator $\hat{J}^2$ are

$$j(j+1) \text{ , with } j = \frac{n}{2} \text{ and } n \in \mathbb{N} \tag{7.38}$$

On irreducible representations its action is proportional to the identity map. For a $(2j+1)$-dimensional representation of the group it is given by:

$$\hat{J}^2 = j(j+1)\mathbb{1} \tag{7.39}$$

Irreducible representations of the group $SU(2)_L \times SU(2)_R$ are classified using the following notation:

$$(j_L, j_R) \tag{7.40}$$

This representation consists of 2-tuples formed of one member of the $(2j_R+1)$-dimensional and one of the $(2j_L+1)$-dimensional irreducible representation of the group $SU(2)$. Hence , its dimension is

$$(2j_L+1)(2j_R+1). \tag{7.41}$$

Another symmetry of QCD is parity. Accordingly, only energy states with definite parity occur. Definite parity means, that the state is eigenstate of the parity transformation $\mathcal{P}$. Consequently the considered symmetry group has to be extended by the parity group and the spectrum will form multiplets of the parity-chiral group [34]:

$$SU(2)_L \times SU(2)_R \times \mathcal{C}, \tag{7.42}$$

where $\mathcal{C}$ contains space-inversion $\mathcal{P}$ and identity.

To construct these multiplets one starts with the action of parity conjugation on quark operators:

$$\hat{\psi}_R \to \hat{\mathcal{P}}\psi_R\hat{\mathcal{P}}^\dagger = P_R\hat{\mathcal{P}}\psi\hat{\mathcal{P}}^\dagger = P_R\gamma_0\hat{\psi} \overset{(7.5)}{=} \gamma_0 P_L\hat{\psi} = \gamma_0\hat{\psi}_L, \tag{7.43}$$

It changes the chirality of the created quark. The effect on a representation of $SU(2)_L \times SU(2)_R$ is:

$$(j_L, j_R) \xrightarrow{\mathcal{P}} (j_R, j_L) \tag{7.44}$$

This implicates that irreducible representations of the parity-chiral group are representations with $j_R = j_L$

$$(j, j) \tag{7.45}$$

or the direct sum of two irreducible representations with $j_R \neq j_L$

$$(j_L, j_R) \oplus (j_R, j_L), \tag{7.46}$$

which contains the elements of both representations and ensures that any parity or chiral transformation acting on an element will always yield an element of the same representation.

One direct consequence of parity-chiral multiplets are parity doublets. As every multiplet is invariant under parity conjugation, a basis of states, that diagonalizes the parity operator, can be found, i.e. states with definite parity. On the other hand the multiplet is also invariant under any chiral transformation, which in general changes parity[19]. So there will always be states of positive and negative parity in any multiplet, and as a result, the spectrum will show almost mass-degenerate states of opposite parity[20], which are called *parity doublets*.

The possible multiplets for baryons can be constructed from the product of three fundamental quark representations. The four quark fields u_L, d_L, u_R, d_R belong to the $q = (\frac{1}{2}, 0) \oplus (0, \frac{1}{2})$ representation. Their product can be reduced into irreducible representations [35]:

$$q \otimes q \otimes q = \left[\left(\tfrac{3}{2}, 0\right) \oplus \left(0, \tfrac{3}{2}\right)\right] \oplus 3 \times \left[\left(1, \tfrac{1}{2}\right) \oplus \left(\tfrac{1}{2}, 1\right)\right] \oplus 5 \times \left[\left(\tfrac{1}{2}, 0\right) \oplus \left(0, \tfrac{1}{2}\right)\right] \tag{7.48}$$

The $\left(\frac{3}{2}, 0\right) \oplus \left(0, \frac{3}{2}\right)$ only contains states with isospin $\frac{3}{2}$ which correspond to Δ-particles, $\left(\frac{1}{2}, 0\right) \oplus \left(0, \frac{1}{2}\right)$ contains only isospin $\frac{1}{2}$ and thus only nucleon excitations. The $\left(1, \frac{1}{2}\right) \oplus \left(\frac{1}{2}, 1\right)$ multiplet contains states with both isospin $\frac{1}{2}$ and $\frac{3}{2}$.

To determine what multiplets are realized in nature, one has to look at the spectroscopy data. If $\left(1, \frac{1}{2}\right) \oplus \left(\frac{1}{2}, 1\right)$ was realized, nucleon excitations and Δ-particles would have degenerate masses [27]. Table 5, shows that nucleons with $m < 1.9\,\mathrm{GeV}$ can clearly be attributed to the $\left(\frac{1}{2}, 0\right) \oplus \left(0, \frac{1}{2}\right)$ representation of the parity-chiral group. States above $1.9\,\mathrm{GeV}$ could belong to the multiplet $\left(1, \frac{1}{2}\right) \oplus \left(\frac{1}{2}, 1\right)$, due the approximate degeneracy between Δ-states and nucleons.

7.5 Generalized Linear Sigma-Model for Baryons

To derive the properties of parity doublet states, that have been referred to above (smallness of pion coupling due to small axial charge, section 7.3), a model is presented, that exhibits chiral restauration. The aim is to construct an effective Lagrangian that allows baryons of opposite parity to be in chiral multiplets [27].

[19] This can be derived using the anti-commutability of γ_5 and γ_0:

$$\begin{aligned} &\psi \xrightarrow{\mathcal{P}} \gamma_0 \psi \\ &\psi \to \phi = \exp(i\tfrac{\pi}{2}\gamma_5)\psi \overset{(7.15)}{=} i\gamma_5\psi \\ &\phi \xrightarrow{\mathcal{P}} i\gamma_5\gamma_0\psi = -\gamma_0\phi \end{aligned} \tag{7.47}$$

[20] Please note that all this is untouched by the fact, that for every state there exists a charge conjugated version (e.g. anti-nucleon), which of course has the same mass and opposite parity

As explained in the last section, the low lying nucleon parity doublets can be interpreted to originate from the parity-chiral multiplet $\left(\frac{1}{2},0\right)\oplus\left(0,\frac{1}{2}\right)$. The model is intended to explain their properties.

A state from the $\left(\frac{1}{2},0\right)\oplus\left(0,\frac{1}{2}\right)$ multiplet can be written as a vector:

$$\Psi=\begin{pmatrix}\Psi_R\\ \Psi_L\end{pmatrix}=\begin{pmatrix}\begin{pmatrix}u_R\\ d_R\end{pmatrix}\\ \begin{pmatrix}u_L\\ d_L\end{pmatrix}\end{pmatrix} \tag{7.49}$$

where $\Psi_{R/L}$ are isospinors as indicated and u_R is a Dirac bispinor. This vector can be written in a different basis:

$$\tilde{\Psi}=\begin{pmatrix}B_+\\ B_-\end{pmatrix}=\begin{pmatrix}\Psi_R+\Psi_L\\ \Psi_R-\Psi_L\end{pmatrix} \tag{7.50}$$

In this basis the upper (lower) component represents a field of positive (negative) parity:

$$\tilde{\Psi}\xrightarrow{\mathcal{P}}\gamma_0\begin{pmatrix}\Psi_L+\Psi_R\\ \Psi_L-\Psi_R\end{pmatrix}=\gamma_0\begin{pmatrix}+B_+\\ -B_-\end{pmatrix}=\gamma_0\sigma_3\Psi, \tag{7.51}$$

where the transformation property of chirality eigenstates

$$\Psi_{R/L}\xrightarrow{\mathcal{P}}\gamma_0\Psi_{L/R} \tag{7.52}$$

has been used and σ_3 is the first Pauli matrix:

$$\sigma_3=\begin{pmatrix}1&0\\ 0&-1\end{pmatrix} \tag{7.53}$$

The effective Lagrangian is constructed as suggest in [36]. It gives to the two opposite parity fields degenerate masses [27]:

$$\mathcal{L}=i\bar{\Psi}\partial\!\!\!/\Psi-m_0\bar{\Psi}\Psi \tag{7.54}$$

$$=i\bar{B}_+\partial\!\!\!/B_++i\bar{B}_-\partial\!\!\!/B_--m_0\bar{B}_+B_+-m_0\bar{B}_-B_- \tag{7.55}$$

This Lagrangian is invariant under chiral transformations. They are defined as:

$$\text{vectorial:}\qquad \Psi_R\to\exp(i\theta_V^a\tau^a)\Psi_R\,,\quad \Psi_L\to\exp(i\theta_V^a\tau^a)\Psi_L \tag{7.56}$$

$$\text{axial:}\qquad \Psi_R\to\exp(i\theta_A^a\tau^a)\Psi_R\,,\quad \Psi_L\to\exp(-i\theta_A^a\tau^a)\Psi_L \tag{7.57}$$

where τ^a are the $SU(2)$ generators that act on the isospinor space:

$$\tau B=\begin{pmatrix}\tau_{11}u+\tau_{12}d\\ \tau_{21}u+\tau_{22}d\end{pmatrix} \tag{7.58}$$

The effect of chiral transformations on the vector Ψ for vectorial rotations is:

$$\Psi\to\exp(i\theta_V^a\tau^a)\Psi \tag{7.59}$$

Axial rotations take a more complex form:

$$\Psi \to \begin{pmatrix} \exp(i\theta_A^a \tau^a)\Psi_R + \exp(-i\theta_A^a \tau^a)\Psi_L \\ \exp(i\theta_A^a \tau^a)\Psi_R - \exp(-i\theta_A^a \tau^a)\Psi_L \end{pmatrix} \tag{7.60}$$

$$= \cos(\theta_A) \begin{pmatrix} B_+ \\ B_- \end{pmatrix} + i\frac{\tau^a \theta_A^a}{\|\theta_A\|} \sin(\|\theta_A\|) \begin{pmatrix} B_- \\ B_+ \end{pmatrix} \tag{7.61}$$

$$= \exp(i\theta_A^a \tau^a \sigma_1)\Psi, \tag{7.62}$$

where σ_1 is the first Pauli matrix:

$$\sigma_1 = \begin{pmatrix} 0 & 1 \\ 1 & 0 \end{pmatrix} \tag{7.63}$$

The Lagrangian is a bilinear form, whose matrix commutes with both τ^a and σ_i. Thus, the form of axial and vectorial transformations given in eqs. (7.59) and (7.62) can be easily used to check the chiral invariance of this model.

This invariance leads to predictions concerning the axial charges of B_+ and B_-. The conserved axial Noether current of the theory is:

$$A_\mu^a = \bar{\Psi}\gamma_\mu \tau^a \sigma_1 \Psi = \bar{B}_+ \gamma_\mu \tau^a B_- + \bar{B}_- \gamma_\mu \tau^a B_+ \tag{7.64}$$

The absence of diagonal terms of the form $\bar{B}_\pm \gamma_\mu \gamma_5 \tau^a B_\pm$ implies that the axial charges g_A of B_+ and B_- are zero [37]. Hence the chiral symmetry properties of chiral parity doublets determine the axial properties of opposite-parity baryons [38].

The Goldberger-Treiman relation

$$g_{\pi B_\pm B_\pm} = \frac{g_A m_{B_\pm}}{f_\pi} \tag{7.65}$$

requires that the pion coupling to these states also vanishes.

7.6 Lattice QCD Test

The lightest excited nucleon with positive parity and spin-1/2 is the Roper resonance, $N(1440)$ [18]:

Name	spin$^{\text{parity}}$	mass/MeV	width/MeV
$N(1440)$	$\frac{1}{2}^+$	$1,440^{+30}_{-20}$	300^{+150}_{-100}

The two lightest negative parity baryons with spin-1/2 are $N^*(1535)$ and $N^*(1650)$ [18]:

Name	spin$^{\text{parity}}$	mass/MeV	width/MeV
$N^*(1535)$	$\frac{1}{2}^-$	$1,535^{+10}_{-10}$	150^{+25}_{-25}
$N^*(1650)$	$\frac{1}{2}^-$	$1,655^{+15}_{-10}$	165^{+20}_{-20}

They are believed to be linear combinations of a three quark state (N_{3q}) and possibly a Lambda(Λ)-Kaon molecule state ($N_{\Lambda K}$).

The three quark state is supposed to be the chiral partner of the Roper resonance. If this parity doublet occurs due to chiral symmetry restauration, its axial charge g_A should be small. The aim of this work is to give an estimate of g_A for the three-quark contribution of the two lowest negative parity nucleons.

7.6.1 The Operator for the Axial Charge

In QCD, the axial charge of the nucleon g_A, which for example determines the beta decay rate of the neutron (cp. eq. 5.4), is defined as:

$$\langle p, \sigma | \hat{\bar{u}} \gamma_\mu \gamma_5 \hat{d} | n, \sigma \rangle = 2 s_\mu g_A \tag{7.66}$$

It can be written as expectation value of a certain component of the chiral axial current:

$$\langle p, \sigma | \hat{\bar{u}} \gamma_\mu \gamma_5 \hat{d} | n, \sigma \rangle = \langle p, \sigma | \hat{A}_\mu^{1+i2} | n, \sigma \rangle \tag{7.67}$$

with

$$\hat{A}_\mu^{1+i2} \equiv \hat{A}_\mu^1 + i \hat{A}_\mu^2 \overset{(7.27)}{=} \hat{\bar{u}} \gamma_\mu \gamma_5 \hat{d}, \tag{7.68}$$

Using the current algebra relation from eq. (7.28):

$$\left[\hat{Q}_V^{1+i2}, \hat{A}_\mu^3 \right] = -\hat{A}_\mu^{1+i2} \tag{7.69}$$

and isospin symmetry one obtains the following relation:

$$\langle p, \sigma | \hat{A}_\mu^3 | p, \sigma \rangle = 2 s_\mu g_A \tag{7.70}$$

If the expression for $\hat{A}_\mu^3$ is inserted

$$\hat{A}_\mu^3 = \hat{\bar{\Psi}} \gamma_\mu \gamma_5 \tau^3 \hat{\Psi} = \hat{\bar{u}} \gamma_\mu \gamma_5 \hat{u} - \hat{\bar{d}} \gamma_\mu \gamma_5 \hat{d} \tag{7.71}$$

it becomes evident, that this matrix takes the form of the forward matrix elements of local operators, introduced in section 5, which can be extracted from ratios of three- and two-point functions.

The same can be applied to the three quark state N_{3q}. As it is presumed to be part of the parity chiral doublet together with the Roper resonance, it possesses isospin-$1/2$ and thus comes in two isospin-projections $N_{3q}(uud)$ and $N_{3q}(udd)$ (corresponding to proton and neutron). Its axial charge analogously is given by

$$\langle N_{3q}, \sigma | A_\mu^3 | N_{3q}, \sigma \rangle = 2 s_\mu g_A \tag{7.72}$$

In terms of local operators defined in eq. (5.11) it corresponds to the following matrix element on the lattice:[21]

$$\langle N_{3q}, \sigma | \hat{\mathcal{O}}^\mu_{\gamma\gamma_5, u} - \hat{\mathcal{O}}^\mu_{\gamma\gamma_5, d} | N_{3q}, \sigma \rangle_{\text{latt}} = \frac{s_\mu^{\text{E}}}{E_N} g_A \tag{7.74}$$

[21] The factor $2E_N$ occurs, because lattice and continuum normalization differ by that factor:

$$|N\rangle_{\text{latt}} = \frac{1}{2E_N} |N\rangle_{\text{cont}} \tag{7.73}$$

In this form the crucial $u - d$ insertion can be seen, which was important in the calculation of the three-point correlator, because it leads to the cancellation of disconnected diagrams (cp. page 45). For the polarized matrix element in the nucleon's rest frame, with spin

$$\vec{s} = \begin{pmatrix} 0 \\ m \\ 0 \end{pmatrix} \tag{7.75}$$

and the corresponding polarization projector (cp. eq. 5.81, using Euclidean gamma matrices)

$$P(\vec{s}\,) - P(-\vec{s}\,) = i\gamma_5^{\mathrm{E}}\gamma_3^{\mathrm{E}} \tag{7.76}$$

on obtains:[22],[23]

$$\langle N_{3q}|\hat{\mathcal{O}}_{g_A}|N_{3q}\rangle_{\mathrm{pol}} = 2ig_A \tag{7.77}$$

The g_A operator used in this work is:

$$\hat{\mathcal{O}}_{g_A} \equiv \hat{\mathcal{O}}^3_{\gamma\gamma_5,u} - \hat{\mathcal{O}}^3_{\gamma\gamma_5,d} \tag{7.78}$$

7.6.2 Estimation of g_A for the Chiral Partner of the Roper

To calculate the matrix element from eq. (7.77) on the lattice, the following three-point correlator with the correct sink time ($0 \ll t \ll L_t/2$) and projectors that lead to the extraction negative parity states is calculated. Its insertion time dependence will show a plateau with the following value (taken from eqs. 5.94 and 5.84):[24]

$$\begin{aligned} C^{\hat{\mathcal{O}}_{g_A}}_{+,\mathrm{pol}}(0, L_t - t)_{\mathrm{plat}} &= \mathcal{Z}^{-1} \sum_{N^*} e^{-tE_{N^*}}\ |Z_{N^*}|^2 \langle N^*|\hat{\mathcal{O}}_{g_A}|N^*\rangle_{\mathrm{pol}} \\ &= -C^{\hat{\mathcal{O}}_{g_A}}_{-,\mathrm{pol}}(0, t)_{\mathrm{plat}} \end{aligned} \tag{7.80}$$

To get rid of the partition function $\mathcal{Z}$, the exponential function containing the unknown energies and the unknown overlap constants Z_{N^*}, the ratio of the three- and the two-point correlator is considered. The sink time for the two-point functions again is chosen, to guarantee that only the negative parity contributions remain (form eqs. 5.70 and 5.71):

$$C_{P_+}(L_t - t, 0) = 2\mathcal{Z}^{-1} \sum_{N^*} |Z_{N^*}|^2 e^{-tE_{N^*}} \tag{7.81}$$

$$= -C_{P_-}(t, 0) \tag{7.82}$$

[22] The imaginary unit originates from the use of Euclidean matrices in the operators eq. (7.74) and the resulting Euclidean spin vector on the right hand side

[23] The polarized matrix element is defined as $\langle N^*|\hat{\mathcal{O}}|N^*\rangle_{\mathrm{pol}} = \langle N^*, \sigma|\hat{\mathcal{O}}|N^*, \sigma\rangle - \langle N^*, -\sigma|\hat{\mathcal{O}}|N^*, -\sigma\rangle$

[24] the charge conjugation operation has been performed using eq. (5.21):

$$\mathcal{C}\hat{\mathcal{O}}^{\mu}_{\gamma\gamma_5,u}\mathcal{C}^{\dagger} = \hat{u}^T C\gamma_\mu\gamma_5 C\hat{\bar{u}}^T = \hat{\bar{u}}\gamma_\mu\gamma_5\hat{u} = \hat{\mathcal{O}}^{\mu}_{\gamma\gamma_5,u} \tag{7.79}$$

The ratio will also show a plateau with the following value:

$$R_{\text{plat}} = \frac{\sum_{N^*} e^{-tE_{N^*}} \ |Z_{N^*}|^2 \langle N^*|\hat{\mathcal{O}}_{g_A}|N^*\rangle_{\text{pol}}}{2\sum_{N^*} e^{-tE_{N^*}} \ |Z_{N^*}|^2} \tag{7.83}$$

In this form, this value is expressed in terms of the matrix elements of the lowest parity states. To derive an estimate for the three quark state, it can be rewritten. In the following the subscript $_{\text{pol}}$ will be omitted.

The general structure of the linear combination mentioned in the last section can be expressed with an angle α:

$$\begin{aligned} |N^*_{1535}\rangle &= \cos\alpha|N_{3\text{q}}\rangle + \sin\alpha|N_{\Lambda\text{K}}\rangle \\ |N^*_{1650}\rangle &= -\sin\alpha|N_{3\text{q}}\rangle + \cos\alpha|N_{\Lambda\text{K}}\rangle \end{aligned} \tag{7.84}$$

It is reasonable to assume that the baryon operator $\hat{\bar{B}}$ from eq. (5.18) has very little overlap with the molecule state that contains a $\bar{s}, s$ quark pair:

$$\langle 0|B(0,\vec{p})|N_{\Lambda\text{K}}\rangle \approx 0 \tag{7.85}$$

$$\Rightarrow \langle 0|B(0,\vec{p})|N^*_{1535}\rangle \approx \cos\alpha\langle 0|B(0,\vec{p})|N_{3\text{q}}\rangle \tag{7.86}$$

$$\langle 0|B(0,\vec{p})|N^*_{1650}\rangle \approx -\sin\alpha\langle 0|B(0,\vec{p})|N_{3\text{q}}\rangle \tag{7.87}$$

These can be used to further reduce the ratio of three- and two-point correlator:

$$2R_{\text{plat}} = \frac{\cos^2\alpha\langle N^*_{1535}|\hat{\mathcal{O}}_{g_A}|N^*_{1535}\rangle + e^{-t\Delta E}\sin^2\alpha\langle N^*_{1650}|\hat{\mathcal{O}}_{g_A}|N^*_{1650}\rangle}{\cos^2\alpha + e^{-t\Delta E}\sin^2\alpha} \tag{7.88}$$

ΔE is the (positive) mass difference of the two N^*-states. The matrix elements can be expressed in the other basis:[25]

$$\langle N^*_{1535}|\hat{\mathcal{O}}_{g_A}|N^*_{1535}\rangle = \cos^2\alpha\langle N_{3\text{q}}|\hat{\mathcal{O}}_{g_A}|N_{3\text{q}}\rangle + \sin^2\alpha\langle N_{\Lambda\text{K}}|\hat{\mathcal{O}}_{g_A}|N_{\Lambda\text{K}}\rangle \tag{7.89}$$

Upon insertion of eq. (7.89), the ratio becomes:

$$\begin{aligned} 2R_{\text{plat}} = \langle N_{3\text{q}}|\hat{\mathcal{O}}_{g_A}|N_{3\text{q}}\rangle\frac{\cos^4\alpha + e^{-t\Delta E}\sin^4\alpha}{\cos^2\alpha + e^{-t\Delta E}\sin^2\alpha} + \langle N_{\Lambda\text{K}}|\hat{\mathcal{O}}_{g_A}|N_{\Lambda\text{K}}\rangle\times \\ \frac{\left(1+e^{-t\Delta E}\right)\cos^2\alpha\sin^2\alpha}{\cos^2\alpha + e^{-t\Delta E}\sin^2\alpha} \end{aligned} \tag{7.90}$$

If $\langle N_{\Lambda\text{K}}|\hat{\mathcal{O}}|N_{\Lambda\text{K}}\rangle$ and $\langle N_{3\text{q}}|\hat{\mathcal{O}}|N_{3\text{q}}\rangle$ are assumed to have the same sign, one can estimate

$$|\langle N_{3\text{q}}|\hat{\mathcal{O}}_{g_A}|N_{3\text{q}}\rangle_{\text{pol}}| \leq 2|R_{\text{plat}}|\frac{\cos^2\alpha + e^{-t\Delta E}\sin^2\alpha}{\cos^4\alpha + e^{-t\Delta E}\sin^4\alpha} \leq 2|R_{\text{plat}}|\left[1+\cosh\left(\frac{t\Delta E}{2}\right)\right] \tag{7.91}$$

Inserting eq. (7.74) yields:

$$|g_A| \leq |R_{\text{plat}}|\left[1+\cosh\left(\frac{t\Delta E}{2}\right)\right] \tag{7.92}$$

[25] Uses $\hat{\mathcal{O}}^\dagger = (\hat{\bar{q}}\gamma_5\gamma_2\hat{q})^\dagger = \hat{\mathcal{O}}$ and the fact that the matrix element $\langle N_{3\text{q}}|\hat{\mathcal{O}}|N_{\Lambda\text{K}}\rangle$ is real valued.

8 Results and Interpretation

8.1 Gauge Configurations and Lattice

For the calculations of this work I used gauge configurations and propagators of the Bern-Graz-Regensburg Collaboration. The lattice had the dimensions

$$N_s^3 \times N_t = 16^3 \times 32. \tag{8.1}$$

I used a quenched ensemble of 100 gauge configurations that were generated using the Lüscher-Weisz action (see section 4.5) with

$$\beta = 7.90 \tag{8.2}$$

The scale, given by the lattice constant, had been determined to be

$$a = 0.148(2)\,\mathrm{fm} \tag{8.3}$$

The spacial lattice volume is

$$V_s = (2.37(3)\,\mathrm{fm})^3. \tag{8.4}$$

The gauge fields have been smeared with hypercubic-blocking [39]. The propagators have been obtained by inversion of the chirally improved Dirac operator; the coefficients used can be found in Appendix D of [6]). For bigger overlap factors Z (eq. 5.38) all appearing source quarks have been Jacobi smeared. Parameters used for Jacobi smearing are

$$\kappa = 0.21,\ N = 18,\ r \approx 0.354\,\mathrm{fm}. \tag{8.5}$$

Propagators were calculated with the following bare quark masses

$$am_q \in \{0.20,\ 0.16,\ 0.12,\ 0.10,\ 0.08,\ 0.16,\ 0.05,\ 0.04,\ 0.03,\ 0.02\} \tag{8.6}$$

8.2 Inversions on the HPC-Cluster Regensburg

The inversions of the Dirac operator on sequential sources were performed in the test-run of the 2009 newly installed high-performance computing cluster (HPCC) at the University of Regensburg. This cluster is made up of 187 nodes that are connected via *InfiniBand*-interfaces. Every node possesses two *AMD Barcelona B3 2,2 GHz* processors with four processors-cores each. This gives a total of 1496 cores that can execute instructions in parallel. The nodes come in two version. 130 nodes are equipped with 32 GiB main-memory and the rest with 16 GiB. They all have 250 to 500 GiB local hard-disc storage and are connected to NFS-servers via Gigabit-LAN. The servers run *SUSE Enterprise Linux (Novell)* and have numerous compiler suites and MPI libraries installed. The queuing system *Torque* handles the distribution and execution of jobs on the nodes.

As explained above, 24,000 independent inversions had to be performed. As each inversion takes about 24 GiB of memory every 32 GiB node performed one inversion at a time running on 8 cores in parallel. The remaining 16 GiB nodes had to be used in pairs of two nodes, running one inversion at a time on 16 cores in parallel.

The program is written in Fortran.

The total task took the equivalent of one week of the complete cpu time of the cluster.

8.3 Determining the Sink Time

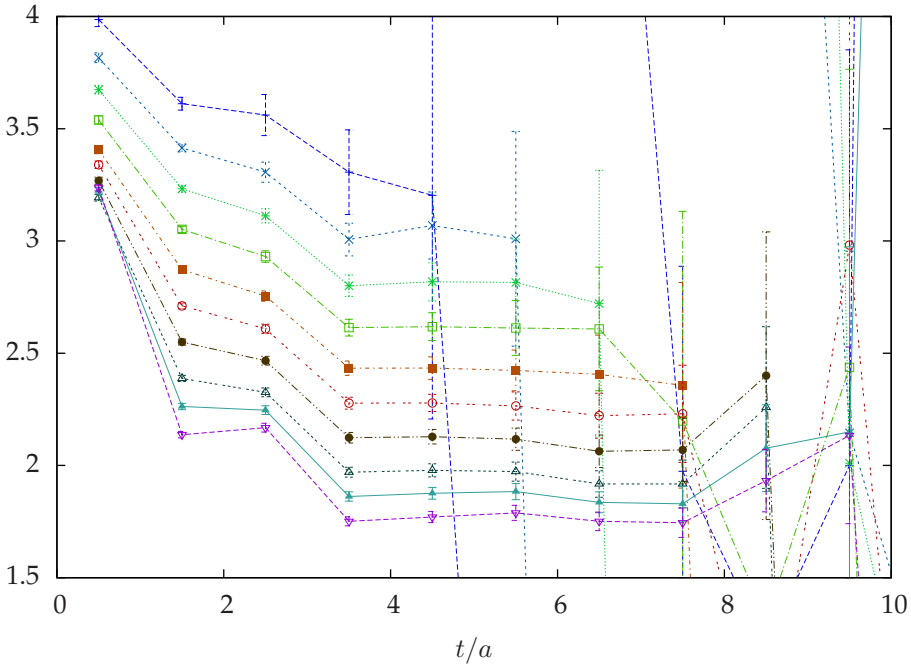

Fig. 5: Effective mass plot of the two-point correlator (figure 2): $m_{\text{eff}}(t+\frac{a}{2}) \equiv \ln(C_{P_-}(t,0)) - \ln(C_{P_-}(t+a,0))$. The effective nucleon masses for ten different quark masses m_i were shifted by $0.2i$. One can see clearly that the ground state is reached after $t = 3a$, where the effective mass shows constant t dependence.

The sink time used in the three point correlator (see eq. 5.74) has to be chosen carefully. It should be far away from 0 and smaller than $L_t/2$. If however the chosen value is too large, the large errors from the two point correlator (cp. figure 1) are going to mess up the result for the ratio of three- and two-point correlator. If the value is too small, the expected plateau behaviour in the τ dependence of the three-point correlator will not evolve, because higher energy contributions do not have enough time to vanish (cp. eq. 5.78). A good indicator for the time the ground state needs to evolve, is the effective mass:

$$m_{\text{eff}}(t+\frac{a}{2}) \equiv \ln(\frac{C_{P_-}(t,0)}{C_{P_-}(t+a,0)}) \tag{8.7}$$

When a plateau is reached, the higher energy contributions have fallen off and only the ground state is measured. Figure 5 shows a plateau after $t = 3a$. Consequently, plateau behaviour of the three-point correlator should occur $3a$ after source time until $3a$ before sink time. To have access to the expected plateau value on at least one or two time slices, the sink time has been chosen to be $t = 9a$. Usually a higher value is chosen to have a larger plateau, but in this work the errors of the two-point correlators forbid the use times later than $9a$.

8.4 Results of the Calculation

To improve statistics and reduce error bars, the two statistically almost independent three-point functions have been calculated (for definition see eq. 5.74):

$$C_{+,\text{pol}}^{\hat{\mathcal{O}}_{g_A}}(\vec{p} = 0, L_t - t, \tau) \tag{8.8}$$

$$C_{-,\text{pol}}^{\hat{\mathcal{O}}_{g_A}}(\vec{p} = 0, t, \tau) \tag{8.9}$$

In the limit of infinitely many gauge configurations they coincide:

$$C_{+,\text{pol}}^{\hat{\mathcal{O}}_{g_A}}(0, L_t - t, L_t - \tau) = -C_{-,\text{pol}}^{\hat{\mathcal{O}}_{g_A}}(0, t, \tau) \tag{8.10}$$

Also two versions of the two-point function have been calculated (for definition see eq. 5.53):

$$C_+(\vec{p} = 0, L_t - t) \tag{8.11}$$

$$C_-(\vec{p} = 0, t) \tag{8.12}$$

that in the limit of an infinite ensemble average obey the similar relation:

$$C_+(0, L_t - t) = -C_-(0, t) \tag{8.13}$$

From these correlators three different ratios have been produced:

$$R_{\text{pos}}(\tau) \equiv \frac{C_{+,\text{pol}}^{\hat{\mathcal{O}}_{g_A}}(0, L_t - t, \tau)}{C_+(0, L_t - t)} \tag{8.14}$$

$$R_{\text{neg}}(\tau) \equiv \frac{C_{-,\text{pol}}^{\hat{\mathcal{O}}_{g_A}}(0, t, \tau)}{C_-(0, t)} \tag{8.15}$$

$$R_{\text{avg}}(\tau) \equiv \frac{C_{+,\text{pol}}^{\hat{\mathcal{O}}_{g_A}}(0, L_t - t, L_t - \tau) - C_{-,\text{pol}}^{\hat{\mathcal{O}}_{g_A}}(0, t, \tau)}{C_+(0, L_t - t) - C_-(0, t)} \tag{8.16}$$

The corresponding plots are found in figures 7, 8 and 9. They also contain the fitted plateau upper and lower error bar (the solid horizontal bars).

As explained in section 7.6.2, the plateau value of the ratio is an unknown combination of two matrix elements. These matrix elements are already regularized. However the renormalization induced by lattice regularization has to be converted to the $\overline{MS}$-scheme to be comparable with continuum results.

To obtain results given in the $\overline{MS}$ renormalization scheme at a scale of $\mu^2 = 1\,\mathrm{GeV}^2$, the lattice results have to be multiplied by a factor. For the inserted operator $\hat{\bar{q}}\gamma_5\gamma_\mu\hat{q}$ the factor has been calculated by Thilo Maurer [6]:

$$Z_A^{\overline{MS}}(\mu^2) = 0.9795(28) \tag{8.17}$$

In figure 6 the normalized plateau values for the four highest quark masses are plotted against the pion mass squared. The pion masses for every bare quark mass were taken from [6].

To derive an estimation for g_A of the presumed chiral partner of the Roper resonance using eq. (7.92), the energy difference ΔE of the two negative parity states has to be estimated. The largest value will occur for the highest quark mass. In lattice units the mass of the lowest negative parity state can be obtained from the value of the plateau in figure 5:

$$(am_{(1535)})^{\text{latt}} = 1.76 \tag{8.18}$$

For an estimation one can assume that the relative difference of the two masses has the same value on the lattice and in experiment. From that it follows:

$$a\Delta E = \frac{m_{(1650)} - m_{(1535)}}{m_{(1535)}}(am_{(1535)})^{\text{latt}} = 0.138 \tag{8.19}$$

If this and $t = 9$ is inserted into eq. (7.92), one obtains:

$$2.2R_{\text{plat}} \leq g_A \leq 0 \tag{8.20}$$

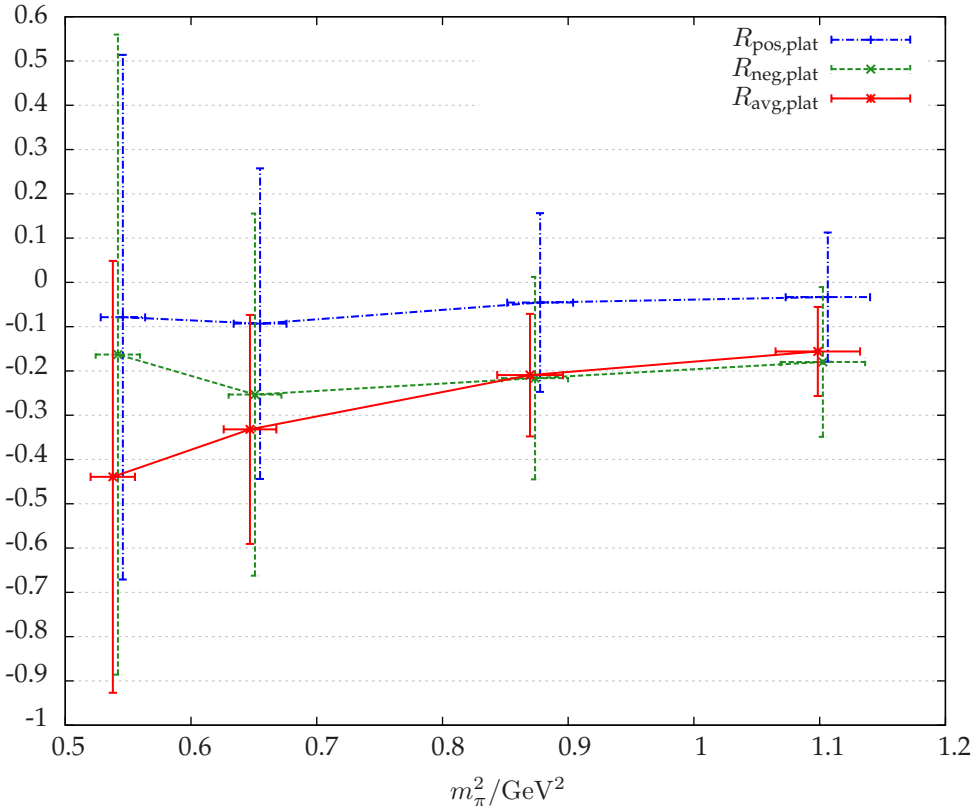

Fig. 6: Plateau values of the ratios for four highest quark masses, plotted against the pion mass squared, renormalized in the $\overline{MS}$-scheme at $\mu^2 = 1\text{GeV}^2$. The three sets are slightly shifted horizontally, to prevent overlapping. The data points can be found in table 6

m_π^2/GeV^2	$R_{\text{pos,plat}}$	$R_{\text{neg,plat}}$	$R_{\text{avg,plat}}$
1.103(34)	−0.03(15)	−0.18(17)	−0.16(10)
0.874(26)	−0.05(20)	−0.22(23)	−0.21(14)
0.651(21)	−0.09(35)	−0.25(41)	−0.33(26)
0.542(18)	−0.08(59)	−0.16(72)	−0.44(49)

Table 6: The plateau values plotted in figure 6

9 Conclusions

The aim of this work was to test the hypothesis of an effective restauration of chiral symmetry in the baryon spectrum. In the course of this work, I passed through several stages:

I introduced QCD as a non-Abelian gauge theory for spin-$1/2$ particles that interact via gluons.

I presented an outline of lattice QCD, the numerical calculation of expectation values related to path integrals in continuum QCD. Important parts in the formulation are the Euclideanization, which produces the real damping factor $e^{-\mathcal{S}_\mathrm{E}}$ and the reduction of the infinitely many integrals to a finite number by restricting the fermion fields to exist only on a finite number of lattice sites and the gauge fields only on the links between them. Also, the discretized version of the fermion and gauge field actions have been introduced and motivated.

Then I explained how hadron properties can be derived from lattice calculations: First I defined the two- and three-point correlation functions and showed how they are calculated on the lattice. After that, I explained what the value of the correlators 'measure' and expressed it in terms of continuum QCD matrix elements.

I also provided a small overview over the numerical and programming aspects of the lattice calculations. Starting from the numerical evaluation of the integrals using statistical methods through to the parallelization of the inversion of the Dirac matrix.

The last section dealt with chiral symmetry. What is chiral symmetry, how is it broken and what implication would an effective restauration have. One consequence of a restauration is the formation of parity-chiral multiplets, which is also seen in the experimental data. In addition to it, one can show using a generalized linear sigma-model for baryon states that form a parity doublet, that for exact chiral symmetry, the axial charges of these states are zero. An effective restauration of this symmetry implies that their axial charges are much smaller than the axial charge of baryons with no chiral partner.

One candidate for a parity doublet in the nucleon spectrum is the Roper resonance $N(1440)$ and possibly a linear combination of the two lightest nucleons with negative parity. The aim of this work was to estimate the axial charge of this state.

Unfortunately the error bars are quite large. One can still conclude, that the axial charge of the lowest three quark state with negative party is definitely smaller than that of the nucleon ($g_A = 1.27$). It does not give reasons to reject the hypothesis of chiral symmetry restauration.

For the highest quark mass, using the ratio of the average (eq. 8.16), the following estimate can be made for the axial charge g_A:

$$0 \leq |g_A| \leq 0.35(22) \tag{9.1}$$

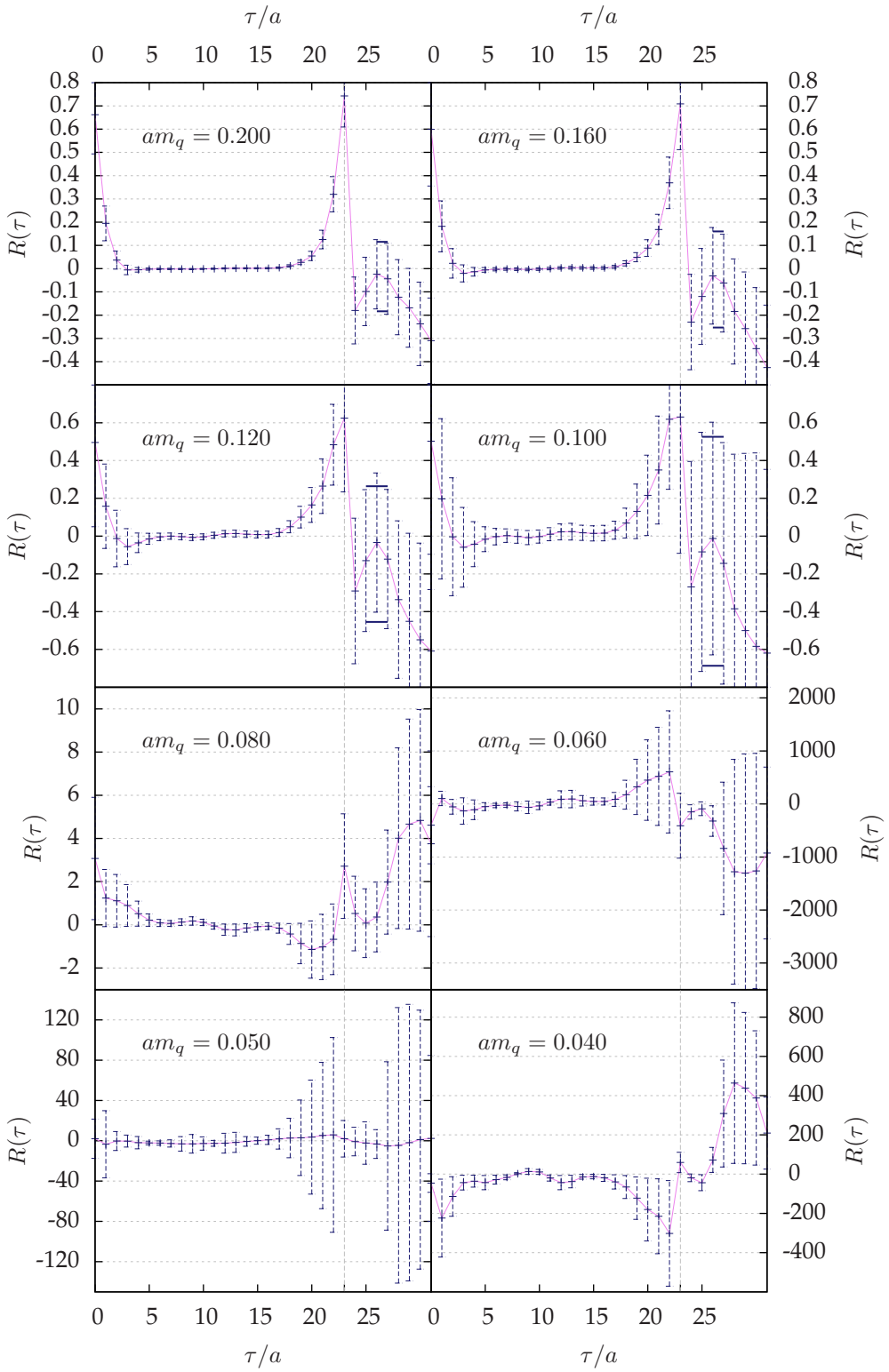

Fig. 7: R_{pos} for the eight heaviest quark masses

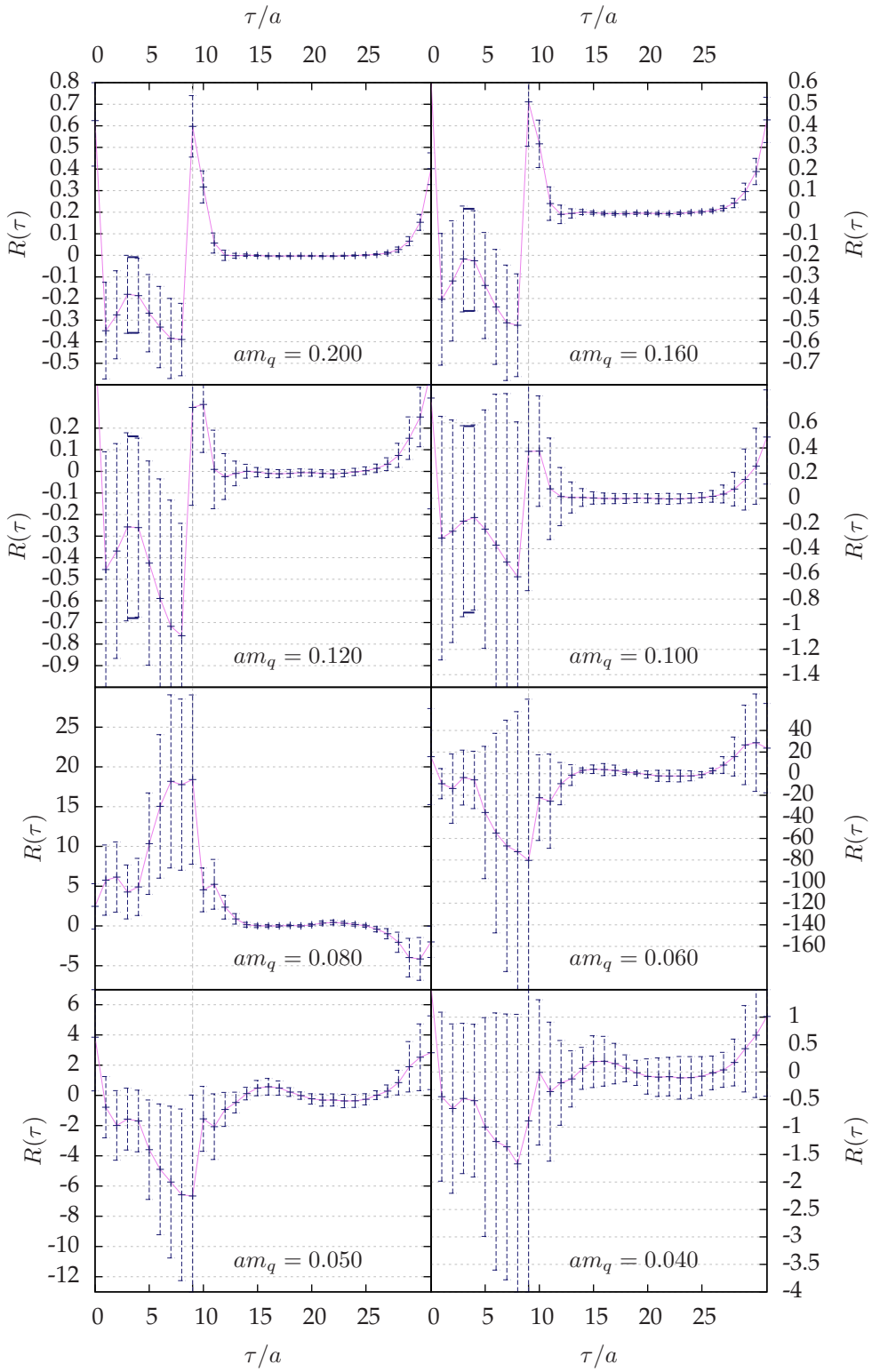

Fig. 8: R_{neg} for the eight heaviest quark masses

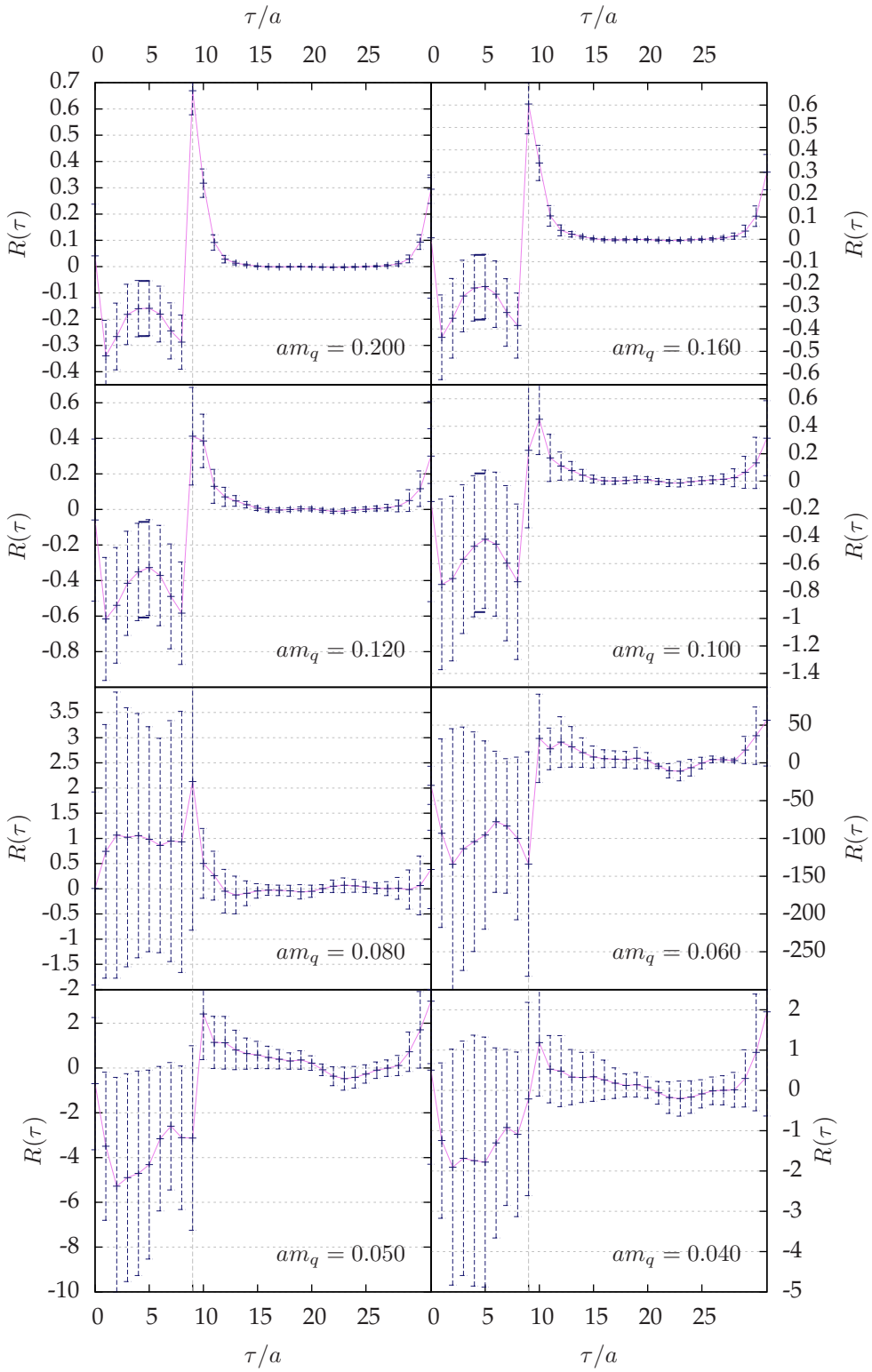

Fig. 9: R_{avg} for the eight heaviest quark masses

References

[1] M. E. Peskin and D. V. Schroeder. *An Introduction to Quantum Field Theory*. Westview Press, 1995. 2

[2] W. Greiner and J. Reinhardt. *Field Quantization*. Springer-Verlag, Berlin, Heidelberg, New York, 1996. 4.1, 4.4

[3] Heinz J. Rothe. *Lattice Gauge Theories. An Introduction*. Word Scientific, Singapore, third edition, 2005. 4.1, 4.4, 4.4.1, 4.7

[4] Konrad Osterwalder and Robert Schrader. Axioms for Euclidean Green's functions. II. *Commun. Math. Phys.*, 42(3):281–305, 1975. 4.1

[5] M. Lüscher. Construction of a selfadjoint, strictly positive transfer matrix for euclidean lattice gauge theories. *Commun. Math. Phys.*, 54(3):283–292, 1977. 4.1, 4.4

[6] Thilo Maurer. *Moments of unpolarized nucleon structure functions in chirally improved lattice quantum chromodynamics*. Diploma thesis, Universität Regensburg, 2007. http://www.thilomaurer.de/diplomathesis.html. 4.4.2, 4.4.3, 4.5, 4.5, 4.7, 4.8, 6.4, 8.1, 8.4, 8.4

[7] H. B. Nielsen and M. Ninomiya. Absence of neutrinos on a lattice : (ii). intuitive topological proof. *Nuclear Physics B*, 193(1):173 – 194, 1981. 4.4.2

[8] H. B. Nielsen and M. Ninomiya. Absence of neutrinos on a lattice : (i). proof by homotopy theory. *Nuclear Physics B*, 185(1):20 – 40, 1981. 4.4.2

[9] Paul H. Ginsparg and Kenneth G. Wilson. A remnant of chiral symmetry on the lattice. *Phys. Rev. D*, 25(10):2649–2657, May 1982. 4.4.3

[10] Nigel Cundy. New solutions to the ginsparg-wilson equation. *Nuclear Physics B*, 802(1-2):92 – 105, 2008. 4.4.3

[11] Christof Gattringer. A new approach to ginsparg-wilson fermions. *Physical Review D*, 63:114501, 2001. 4.4.3, 4.4.3

[12] Christof Gattringer, Ivan Hip, and C. B. Lang. Approximate Ginsparg-Wilson fermions: A first test. *Nucl. Phys.*, B597:451–474, 2001. 4.4.3

[13] Kenneth G. Wilson. Confinement of quarks. *Phys. Rev. D*, 10(8):2445–2459, Oct 1974. 4.5

[14] M. Lüscher and P. Weisz. On-shell improved lattice gauge theories. *Commun. Math. Phys.*, 97(1-2):59–77, 1985. 4.5

[15] G. Curci, P. Menotti, and G. Paffuti. Symanzik's improved lagrangian for lattice gauge theory. *Physics Letters B*, 130(3-4):205 – 208, 1983. 4.5

[16] G. Peter Lepage and Paul B. Mackenzie. On the viability of lattice perturbation theory. *Phys. Rev.*, D48:2250–2264, 1993. 4.5

[17] Mark G. Alford, W. Dimm, G. P. Lepage, G. Hockney, and P. B. Mackenzie. Lattice QCD on small computers. *Phys. Lett.*, B361:87–94, 1995. 4.5

[18] C. Amsler et al. (Particle Data Group). Review of particle physics. *Physics Letters B*, 667(1):1, 2008. 5, 3, 4, 7.6

[19] R. Horsley. *The hadronic structure of matter - a lattice approach*. habilitation thesis, 1999. 5

[20] R. Horsley. *The lattice calculation of moments of structure functions*. 2004. Plenary talk at Hadron Physics I3 Topical Workshop, St. Andrews, UK. http://arxiv.org/abs/hep-lat/0412007v1. 5

[21] UKQCD Collaboration. Gauge-invariant smearing and matrix correlators using wilson fermions at beta=6.2. *Physical Review D*, 47:5128, 1993. 5.2

[22] C. Best, M. Gockeler, R. Horsley, E. M. Ilgenfritz, H. Perlt, P. Rakow, A. Schafer, G. Schierholz, A. Schiller, and S. Schramm. Pion and rho structure functions from lattice qcd. *Physical Review D*, 56:2743, 1997. 5.2

[23] Simon Duane, A. D. Kennedy, Brian J. Pendleton, and Duncan Roweth. Hybrid monte carlo. *Physics Letters B*, 195(2):216 – 222, 1987. 6.1

[24] H. A. VAN DER VORST. BI-CGstab: A fast and smoothly converging variant of BI-CG for the solution of nonsymmetric linear systems. *SIAM Journal on Scientific and Statistical Computing*, 13(2):631–644, 1992. 6.2.4

[25] B. Jegerlehner. Multiple mass solvers. *Nuclear Physics B - Proceedings Supplements*, 63:958, 1998. http://arxiv.org/abs/hep-lat/9708029v1. 6.2.4

[26] Reinhard Alkofer and Hugo Reinhardt. *Chiral Quark Dynamics*. Springer-Verlag, Berlin, Heidelberg, New York, 1995. 7.2

[27] L.Ya. Glozman. Restoration of chiral and $U(1)_a$ symmetries in excited hadrons. *Physics Reports*, 444(1):1 – 49, 2007. 7.2, 7.3, 5, 7.4, 7.5, 7.5

[28] Murray Gell-Mann, R. J. Oakes, and B. Renner. Behavior of current divergences under $SU(3) \times SU(3)$. *Phys. Rev.*, 175(5):2195–2199, Nov 1968. 7.2

[29] L. Ya. Glozman. Parity doublets and chiral symmetry restoration in baryon spectrum. *Physics Letters B*, 475(3-4):329 – 334, 2000. 7.3, 7.3, 5

[30] B. L. Ioffe. Calculation of baryon masses in quantum chromodynamics. *Nuclear Physics B*, 188(2):317 – 341, 1981. 7.3

[31] Erratum. *Nuclear Physics B*, 191(2):591 – 592, 1981. 7.3

[32] L. Ya. Glozman. Alternative experimental evidence for chiral restoration in excited baryons. *Physical Review Letters*, 99(19):191602, 2007. 7.3

[33] Thomas D. Cohen and Leonid Ya. Glozman. Chiral multiplets versus parity doublets in highly excited baryons. *Phys. Rev. D*, 65(1):016006, Dec 2001. 7.4

[34] L. Ya. Glozman. Chiral symmetry restoration in hadron spectra. *Progress in Particle and Nuclear Physics*, 50(2):247 – 257, 2003. 7.4

[35] Thomas D. Cohen and Xiangdong Ji. Chiral multiplets of hadron currents. *Phys. Rev. D*, 55(11):6870–6876, Jun 1997. 7.4

[36] B.W. Lee. *Chiral Dynamics*. Gordon and Breach, New York, 1972. 7.5

[37] R. L. Jaffe, Dan Pirjol, and Antonello Scardicchio. Parity doubling and $SU(2)_L \times SU(2)_R$ restoration in the hadron spectrum. *Physical Review Letters*, 96(12):121601, 2006. 7.5

[38] L.Ya. Glozman and A.V. Nefediev. Chiral restoration in excited nucleons versus $SU(6)$. *Nuclear Physics A*, 807(1-2):38 – 47, 2008. 7.5

[39] Anna Hasenfratz and Francesco Knechtli. Flavor symmetry and the static potential with hypercubic blocking. *Phys. Rev. D*, 64(3):034504, Jul 2001. http://arxiv.org/abs/hep-lat/0103029v2. 8.1

ERKLÄRUNG

Hiermit erkläre ich, dass ich die Diplomarbeit selbständig angefertigt und keine Hilfsmittel außer den in der Arbeit angegebenen benutzt habe.

Regensburg, den ....
(Unterschrift)